

129456

**ISTANBUL TECHNICAL UNIVERSITY ★ EURASIA INSTITUTE OF  
EARTH SCIENCES**

**DEPOSITIONAL CONDITIONS OF THE HOLOCENE SAPROPEL IN THE  
BLACK SEA**

**MSc Thesis by  
Ümmühan SANCAR**

**Institute Number: 621981001**

**Date of submission : May 2002**

128456

**Date of defence examination: May 2002**

**Supervisor (Chairman): Prof.Dr. Namık ÇAĞATAY**

**Members of the Examining Committee: Prof.Dr. Nüzhet DALFES (ITU)**

**Assoc.Doç.Dr. Nuray BALKIS (IU)**

**MAY 2002**

**T.C. YÜKSEKÖĞRETİM KURULU  
DOKÜMANTASYON MERKEZİ**

**İSTANBUL TEKNİK ÜNİVERSİTESİ ★ AVRASYA YERBİLİMLERİ**  
**ENSTİTÜSÜ**

**KARADENİZ'DE HOLOSEN SAPROPELİNİN OLUŞUM**  
**KOŞULLARININ ARAŞTIRILMASI**

**YÜKSEK LİSANS TEZİ**  
**Ümmühan SANCAR**  
**( 621981001 )**

**Tezin Enstitüye Verildiği Tarih: Mayıs 2002**  
**Tezin Savunulduğu Tarih: Mayıs 2002**

**Tez Danışmanı: Prof. Dr. Namık ÇAĞATAY**  
**Diğer Jüri Üyeleri: Prof. Dr. Nüzhet DALFES**  
**Yrd.Doç. Dr. Nuray BALKIS**

**MAYIS 2002**

## ACKNOWLEDGEMENTS

I wish to express my sincere appreciation to all the individuals and organizations that contributed to this study.

I would like to thank all the people who helped me develop an interest in sedimentology, natural sciences and marine geology. I am indebted to Namık ÇAĞATAY, my thesis advisor, for all his efforts, advice and guidance throughout the progress of this thesis work and master programme in general.

I express my sincere gratitude to Naci GÖRÜR, who supervised my undergraduate studies, made every effort to improve my educational background and introduced me to Namık ÇAĞATAY.

I would like to thank Aral OKAY for guiding me to take microphotographs of fossils.

I would like to thank Emin GÜNGÖR and Leyla TOLUN provided the IAEA and MTA core samples for this study.

I would like to thank all the staff in the General Geology Division and Eurasia Institute of Earth Sciences, and in particular to Demet BİLTEKİN for their help during my study.

Finally I would like to express the deepest appreciation to my parents, who made every effort for my education and happiness.

Ümmühan SANCAR  
MAY 2002

## CONTENTS

	<u>Page Number</u>
<b>ACKNOWLEDGEMENTS</b>	ii
<b>CONTENTS</b>	iii
<b>LIST OF FIGURES</b>	v
<b>LIST OF TABLES</b>	vii
<b>SUMMARY</b>	viii
<b>ÖZET</b>	x
<b>PART 1. INTRODUCTION</b>	<b>1</b>
1.1. Oceanography, Recent Sedimentary History and Holocene Sapropel of the Black Sea.	1
1.2. The Objectives and Outline of the Study	7
<b>PART 2. METHODS OF STUDY</b>	<b>8</b>
2.1. Sample Collection	8
2.2. Sample Preparation	8
2.3. Geochemical Analyses	9
2.3.1. Organic Carbon Analyses	9
2.3.2. Total Carbonate Analyses	9
2.3.3. Metal Analysis by ICP-ES (Inductively Coupled Plasma Emission Mass Spectrometry)	10
<b>PART 3. RESULTS</b>	<b>13</b>
3.1. General Lithological Description of the Cores	13
3.2. Mineralogy and Paleontology	15
3.2.1. Core BS 15	15
3.2.2. Core BS 23 (2)	16
3.3. Geochemistry	22
3.3.1. Organic Carbon and Carbonate Contents	22
3.3.2. Metal Distributions	23
3.3.2.1. Core BS 9	23
3.3.2.2. Core BS 15	29
3.3.2.3. Core BS 23 (2)	33
3.3.2.4. Core 46	44

	<b><u>Page Number</u></b>
<b>PART 4. DISCUSSIONS AND CONCLUSIONS</b>	<b>53</b>
4.1. Discussions	53
4.1.1. Detrital Input.	53
4.1.2. Organic Productivity	61
4.1.3. Redox conditions during the sapropel deposition	63
4.2. Conclusions	65
<b>REFERENCES</b>	<b>69</b>
<b>CURRICULUM VITAE</b>	<b>78</b>



## LIST OF FIGURES

	<u>Page Number</u>
<b>Fig 2.1.</b> Location of the studied cores in the Black Sea basin.....	11
<b>Fig 3.1.</b> Lithological logs of the studied cores from the Black Sea.....	14
<b>Fig 3.2.</b> Photomicrographs of Holocene coccoliths in Core BS 23 (2).....	18
<b>Fig 3.3.</b> Photomicrographs of Holocene Diatoms in Core BS 23 (2).....	20
<b>Fig 3.4.</b> Photomicrographs of Pollen in Core BS 23 (2).....	21
<b>Fig 3.5.</b> Concentration/depth profiles of Corg (wt %), total carbonate (wt %) in Cores BS 9, BS 15, BS 23 (2) and 46.....	24
<b>Fig 3.6.</b> Concentration/depth profiles of Mn, Fe, Cu, Zn, V, Cr, Ba and Mo in Core BS 9. All metal data are as weight ratios to Al ( $\times 10^{-4}$ ), except for Fe (x1).....	26
<b>Fig 3.7.</b> Concentration/depth profiles of Sb, Pb, Co, Ni, Sc, Sr and As in Core BS 9. All metal data are as weight ratios to Al ( $\times 10^{-4}$ ).....	28
<b>Fig 3.8.</b> Concentration/depth profiles of Mn, Fe, Cu, Zn, V, Cr, Ba and Mo in Core BS 15. All metal data are as weight ratios to Al ( $\times 10^{-4}$ ) except for Fe(x1).....	31
<b>Fig 3.9.</b> Concentration/depth profiles of Sb, Pb, Co, Ni, Sc, Sr and As in Core BS 15. All metal data are as weight ratios to Al ( $\times 10^{-4}$ ).....	32
<b>Fig 3.10.</b> Concentration/depth profiles of Mn, Fe, As, S, Cu, Zn, Cd, Pb and Sb in Core BS 23 (2). All metal data are as weight ratios to Al( $\times 10^{-4}$ ), except for Fe and S (x1).....	34
<b>Fig 3.11.</b> Concentration/depth profiles of Ni, Co, Ba, Mo, P, U, Th, V and Cr in Core BS 23 (2). All metal data are as weight ratios to Al ( $\times 10^{-4}$ ), except for P(x1).....	38
<b>Fig 3.12.</b> Concentration/depth profiles of Sr, Rb, Ca, Mg, Nb, Zr, Na and K in Core BS 23(2). All metal data are as weight ratios to Al ( $\times 10^{-4}$ ), except for Ca, Mg, Na and K (x1).....	39
<b>Fig 3.13.</b> Concentration/depth profiles of Ce, Ta, Li, Ti, La, Y and Sc, in Core BS 23 (2). All metal data are as weight ratios to Al ( $\times 10^{-4}$ ), except for Ti (x1).....	42
<b>Fig 3.14.</b> Concentration/depth profiles of Mg/Ca, Sr/Ca, Cd/Ca and U/Th in Core BS 23(2).....	43
<b>Fig 3.15.</b> Concentration/depth profiles of Mn, Fe, As, S, Cu, Zn, Cd, Pb and Sb in Core 46. All metal data are as weight ratios to Al ( $\times 10^{-4}$ ) except for Fe and S (x1).....	45

<b>Fig 3.16.</b> Concentration/depth profiles of Ni, Co, Ba, Mo, P, U, Th, V and Cr in Core 46. All metal data are as weight ratios to Al ( $\times 10^{-4}$ ), except for P (x1).....	48
<b>Fig 3.17.</b> Concentration/depth profiles of Sr, Rb, Ca, Mg, Nb, Zr, Na and K in Core 46. All metal data are as weight ratios to Al ( $\times 10^{-4}$ ) except for Ca, Mg, Na and K (x1).....	49
<b>Fig 3.18.</b> Concentration/depth profiles of Ce, Ta, Li, Ti, La, Y and Sc, in Core 46. All metal data are as weight ratios to Al ( $\times 10^{-4}$ ) except for Ti (x1).....	51
<b>Fig 3.19.</b> Concentration/depth profiles of Mg/Ca, Sr/Ca, Cd/Ca and U/Th in Core 46.....	52



## LIST OF TABLES

	<u>Page Number</u>
<b>Table 2.1.</b> The precision and accuracy values of the cores.....	12
<b>Table 3.1.</b> The average and range values of Corg, CaCO <sub>3</sub> and metals in sapropel and coccolith unit in Core BS 9& BS 15.....	23
<b>Table 3.2.</b> The average and range values of Corg, CaCO <sub>3</sub> and metal/Al ratios insapropel and coccolith unit in Core BS 9& BS 15.....	26
<b>Table 3.3.</b> The average and range values of Corg, CaCO <sub>3</sub> and metals in sapropel and coccolith unit in Core BS 23 (2)& 46.....	35
<b>Table 3.4.</b> The average and range values of Corg, CaCO <sub>3</sub> and metals in sapropel and coccolith unit in Core BS 23 (2)& 46.....	36
<b>Table 3.5.</b> Chemical composition of the sediments in Core BS 9 from the Western basin.....	27
<b>Table 3.6.</b> Chemical composition of the sediments in Core BS 15 from the Western basin.....	30
<b>Table 3.7.</b> Chemical composition of the sediments in Core BS 23 (2) from The eastern basin.....	40
<b>Table 3.8.</b> Chemical composition of the sediments in Core 46 from the eastern basin.....	46
<b>Table 3.9.</b> Correlation coefficients of elements for the coccolith unit in Cores BS 23 (2)& 46 from the eastern basin.....	55
<b>Table 3.10.</b> Correlation coefficients of elements for the sapropel unit in Cores .BS 23 (2)& 46 from the eastern basin.....	56
<b>Table 3.11.</b> Correlation coefficients of elements for the coccolith unit in Cores BS 9, BS 15,BS 23 (2)& 46.....	59
<b>Table 3.12.</b> Correlation coefficients of elements for the sapropel unit in Cores BS 15, BS 23 (2)& 46.....	60



## SUMMARY

The objective of this thesis is to investigate the water column oxygen and organic productivity conditions during the deposition of the Black Sea sapropel, using inorganic geochemical, paleontological and sedimentological methods.

Four cores were studied from Black sea basin two each from western (Core BS 9& BS 15) and eastern basins (Core BS 23 (2)&46). These cores include two sedimentary units. These units were deposited during the last 3000 and 7000-3000 yr BP, respectively from top to base are a laminated coccolith unit and organic rich sapropel.

These studied cores give important results concerning the depositional conditions of the two stratigraphic units. Firstly, the high values of total carbonate content is a result of high concentrations of calcite coccoliths of *Emiliana huxleyi* forming coccolith laminae in this unit. This laminae are the product of annual summer plankton blooms when the light intensity and temperature are optimal for a maximum growth. Secondly, the Carbonate, Ca/Al and Sr/Al profiles also shows biogenic input and elevated values in the coccolith unit. The higher values of Sr/Al in the coccolith unit in the western basin than those in the eastern basin indicate that there are greater biogenic carbonate flux and relatively low detrital input in the former basin compared to the latter basin.

Another important component of the Black Sea sediments is the detrital mineral and organic matter which have been transported to the basin via the rivers. The mineralogical composition and grain size of detrital input is consistent with the enrichment of lithophile elements, such as K, Na, Mg, Rb, Cr, Ti and Zr in coccolith unit. These metals, together with sharp increases in heavy metals of anthropogenic origin (Cu, Zn, Pb, Sb and As), in the top few cm of the cores are due to anthropogenic activity in the last few hundred years.

The differences in the depth of the onset of the enrichment in different cores are because of different sedimentation rates at the different core sites. The sequence of this depth distribution indicate that the sedimentation rate is in the order of Core BS 9 > Core BS 15 > Core BS 23(2).

The trends of Ba/Al profiles are generally conformable with those of Corg profiles in the studied cores, indicating the proxy character of this ratio for organic productivity in the Black Sea sediments. Ba/Al ratio is the highest in the sapropel unit in Core BS 15, followed by Core BS 23(2) and Core 46. These trends suggest that the organic productivity was higher in the western basin than in the eastern basin during the sapropel deposition.

High Ba, Mo, P, Ni and V show strong correlation between each other in organic-rich sediments. In the coccolith unit, Ba/Al ratio increases in the order: Core 46 < BS 23(2) < BS 9 < BS15, again suggesting higher organic productivity in the western Black Sea basin compared to the eastern Black Sea basin during the last 3000 years. The sharp enrichment of Ba in the few cm-thick core tops is an important indicator of the recent eutrophication of the Black Sea.

The enrichments of Redox sensitive elements such as Mn and Fe in and above the Black Sea sapropel are not observed in both the eastern and western Black Sea basins strongly suggesting that the sapropel unit was deposited under anoxic water conditions.

The enrichment chalcophile (Pb, Cu, Zn, Cd, Ni, As, S and Sb) elements in the Black Sea sapropel in studied cores also strongly suggests that this layer was deposited under anoxic bottom waters. High correlation coefficients between Fe, Co, As and S support close relationship of these metals with sulphide phases in the sapropel unit. The elevated values of Mo, Ni and V are observed in sapropel unit in Core BS 15, BS 23 (2) and 46. These metals are probably concentrated in both the organic and sulphide fractions.



## ÖZET

Tezin amacı, Karadeniz'e Akdeniz sularının girmesinden sonra orta Holosen'de oluşan sapropel biriminin çökeldiği su sütunu koşullarını ve organik üretimi inorganik jeokimyasal ve paleontolojik yöntemlerle belirlemektir.

Karadeniz'de ikisi batıdan (BS 9&BS 15) ve ikisi doğudan (BS 23 (2)& 46) olmak üzere 4 karot çalışılmıştır. Bu karotlar iki sedimanter birim içerirler. Bu kokolit ve sapropel birimi sırasıyla günümüzden son 3000 ve 7000-3000 yıl önce çökelmiştir.

Çalışılan karotlar sapropel biriminin çökme koşulları ile ilgili olarak önemli sonuçlar vermiştir. İlk olarak kokolit laminalı birimde yüksek toplam karbonat değerleri bu birimdeki kokolit laminaları oluşturan *Emiliana huxleyi* kalsitik kokolit konsantrasyonlarının yüksek olması nedeniyledir. Bu laminalar ışık yoğunluğu ve sıcaklığın büyüme için en elverişli olduğu yıllık yaz plankton patlamalarının ürünüdür. Karbonata benzer şekilde, Ca ve Sr profilleri biyojenik akıyı gösterir ve kokolit biriminde yüksek değerler göstermiştir. Kokolit biriminde batı Karadeniz havzasında doğu havzasına göre daha yüksek Sr/Al değerleri izlenmiştir. Bu batı havzasında daha çok biyojenik karbonat akıyı ve kısmen düşük detrital girdiyi göstermektedir.

Karadeniz sedimentlerinin diğer önemli bileşeni nehirler yoluyla taşınan organik madde ve detrital minerallerdir. Kokolit biriminde K, Na, Mg, Rb, Cr, Ti, Zr gibi litofil elementlerin zenginleşmesi mineralojik bileşim ve detrital tane büyüklüğü akışı ile uyumludur. Bu metallerle birlikte antropojenik kökenli ağır metallerin (Cu, Zn, Pb, Sb and As) karotların üst birkaç cm.'sinde hızlı artışı son birkaç yüzyıldaki antropojenik etkinlikle ilgilidir.

Farklı karotlardaki zenginleşmelerin başladığı derinliklerdeki farklılıklar, farklı karot alanlarındaki farklı sedimantasyon hızları nedeniyledir. Buna göre sedimantasyon hızının sırası Core BS 9>BS 15> BS 23 (2) şeklindedir.

Karadeniz sedimentleri içinde organik üretimi gösteren Ba/Al oranı karot BS15 te sapropel biriminde en yüksektir. Bunu Core BS 23 (2) ve Core 46 izlemektedir. Aynı sıra adı geçen karotlarda kokolit biriminde de izlenmiştir. Bu sıraya göre gerek sapropel ve gerekse kokolit çökelişi sırasında batı havzada doğu havzaya göre daha yüksek organik üretim gerçekleşmiştir.

Karadeniz karotlarında sapropel biriminde Ba, Mo, Ni ve V ile organik karbon arasında kuvvetli korelasyon görülmüştür. Bu kuvvetli korelasyonlar adı geçen metallerin organik madde ile ilişkisini göstermektedir..

Karotun üst birkaç cm.'sinde Baryumun hızla artışı Karadeniz' de yakın zamandaki aşırı organik üretimin(ötrifikasyon) önemli göstergesidir

Mn ve Fe gibi redoksa duyarlı elementlerin Karadeniz sapropeli içinde ve üzerinde hem doğu hemde batı Karadeniz havzasında zenginleşme göstermemesi sapropel biriminin oksijensiz (anokzik) dip suyu koşulları altında çökeldiğini kuvvetle desteklemektedir. Karadeniz sapropeli içinde kalkofil element (Fe, Cu, Zn, Cd, Ni, Sb,As ve S) zenginleşmesi bu sonucu desteklemektedir.

Fe, Co, As ve S arasındaki yüksek korelasyon katsayıları, bu metallerin sapropel biriminde sülfid fazında bulunduğunu göstermektedir. Sapropel biriminde çok yüksek Mo, Ni, V değerleri Core BS 15 ve BS 23 (2) de gözlemlenmektedir. Bu metaller büyük olasılıkla hem organik maddenin yapısında hemde sülfid fazında konsantre olmuştur.



## **1. INTRODUCTION**

### **1.1. Oceanography, Recent Sedimentary History and Holocene Sapropel of the Black Sea**

Black Sea is the largest modern anoxic basin in the world with a maximum depth of 2250 m. It is a tectonically restricted basin connected to Mediterranean and the world ocean system via the Sea of Marmara and the Straits of Bosphorus and Dardanelles.

The present sill depths of Bosphorus and Dardanelles Straits are 35m and 64m, respectively (Gunnerson and Özturgut, 1974). The Black Sea has a positive water balance and exports waters of low salinity to the Mediterranean, the positive water balance is supported by substantial riverine input of fresh water from Danube drainage system to the west, from rivers draining the southern part of the Russian and Caucasus and Anatolian drainages to the east and south (Shimkus and Trimonis, 1974). The Bosphorus Strait limits the influx of relatively warm, saline Mediterranean surface waters to the basin (Özsoy and Ünlüata, 1997). The Black Sea has a pycnocline at depth of about 100-150 m, separating aerated brackish waters (~18 ‰) from anaerobic, H<sub>2</sub>S-rich more saline waters (~ 22.5 ‰). However, The pycnocline depth of Black Sea occur at ~75m in the centre and at ~210m at margins (Murray *et al.*, 1991).

The Black Sea basin consists of four physiographic parts: continental shelf, continental slope, basin apron and abyssal plain (Ross *et al.*, 1974; Ross *et al.*, 1978).

The northwest shelf of the Black Sea is much wider than the Anatolian Coastline and Caucasus shelves (<20km). Some canyons trending at roughly right angles to the coast have dissected the southern shelf and slope. These canyons are important in transportation of sediment loads to the abyssal plains that cover large area in the central part.

The Holocene Black Sea sediments deposited in the last 30000 year consist of three units. The youngest is a modern, finely laminated coccolith marl (Recent unit of Soviet workers and Unit 1 of Ross *et al.*, 1970). This is underlain by a micro laminated organic-rich sapropel (Old Black Sea unit of Soviet workers and Unit 2 of Ross *et al.*, 1970). Laminated carbonate-poor clays (New Euxinian unit of Soviet workers: Unit 3 of Ross *et al.*, 1970) comprise the oldest unit recovered. These three units can be traced over most of the deep water area of the Black Sea and reflect the evolution of hydrographic conditions in the basin following the last glaciation. In the last glacial epoch and deglaciation, the Black Sea was a fresh water lake and a lacustrine clay unit (Unit 3) was deposited when the Black Sea was isolated from the Mediterranean (Degens and Ross, 1972; Ross and Degens, 1974). The last connection with the Mediterranean was established through the Bosphorus at 7150 yr BP (Ryan *et al.*, 1997). After this connection, high organic productivity and restricted circulation conditions caused deposition of the sapropel unit (Unit 2) about between 7000 and 3000 yr BP. The coccolithophore *Emiliania huxleyi* invaded the basin at about 3000yr BP and present oceanographic conditions were established with the deposition the coccolith microlaminated mud. Based on modern AMS <sup>14</sup>C datings of numerous core samples from various parts of the basin, Jones and Gagnon (1994) determined the calibrated ages of 2720 and 7900 yr BP for the Unit 1 / Unit 2 and Unit 2 / Unit 3 boundaries, respectively. Later, the same boundaries were dated at 2000 and 7800yr by Arthur and Dean (1998).

Çağatay *et al.* (1990) found sapropel (Unit 2) is about 40 cm thickness and consist mainly organic matter with some coccolith remains, clays, inorganically precipitated aragonite, iron monosulfides and pyrite. The organic carbon content of the sapropel unit ranges up to 14.25 % and average 10 %.

The average Corg contents of Unit 1 is ~3 %. The surface sediments from all physiographic regions of the southern part of the Black Sea basin contain an average of 2.3 % Corg. The areal distribution of Corg contents of composite samples comprising all the three units shows an increase from < 1 % on the shelf to > 5% on the abyssal plains (Çağatay, 1987; Çağatay *et al.*, 1990). This distribution closely approximates that of sedimentation rates given by Ross *et al* (1970).

According to Arthur and Dean (1998), the sapropel consists of ~50 cm of finely laminated, olive-black sapropel found underlying Unit 1 in the deep basins but thickens to 150 cm or more and becomes lighter in colour in shallow waters because of a much higher accumulation rate of detrital clastic material. The sapropel contains 1-20 % Corg and 5-15 % CaCO<sub>3</sub>. The contents of the latter two components are higher in the deep basin and lower in the shallower water due primarily to dilution by detrital clastic material. At the base of the sapropel, there is a white laminated band consisting of rounded needles of aragonite ('rice grains' of Ross and Degens, 1974). Arthur and Dean (1998), subdivided sapropel unit on the basis of colour, organic carbon content and the presence of the laminae at the base into two subunits. Subunit IIb<sub>1</sub> is distinguished from Subunit IIb<sub>2</sub> on the basis of the presence of aragonite laminae in subunit IIb<sub>2</sub> and the prominent peak in organic carbon content in Subunit IIb<sub>1</sub>. They agree that increased primary productivity in Unit II relative to Unit III played an important role in forming the Unit II sapropel. However, they conclude that the entire water column below ~200 m was sufficiently oxygen deficient at the beginning of the deposition of Unit II to permit preservation of the fine laminations. They believe that the bottom waters of the Black Sea became totally anoxic and sulphidic (with free H<sub>2</sub>S in the bottom waters) within a few hundred years after the initiation of deposition of Unit 2.

The Holocene Black Sea sediments consist of four units according to Calvert (1990). Unit A consists of laminated, coccolith-bearing marls with carbon values ranging from 0.66 to 3.88 %. Unit B is very homogeneous with 1.63 ± 0.09 % Corg and 13.4 ± 0.17 % CaCO<sub>3</sub>. Unit C is the sapropel that organic carbon content of 14.4 % and Unit D has the lowest Corg contents of the entire core and contains 15.6 to 26.0 % CaCO<sub>3</sub>.

These sedimentary units, which are distinguished by carbon and carbonate profiles, has been interpreted by Calvert *et al.* (1987) to represent: (1) the modern sediment facies of Black Sea (Unit A) which is equivalent to the Recent horizon of Soviet workers (Arkangel'skiy and Strakhov, 1938) and Unit 1 of Ross *et al.* (1970) (2) the recent sapropel (Unit C) which is equivalent to the Old Black Sea Horizon of Soviet workers and Unit 2 of Ross *et al.* (1970), and (3) laminated calcareous (lacustrine) clays (Unit D) which are equivalent to New Euxinic horizon of Soviet workers and Unit 3 of Ross *et al.* (1970).

The homogeneous (Unit B) separating the modern facies and the sapropel in Cores 1432 and 1470 is interpreted to be a homogenite or turbidite horizon: such sediments are evidently very common in Cores collected from the deep Black Sea (*Degens et al.*, 1980), although they have not previously been described from the cores collected by the ATLANTIS II in 1969.

The composition of organic matter in the sapropel unit has been extensively studied by different methods. These various studies have often produced contradictory results concerning the origin of the organic matter in the sapropel. According to Simoneit (1974, 1978) suggests that the organic matter is mainly of terrestrial origin and consists of spores, pollen and other plant parts containing sterols and fatty acids. Volkov & Fomina (1974) further recognized the presence of bitumen, humic and fulvic acids. Similarly, Hunt (1974) concluded that the hydrocarbon composition of the organic matter is enriched in aromatic and asphaltic compounds of terrestrial origin, but poor in paraffin compounds of marine organic affinity. However, the results of Pelet and Debyser (1977) and Lee *et al.* (1980) showed that the marine component of the organic matter is more important than the terrestrial one. Furthermore, infra-red spectroscopic studies by Huc *et al.* (1978) indicate that the sapropel is composed predominantly of aliphatic hydrocarbons.

Çağatay (1999) demonstrate that the elemental C/N of the sapropel in Core 46 in the eastern Black Sea ranges from 12 to 16.4 and averages 14.5. Considering the C/N of marine plankton and zooplankton lies between 5 and 8 and that of land plants between 20-200 (Emerson, 1988), the C/N values of the Black Sea sapropel suggest that the organic carbon is a mixture of marine and terrestrial material.



Recent  $\delta^{13}\text{C}$  data obtained by Tolun *et al.* (1999) suggest a significant contribution of terrestrial organic matter. Recent studies, involving Py/GC/MS analysis (Didyk *et al.*, 1978; Ergin *et al.*, 1996; Brown *et al.*, 2000; van de Meent *et al.*, 1980), Gas Chromatography-Mass Spectrometry (GC-MS) analysis, together with  $^{13}\text{C}$  magnetic resonance spectrometry (Brown *et al.*, 2000), demonstrated that the sapropel is a Type 1 kerogen, having similar organic structures to oil shales. Rock-Eval analysis of the sapropel unit produced very high hydrogen index values that also strongly suggest Type 1 kerogen of marine algal origin (Espitalié *et al.*, 1977; Volkov and Fomina, 1974; Calvert, 1987). Py/GC/MS analysis shows that the principal organic components in sapropel are alkanes, alkenes, alkyl benzenes, alkyl naphthalenes and a few phenols.

Tolun (2001) studied the organic geochemistry of the Black Sea sapropel in Core 46 using elemental C/N analysis, Rock Eval Pyrolysis and C-isotope analysis. The results show that the organic matter in the lower part of the sapropel starts with predominantly terrestrial organic matter input, which gradually become more marine towards the upper part and in the coccolith unit. In the view of these recent results, it can be concluded that organic matter in the sapropel unit is mostly of marine planktonic origin, with local and variable contribution of a terrestrial component causing some variation in the composition.

Formation of any sapropel requires some special water column conditions:

- 1) increase in surface water productivity,
- 2) restricted bottom water circulation and anoxic bottom water conditions (Demaison and Moore, 1980; Schrader and Maderne, 1981; Calvert and Price, 1983; Thunell and Williams, 1989; Pederson and Calvert, 1990; Calvert *et al.*, 1992; Emeis *et al.*, 1996; Thomson *et al.*, 1995).

Stagnant oceanic bottom waters with a low concentration or absence of oxygen (anoxia) were considered for a long time as the main prerequisite for the accumulation of high amounts of organic matter in sediments (Demaison and Moore, 1980).

However, recently, two contrasting models have been developed to explain the deposition of organic matter rich sediments in marine realm, either (1) by preservation under anoxic conditions in a static situation or (2) by high primary productivity in a dynamic system (Pedersen and Calvert, 1990; Demaison, 1991; Pedersen and Calvert, 1991).

The relative importance of these two dominant controlling parameters is still being heavily debated, although Stein (1986 a,b; 1990) conceived that either one of these parameters could play a decisive role in different oceanographic situations. Another parameter brought into a discussion more recently is the protective role for organic matter adsorption on mineral surfaces and its influence on organic matter accumulation in marine sediments (Keil *et al.*, 1994a, b; Mayer, 1994; Ransom *et al.*, 1998).

According to first model, the lack of replenishment of oxygen by restricted circulation in the bottom water can lead to anoxic or suboxic conditions in the water column and at the sediment / water interface.

In the Black Sea, this is caused by the development of a very stable halocline (preventing vertical mixing) at about 100 m to 150 m water depth. The surface layer is fed by relatively light, riverine freshwater which overlies the salty Mediterranean water. Over time, oxidation of sinking remnants of decayed organisms could consume all the free oxygen in the deeper water, which was not effectively replenished by Mediterranean water spilling over the Bosphorus sill.

Presently, the deep water in the Black Sea contains hydrogen sulfide restricting life to anaerobic microorganisms that are commonly thought to degrade organic matter less rapidly than aerobic bacteria. Lack of intense organic matter degradation under anoxic conditions would then not necessarily require high surface water bioproductivity for high organic carbon concentrations to occur in the sediment.

The productivity model is based on high primary productivity in the photic zone of the ocean as it presently occurs in areas of coastal upwelling primarily on the western continental margins, along the equator and as a monsoon-driven phenomenon in the Arabian Sea (Rullkötter, 2000). Upwelling brings high amounts of nutrients to the surface, which stimulates phytoplanktonic growth (e.g. Suess and Thiede 1983, Thiede and Suess 1983, Summerhayes *et al.*, 1992).

On continental margins, the formation of oxygen-depleted water masses (oxygen minimum zones) usually implies that they impinge on the ocean bottom where they create depositional conditions similar to those in a stagnant basin (e.g. Pedersen and Calvert 1990, 1991; Demaison, 1991). Finally, the first model requires anoxic bottom water conditions so that organic matter is deposited.

On the other hand, the high productivity model does not primarily require anoxic bottom water conditions (Calvert, 1990).

Based on the distribution of Mn, I and Br in the deep water sediments, Calvert (1990) suggest that the surface of the sediment and hence the bottom water was well oxygenated at the time of the sapropel deposition in the Black Sea.

## **1.2. The Objectives and Outline of the Study**

As can be seen from the foregoing discussion, the Holocene sapropel in the Black Sea has been the subject of numerous studies. However, depositional conditions, especially concerning water-column oxygen levels, during the deposition of this sapropel are still highly controversial.

The objective of this thesis is to investigate the water column oxygen and organic productivity conditions during the deposition of the Black Sea sapropel, using inorganic geochemical, paleontological and sedimentological methods.

For this study, high-resolution sampling analyses of three multi-corer cores and one gravity core recovered from the deep eastern and western Black Sea basins were carried out. The core samples were analysed for wide range of elements (Fe, Mn, Cu, V, Ni, Cr, Mo, As, S, U, Th, Cd, Sb, Co, Pb, Zn Sr, Ca, P, La, Cr, Mg, Ti, Na, K, Ce, Y, Nb, Ta, Sc and Li) and for organic productivity proxies (organic carbon, carbonate and Ba). The samples were also studied under microscope for their mineral composition and nanno- and micro-fossil content. Distribution of these parameters along the depth of the cores was interpreted in terms of depositional conditions during the sapropel deposition.

## **2. METHODS OF STUDY**

### **2.1. Sample Collection**

Four cores were studied from Black Sea basin two each from western and eastern basins (Fig 2.1). The western basin multi-corer cores were collected from the western continental margin in 1998 during the IAEA-RADEUX cruise (Core BS-9: 44° 28.118' N, 31° 15 .178'E, 600 m water depth; Core BS-15: 43° 29 .094'N, 30° 42 .367' E, 1319 m water depth). The gravity core in the eastern basin was collected by R/V Çarşamba for MTA study in 1978 (Core 46: 43° 00 00N, 36° 45 E, 2160 m water depth). The multi-corer core in the eastern basin was collected in 2000 during the IAEA-RADEUX cruise (Core BS 23 (2): 42° 57.506'N, 37 °22 .403' E, 2167 m water depth).

### **2.2. Sample Preparation**

The samples were dried to constant weight at 70° C and ground to fine powder in an agate mortar. Core BS 9 was subsampled at about 1 cm intervals to 5 cm depth, 2 cm interval between 15 cm and 30 cm depth, and 5 cm interval between 30 and 50cm depth.

Core BS 15 has a total length about 50 cm. The first 10 cm of this core were subsampled at about 1 cm intervals, followed by 2 cm sampling interval between 10 and 20 depth, and 5 cm sampling interval between 20 and 50 cm depth.

Core BS 23, has a total length about 38.5 cm depth. The sampling resolution for this core was 0.5 cm until 5 cm, 1 cm between 5 and 14 cm, and 2 cm between 14 and 38.5 cm core depth.

Core 46 has a total length at 142 cm. Generally; this core was sampled at 5 to 10 cm intervals.

### **2.3. Geochemical Analyses**

#### **2.3.1. Organic Carbon Analyses**

Organic Carbon (Corg) content of the samples was determined by Walkey-Blake method. This method involves the titration with ferrous aluminium sulphate of the dichromate left after a wet combustion of the sample with potassium dichromate (Gaudette *et al.* 1974; Loring and Rantala, 1992).

0.01, 0.02, 0.03, 0.04, 0.05, 0.06 g glucose are used as standards for the calibration. Corg content is calculated using the calibration curve and a dilution factor. 0.5 g of dried and powdered samples are placed in 500 ml flasks, 10 ml 1N dichromate solution is added by pipet and mixed. Then, 20 ml H<sub>2</sub>SO<sub>4</sub> is added and mixed for one minute, and left for thirty minutes with frequent mixing. Samples are diluted with 200 ml distilled water and added 10 ml H<sub>3</sub>PO<sub>4</sub>, 0.2 g NaF and 1ml diphenyl-amin. Finally, the sample solution is backtitrated with 0.4N Fe (NH<sub>4</sub>)<sub>2</sub> (SO<sub>4</sub>)<sub>2</sub> 6H<sub>2</sub>O solution.

#### **2.3.2. Total Carbonate Analyses**

Total Carbonate contents were determined by a gasometric-volumetric method after a 4 M HCl treatment of the samples (Loring and Rantala, 1992). 0.02, 0.04, 0.08, 0.1, 0.15, 0.2, 0.25, 0.3 g pure CaCO<sub>3</sub> are measured to prepare a standard curve. 0.5 g sample dried and powdered samples is weighed into small vial and the vial is placed in a 250 ml flask. 10 ml HCl is added to the flask so that it has no contact with the sample. The flask is shut with a stopper and is mixed so that the sample and HCl are mixed to react. As result of this reaction, CO<sub>2</sub> is released and the volume of the evolved CO<sub>2</sub> is measured by the change of the coloured liquid in burette.

### **2.3.3. Metal Analysis by ICP-ES (Inductively Coupled Plasma Emission Mass Spectrometry)**

For the ICP-ES multi element analysis, the samples were dissolved by a total digestion involving hot HF+ HCl + HNO<sub>3</sub> acid mixture. The final solution for the analysis was in dilutes Aqua Regia (HCl-HNO<sub>3</sub>). The sample solutions were analysed for Al, Fe, Mn, S, As, Cu, Zn, Co, Ni, Na, K, V, Cr, Ba, Mo, Ca, Mg, Sr, Rb, Nb, Zr, La, Y, U, Th, Ce, Ta, Sc, Pb, Cd, Sb, Cd, Ti, Li and P using ICP-ES. The precision and accuracy of the analyses were checked by analysing international standards (CT-3 and G-2) and replicate samples (Table 2.1). They were found to be better than 10 % at 95 % significance level. The metal concentrations were normalized to Al (weight ratios) to minimize the mineralogical and grain size effects, especially the effects due to dilution by CaCO<sub>3</sub> (e.g. Loring and Rantala, 1992).



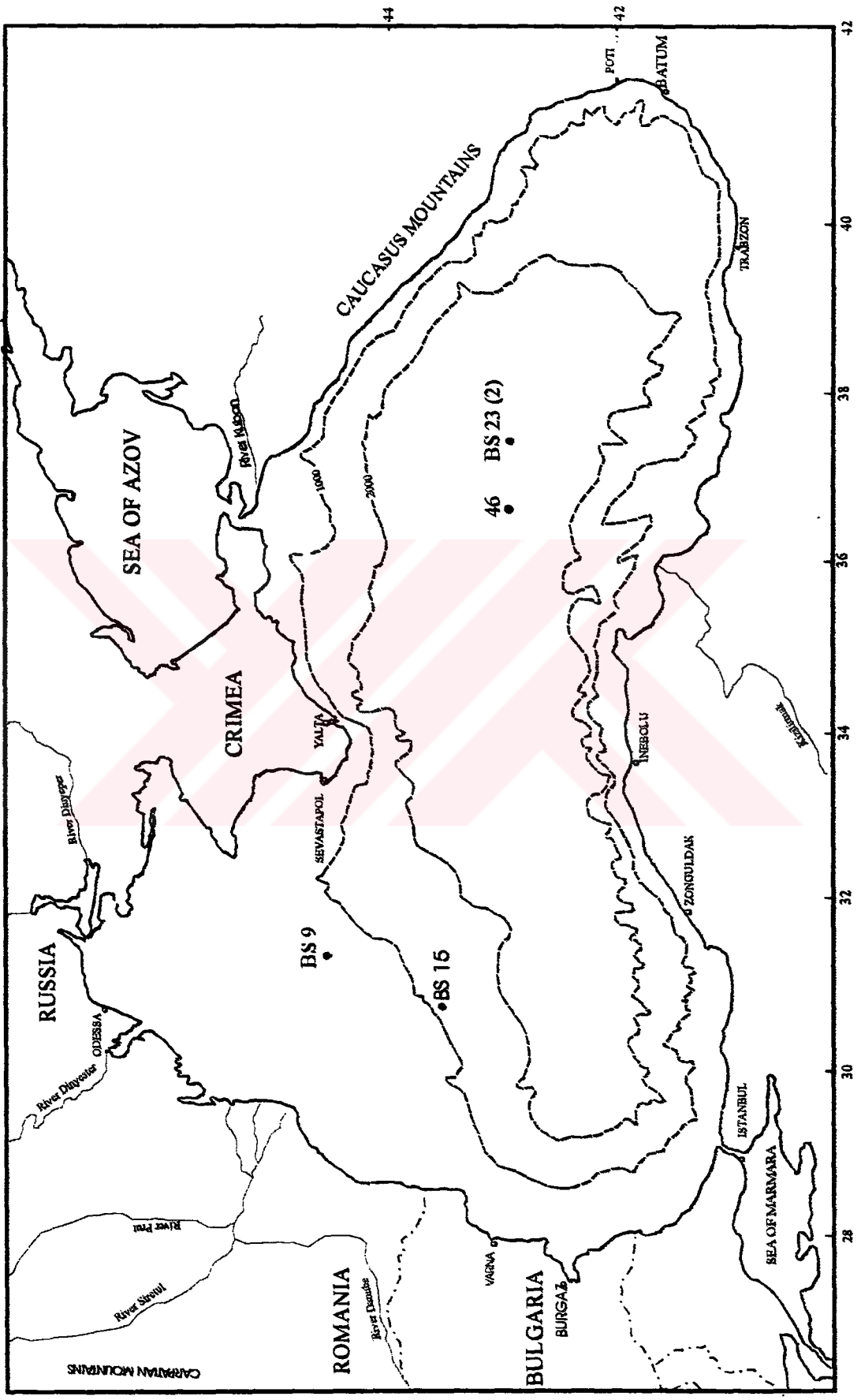


Fig 2.1. Location of the studied cores in the Black Sea basin. Isobaths in meters.

Table 2.1. Precision of the ICP metal analysis as shown by triplicate and duplicate analysis of some international standards (CT3, G-2) and Black Sea Core samples.

Ele.	Cu	Pb	Zn	Ni	Co	Mn	Fe	As	V	Ca	Mg	P	Cr	Ba	Al	S
Örn.	ppm	ppm	ppm	ppm	ppm	ppm	%	ppm	ppm	%	%	%	ppm	ppm	%	%
CT3	65	44	184	41	15	1037	3.97	58	144	1.62	0.97	.111	267	1124	7.17	<.02
CT3	64	43	182	38	14	1013	4.09	58	137	1.50	0.96	.103	263	1038	7.24	<.02
CT3	65	42	187	41	15	1048	4.03	56	140	1.53	0.97	.111	266	1049	7.32	<.02
G-2	2	21	50	10	6	826	2.47	5	59	2.72	0.74	.100	59	954	7.72	<.02
G-2	3	22	51	9	6	829	2.32	<2	59	2.84	0.69	.105	75	1051	7.90	<.02
G-2	2	21	54	8	5	788	2.48	2	59	2.71	0.72	.096	70	1002	8.11	<.02
B23 14-6	50	11	43	64	24	425	2.16	18	85	20.99	0.85	.053	32	161	2.30	1.61
B23 14-6	50	23	44	63	24	428	2.17	19	86	20.69	0.86	.052	31	162	2.32	1.60
46- 12	169	19	86	154	34	421	3.04	18	317	3.19	1.51	.110	74	114	5.80	2.01
46- 12	169	19	83	155	32	435	3.07	19	316	3.18	1.54	.112	74	109	5.50	2.02



### **3. RESULTS**

#### **3.1. General Lithological Description of the Cores**

Only two cores, BS 15 and BS 23(2) were described under microscope using preparation of smear slides. Unground, original samples of other cores ( BS 9 and 46) were not available for this study ( Fig 3.1).

In Core BS 23 (2), first 2 cm consists of a fluffy layer. Between 2 and 5 cm depth the sediment is semi-liquid, dark gray coccolithic ooze, followed downward by 23.5 cm-thick greenish-gray coloured coccolith ooze. The lower 10 cm part of the core consists of dark sapropel with an intervening coccolith ooze interval between 31.5 and 32.5 cm depth (Fig 3.1).

Core 46 consists of coccolithic ooze from the core top until 46 cm depth. It is followed downward by the sapropel unit with intervening coccolith ooze intervals at 51-55 cm, 95-105 cm and 122-123 cm depths (Fig 3.1).

The length of Core BS 9 is 53 cm ( Fig 3.1). However, the last 3 cm sapropel part of the core was not available for sampling for geochemical analyses. The top 50 cm part of this core consists of coccolithic ooze which is greenish-grey, very soft at top; soft and organic- and carbonate-rich at the base (Fig 3.1).

The top 4.5 cm of sediment in Core BS 15 consists of a fluffy layer, with green and white spots (Fig 3.1). Suspension density increases downward in the fluffy layer. The 28 cm-thick coccolithic ooze below the fluffy layer is greenish-grey with microlaminae ( brown, grey, white, dark-grey). It is semiliquid at the top and very soft , elastic, sticky, organic carbon and carbonate rich at the base.

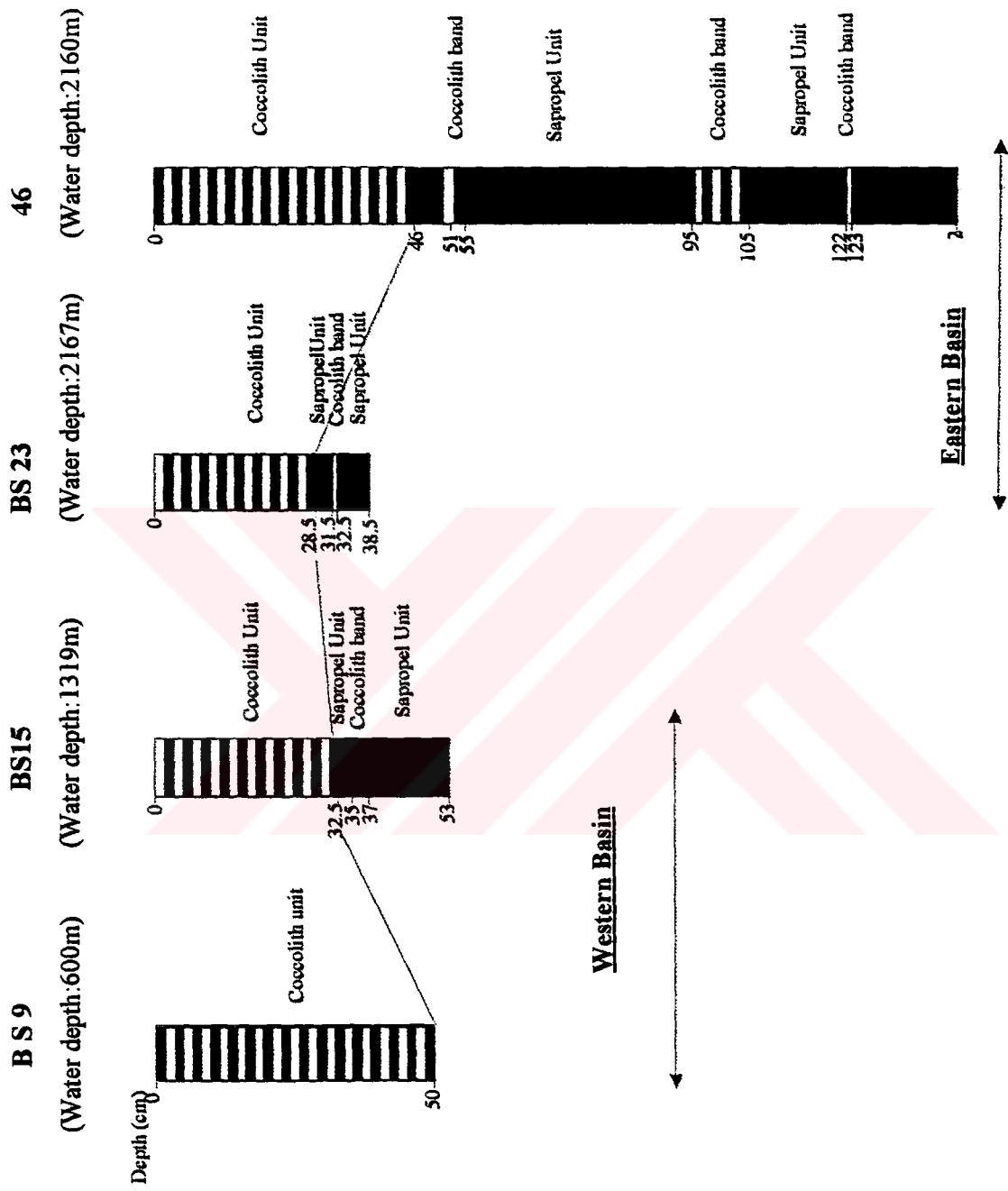


Fig 3.1. Lithological logs of studied cores from the Black Sea.

Sapropel interval in this core from 32.5 to 53 cm depth an intervening greenish gray, microlaminated coccolithic ooze between 35-37 cm depth.

## **3.2. Mineralogy and Paleontology**

### **3.2.1. Core BS 15**

The top 4 cm-thick fluffy layer in Core BS 15 consists mainly of detrital calcite, quartz and minor opaque minerals. The size of quartz is between 0.05 mm and 0.08 mm, angular, and contains about 5-10 % of total samples. Calcite is mainly of biogenic origin consisting predominantly of coccolith tests. Calcite plates of the coccolith origin are 1-2  $\mu\text{m}$  in diameter and beyond the resolution of the optical microscope. This type of calcite appears as highly birefringent very fine specs under the microscope. However, there is also some detrital calcite is present. Such detrital calcite in the fluffy layer is subrounded and constitutes about 10 % of total sample. The size of detrital calcite grains varies 0.03 and 0.05 mm. The grain size of opaque minerals is about 0.04 mm. They are subrounded and form 5 % of total samples. There is lesser amount of angular plagioclase having about 0.04 mm grain size and constituting 5 % of total sample. The grain size between 4 and 5 cm depth is smaller than the underlying part of the core. The coccolithic ooze below the fluffy layer is composed mainly of detrital calcite, quartz, opaque minerals and lesser amounts of plagioclase and chlorite. Between 5 and 32.5 cm depth, the size of quartz is between 0.06-0.1 mm, but it decreases downcore below this layer. Quartz in this interval makes up about 20 % of the sediment. Detrital calcite in this interval is subrounded, with 0.03-0.06 mm grain size, and constitutes 20 % of the sediment. The sapropelic interval of the core is 32.5 cm and 35 cm depth and contains quartz, detrital calcite, plagioclase, opaque minerals and chlorite. Quartz grain size in sapropel is smaller than that in the overlying coccolith ooze unit, ranging between 0.05 and 0.08 mm. Quartz is subangular and compose about 5-10 % of the sapropel.

The percentage of quartz mineral in the sapropel is much less than that in the coccolithic ooze. There is no significant change in the grain size of the detrital calcite, but its percentage decrease in the sapropel relative to coccolith unit. The sapropel contains 5% each of plagioclase and chlorite. The coccolithic ooze intervals between 35-37 cm contain calcite, plagioclase, quartz, chlorite and opaque minerals. The percentages of quartz and detrital calcite increase in this interval compared with the overlying unit. The grain size of quartz is about 0.05-0.1 mm. Calcite varies between 0.02 and 0.04 mm in grain size, and make up 10 % of the sediment. Plagioclase is found between 36 and 41 cm depth. There is no change in the size of opaque minerals. Biotite is present rarely at 25 cm, 31 cm and 35 cm depths.

As a result of paleontological studies, reworked and transported *Maetra subtruncata* are observed in in this core. It is observed between 4-6 cm, 14-16 cm in coccolith unit, and between 30-41 cm depth in sapropel unit. It is found in mid-salinity waters and lives about 50 m water depth, which are proofs of its reworked nature.

### 3.2.2. Core BS 23(2)

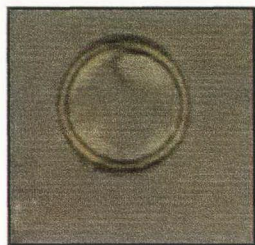
The coccolithic layer, between the core top and 28.5 cm depth contains mainly quartz, carbonate, opaque minerals, with lesser amounts of plagioclase, biotite and chlorite. Quartz consists mainly of fine silt size (30 µm) angular grains, constituting about 5 % of the sediment. The size of detrital calcite in the coccolith ooze is between 0.01 and 0.03mm. They are sub rounded and make up 10 % of the sediment. There is a sharp increase in the amount of carbonate minerals, in 10-11 cm, and 20-22 cm intervals. This increase is reflected in the carbonate analysis of Core BS 23 (2) (Fig 3.5). The 10 cm-thick sapropelic layer at the base of the core consists mainly of quartz, detrital calcite and opaque minerals. Quartz grain size is between 0.02-0.03 mm. It is subangular and forms 5-10 % of the sapropel. The size of detrital calcite grains is about 0.02-0.04 mm. They are subangular and constitute 5- 10 % of the sapropel. The amounts of quartz, detrital calcite, chlorite and biotite are considerably lower in the sapropel unit than they are in the coccolith unit.

The coccolith ooze contains mainly *Emiliana huxleyi* ,and *Scyphosphaera sp.*, and lesser amount of *Braarudosphaera bigelowi* (Fig 3.2). Coccolith unit is composed predominantly of calcitic plates of *Emiliana huxleyi* (Lohmann).

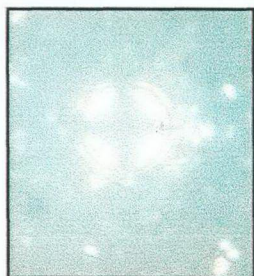
Calcite plates of the coccolith origin are 1-2  $\mu\text{m}$  in diameter and beyond the resolution of the optical microscope. This type of calcite appears as highly birefringent very fine specs under the microscope. The white layers in coccolith unit are composed almost exclusively of coccoliths of *Emiliana huxleyi* suggesting that they resulted from cyclic plankton blooms of this species. The geometry of *Emiliana huxleyi* coccoliths indicates that the Black Sea population in bottom sediment laminae is a product of annual summer blooms when the light intensity and temperature were optimal for maximum growth. The unique recording of these events in the bottom sediment is attributed to the exclusion of bottom-burrowing organisms owing to the non-oxygenated nature of the Black Sea bottom waters (Degens *et al.*, 1970, Bukry, 1974). *Braarudosphaera bigelowi* is observed between 14 and 38 cm depth. This coccolith species are found both in sapropel and coccolith units. However, its abundance increases in sapropelic levels.

The presences of Holocene coccoliths representing *Braarudosphaera bigelowi* and *Emiliana huxleyi* and the absence of certain other Holocene coccoliths from Black Sea sediment provide information on paleoecologic conditions of the Black Sea as contrasted with other bodies of water. Freshening of the Black Sea by major rivers and a restricted marine interchange at the Bosphorus help to account for present-day low surface salinities of 17-18 ‰. Open oceans average about 35 ‰.

*Braarudosphaera bigelowi* were not observed in Red Sea because of high surface salinities is 37-41 ‰. Its presence in the Black Sea is widespread, although not abundant. The assumption that *B. bigelowi* is deterred from developing in the Red Sea by high salinities is supported by evidence from living populations of other areas, the greatest concentration of these species are in coastal waters of low salinity such as the Gulf of Maine (salinity: 31.8-32.7 ‰) (Grand and Braarud, 1935; Braarud, 1963) and the Gulf of Panama (salinity: 26.8-32.5 ‰) (Smayada, 1966). The widespread occurrence of *B. bigelowi* in the Black Sea clearly indicates the ability of this species to thrive in unusually low salinities. The available information from other areas is in agreement suggesting that this species is excluded from contemporary waters of high salinity. *Scyphosphaera sp.* is observed in all levels of the core (Fig 3.2). The sediments also contain diatoms, pollens and dinoflagellates.

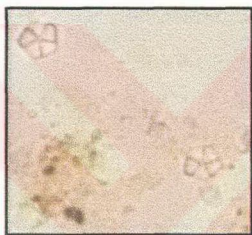


A

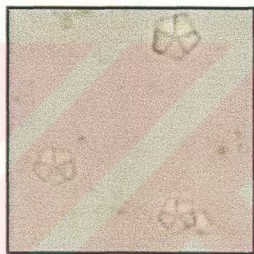


B

0 33µm



C



D

Fig 3.2. Photomicrographs of Holocene Coccoliths in Core BS 23 (2) (BF: bright field, XP: cross Polarized). Scale : The horizontal edge of the squares A and B figures are 99 µm and that of C and D figures are 130 µm. The scale bar is 33µm long.

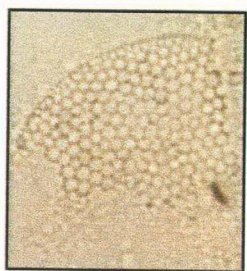
A. *Scyphosphaera* ? sp., 36-38 cm depth, BF.

B. *Scyphosphaera* ? sp., 36-38 cm depth, XP.

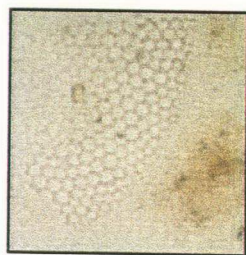
C-D. *Braarudosphaera bigelowi* (Grand and Braarud, 1935), 36-38 cm depth, XP.

The diatoms in this core are *Coscinodiscus marginatus*, *Thalassiosira* sp., *Thalassiosira oestrupi*, *Roperia* sp. (Maynard, 1974) (Fig 3.3). *Coscinodiscus marginatus* is observed in smear slides of samples, between 0-2 cm and 12-14 cm depth in the coccolith unit (Fig 3.3. A-B). *Thalassiosira oestrupi* is found between 0-9 cm depth in the coccolith unit (Fig 3.3. C-D). *Roperia* sp. is found between 3-5 cm depth in the coccolith unit (Fig 3.3. E-F). The diatoms were not observed in the sapropel units. The pollens belong to tree populations, such as coniferae (e.g., *Pinus*), *Alnus*, *Quercus*, and to step vegetation (e.g. *Chenopodiaceae*) (Fig 3.4). *Pinus* is observed at top 2 cm core and between 3-22 cm and 26-32 cm depth (Fig 3.4 B). *Alnus* is observed between 12-13 cm depth (Fig 3.4.A). The *Alnus* pollen belongs to the *glutinosa* and *incana* species, which are common in alder plots of mountain and plain areas. *Quercus* is found rarely between 24- 26 cm depth (Fig 3.4 C). *Carpinus* is observed between 2.5-3.0 cm depth and between 26-34cm depth (Fig 3.4. D). Plant pollens such as *Chenopodiaceae* are observed 4.5-5.0 cm depth of core (Fig 3.4 E). *Ostrya* is observed between 4.5-5 cm over smear slide (Fig 3.4 F).

A wide dispersal of the *Pinus* pollen in marine sediments as recorded by Koreneva (1966) may be inferred that the pollen, which is transported mostly by rivers, becomes scarcer with increasing distance off shore in comparison to pollen transported by wind. The abundance of *Alnus* (alder) pollen in Cores is probably the result of creation of more adequate environments for this tree in the Black Sea drainage area as a result of the higher sea level and higher stream base level after the late glacial maximum (Traverse, 1974; Roman, 1974)).

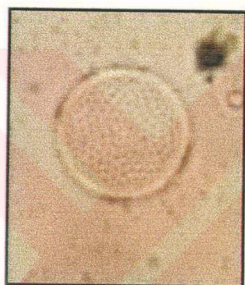


A



B

0 33μm

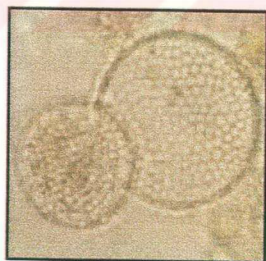


C

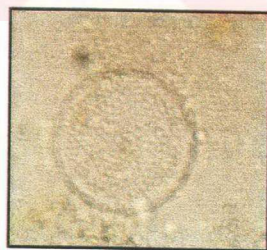


D

0 33μm



E



F

Fig 3.3. Photomicrographs of Holocene Diatoms in core BS 23 (2). Scale: The horizontal edge of the squares of each figure is 99 μm. The scale bar is 33 μm long.

A-B. *Coscinodiscus marginatus*, 1.5-2.0cm (A) and 6-7 cm (B) depths;  
C-D. *Thalassiosira* (*T. oestrupii*?), 1.5-2.0cm (C) and 6-7 cm depth;  
E-F. *Roperia* sp., 3-3,5cm, (E) and 4.5-5cm (F) depth.



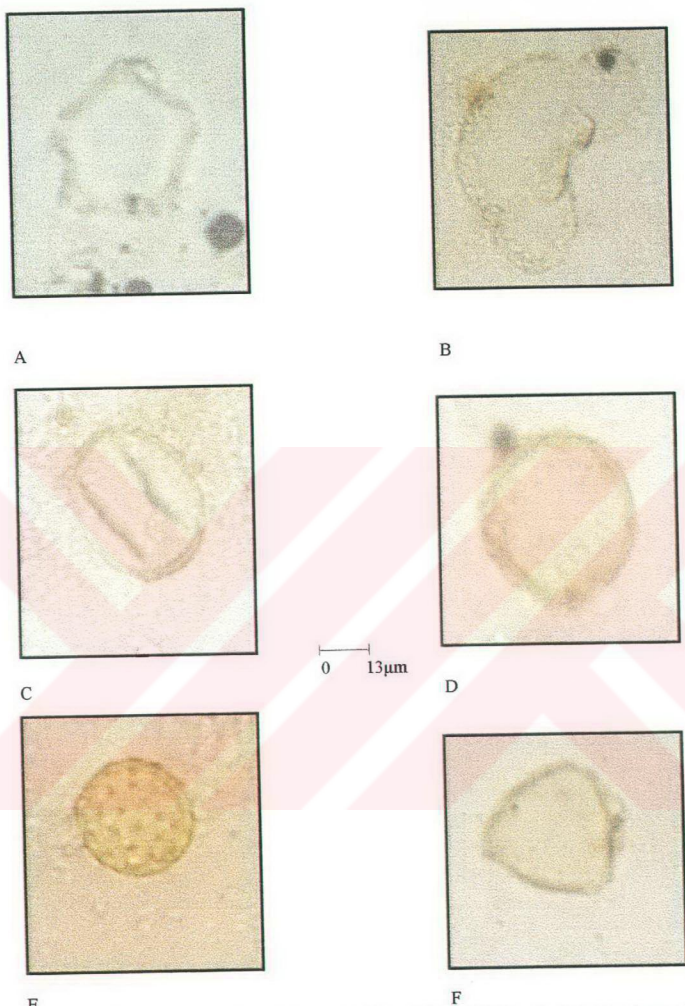


Fig 3.4. Photomicrographs of Pollen in Core BS 23 (2). Scale: The horizontal edge of A, B, C, D, E, and F figures are 26 $\mu$ m, 59 $\mu$ m, 39 $\mu$ m, 26 $\mu$ m, 26 $\mu$ m and 39 $\mu$ m, respectively. The scale bar is 13 $\mu$ m long. A. *Alnus* sp., 12-13 cm depth; B. *Pinus* sp., 20-22 cm depth; C. *Quercus* sp., 24-26cm depth; D. *Carpinus* sp., 26-28 cm depth; E. *Chenopodiacea* sp., 4.5-5.0 cm depth; F. *Ostrya* sp., 4.5-5.0 cm

### 3.3. Geochemistry

#### 3.3.1. Organic Carbon and Carbonate Contents

Organic Carbon ( $C_{org}$ ) and Carbonate profiles in Core BS 9 show a fluctuated distribution along the core depth with the maximum  $C_{org}$  and Carbonate values at 38cm depth and 20 cm depth, respectively. The  $C_{org}$  and Carbonate values in this core in the coccolith unit average 2.7 wt % and 35 wt %, ranges between 2-5 wt % and 22.5-50 wt %, respectively (Table 3.1). Organic Carbon content increases to the base of the Core in BS 9 (Fig 3.5).

The  $C_{org}$  content in the coccolith unit and in the sapropel unit averages 4.11 wt % and 7.96 wt % at Core BS 15, respectively (Fig 3.5, Table 3.1.).  $C_{org}$  content start to increase at 28 cm depth in the sapropel unit. The carbonate content in the sapropel unit at Core BS15 averages 33.15 wt %. However, the carbonate values show an enrichment in coccolith unit, with carbonate concentration of the coccolith unit being about two times as high as that of the sapropel unit. There is a carbonate peak at 10 cm depth and between 10 and 30 cm depth. Carbonate show a higher values in the coccolith unit, followed by a decrease in the sapropel unit. While the highest  $CaCO_3$  value is at 9.5 cm depth in coccolith unit, the highest  $C_{org}$  value is at 42.5 cm depth in sapropel unit.

The  $C_{org}$  content in the sapropel and coccolith units in Core 46 averages 13.05 wt % and 2.39 wt %, ranges between 12.37-14.25 wt % and 0.86-5.38 wt %. Whereas the carbonate content ranges between 3.1-28.1 wt % and 13.59-61.43 wt %, and averages 28.36 wt % and 8.0 wt %, respectively (Fig 3.5, Table 3.1). The carbonate content in coccolith and in sapropel respectively. The highest Carbonate value is at 42.5 cm depth in the coccolith unit and the highest  $C_{org}$  values are located in last 18 cm depth of the Core 46 in the sapropel unit.

The  $C_{org}$  content in the sapropel and coccolith units averages at 10.65 wt % and 4.77 wt %, and ranges between 8.14-12.2 wt % and 3.22-7.7wt % at Core BS 23 (2), respectively. (Fig 3.5, Table 3.1.) The total carbonate concentration of the coccolith and sapropel units averages 38.64 and 15.18 %, respectively.

The high carbonate contents of the coccolith unit in all core levels results mainly from the calcitic coccoliths of *Emiliana huxleyi*.

The highest carbonate values are found in the coccolith unit where the coccoliths are particularly concentrated. As in the other cores, the  $C_{org}$  content of the sapropel unit is much higher than that of the coccolith unit, whereas the total carbonate is more enriched in the latter unit.

Considering the total carbonate contents of the coccolith unit in the cores, the sites of Core BS 9 and Core 46 in the western and eastern basins respectively receives higher amount of siliclastic influx than the sites of Core BS 15 and BS 23 (2) in the western and eastern basins, respectively.

### 3.3.2. Metal Distribution

#### 3.3.2.1. Core BS 9

Aluminium normalized Mn and Fe profiles show similar downcore distribution patterns along the core. Fe/Al and Mn/Al averages 0.4 and  $83 \times 10^{-4}$  in the coccolith unit (Fig 3.6., Table 3.1, Table 3.2). These elements show distinct increase starting at 3 cm depth towards the core top.

Table 3.1. The average and range values of  $C_{org}$ ,  $CaCO_3$  and metals in sapropel and coccolith unit in Core BS 9 & BS 15 from the eastern Black Sea basin.

	Core BS 9		Core BS 15			
	Coccolith Unit		Coccolith Unit		Sapropel Unit	
	Range	Average	Range	Average	Range	Average
$C_{org}$ (%)	2-5	2.7	3.46-5.58	4.11	5.61-10.4	7.96
$CaCO_3$ (%)	22.5-50	35	56.43-81.3	66.78	26.2-37.1	33.15
Al (%)	1.0-1.99	1.4	1.6-3.8	2.9	2.9-6.41	5.2
Fe (%)	1.36-4.01	2.4	1.0-2.4	1.7	2.0-3.8	2.9
Mn (ppm)	328-493	437	338.546	444	354-520	416
Cu (ppm)	49-98	81	36-101	62	64-129	106
Zn (ppm)	46-170	81	28-183	70	52-113	85
V (ppm)	54-127	83	47-86.	64	76-154	120
Cr (ppm)	32-169	90	4-75	51	60-128	102
Sr (ppm)	179-1644	975	1159-2190	1624	525-1706	964
Mo (ppm)	4-88	33	7-34	13	32-89	61
Ba (ppm)	332-1362	623	285-1815	551	1016-2089	1689
Ni (ppm)	4-60	10	6-65	15	58-84	75
Co (ppm)	2-20.	3	2-20	4	2-32	23
Sc (ppm)	4.5-18	10	4-8	7	8-14	12
As (ppm)	20-24	21	20	20	20	20
Sb (ppm)	20-24	21	28-33	23	30	30
Pb (ppm)	20-24	21	30-274	43	30	30

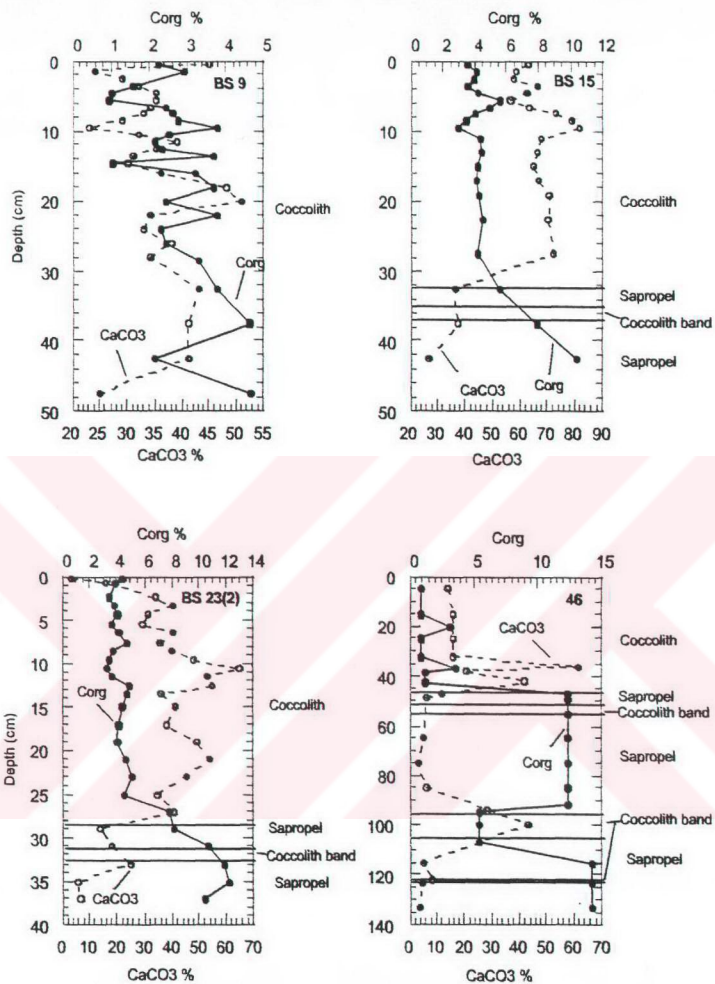


Fig 3.5. Concentration/ depth profiles of  $C_{org}$  (wt %) and total carbonate (wt %)  $CaCO_3$  in the Core BS 9, BS 15, BS 23 (2) and 46.

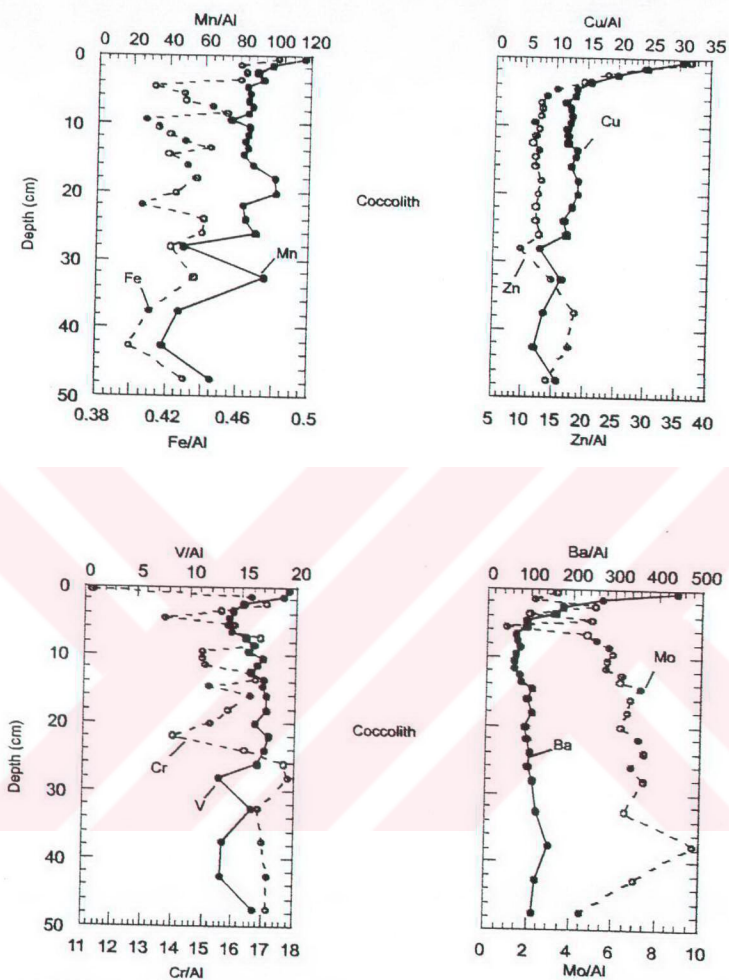


Fig 3.6. Concentration /depth profiles of Mn, Fe, Cu, Zn, V, Cr, Ba, and Mo in Core BS 9. All metal data are as weight ratios to Al ( $\times 10^{-4}$ ), except for Fe ( $\times 1$ ).

Chalcophile elements, such as Pb, Cu, Zn, As and Sb also display a similar, but much sharper trend in top 3 cm depth (Fig 3.6, Fig 3.7, Table 3.1, Table 3.2, Table 3.5).

Ba/Al display an increase from  $268 \times 10^{-4}$  to  $441 \times 10^{-4}$  at top 3 cm depth (Fig 3.6., Table 3.5). Mo /Al average  $6 \times 10^{-4}$  in the coccolith unit, reaching a maximum content at 37.5 cm core depth (Fig 3.6, Table 3.1, Table 3.2, Table 3.5). Ni/Al and Co/Al averages  $1.5 \times 10^{-4}$  and  $0.5 \times 10^{-4}$  in the coccolith unit. They show increase in the top 3 cm of the core, but their increase is smaller than that of Pb/Al, Cu/Al, Zn/Al, As/Al and Ba/Al (Fig 3.6, Fig 3.7., Table 3.5). The behaviour of Sr in general is similar to that of Ca. Sr/Al averages  $210 \times 10^{-4}$ , it shows elevated values in first 3 cm of the core (Fig 3.7, Table 3.1, Table 3.2, Table 3.5).

V/Al and Cr/Al show different trends in top of the core (Fig 3.6, Table 3.5). V increases, whereas Cr decreases at top 3 cm interval of the core. Sc/Al averages  $1.6 \times 10^{-4}$  in the coccolith unit (Fig 3.7, Table 3.1, Table 3.2, Table 3.5). It has a uniform profile along the core depth in the coccolith unit.

Table 3.2. The average and range values of Corg, CaCO<sub>3</sub> and /Al normalized metal values in sapropel and coccolith units in Cores BS 9 & BS 15 from the eastern Black Sea basin. Metal/Al ratios should be multiplied by 10<sup>-4</sup>, except for Fe/Al which the factor is 1.

	Core BS 9		Core BS 15			
	Coccolith Unit		Coccolith Unit		Sapropel Unit	
	Range	Average	Range	Average	Range	Average
Corg (%)	2-5	2.7	3.46-5.58	4.11	5.61-10.4	7.96
CaCO <sub>3</sub> (%)	22.5-50	35	56.43-81.3	66.78	26.2-37.1	33.15
Fe/Al	0.4-0.5	0.43	0.6-1	0.6	0.4-0.7	0.6
Mn/Al	116-37	83	131-213	154	55-150	89
Cu/Al	7-31	13	18-33	23	19-22	21
Zn/Al	11-37	15	18-61	23	15-18	17
V/Al	13-19	16	19-31	23	22-27	24
Cr/Al	14-17	16	3-21	16	17-21	20
Sr/Al	18-544	210	334-1377	588	82-591	240
Mo/Al	1-7	6	2-14	4.5	7-13	12
Ba/Al	63-441	119	101-601	205	295-352	328
Ni/Al	1-6	1.5	2-27	6	13-20	15
Co/Al	1-2	0.5	0.5-10	2	0.3-9	5
Sc/Al	1.5-2	1.6	2-3	2.4	2-3	2
As/Al	2-8	4	5-13	7	3-7	4
Sb/Al	3.1-11.99	6	8-19	11	5-10	6
Pb/Al	3.1-11.99	6	91-8	16	5-10	6

Table 3.5. Chemical composition of the sediments in Core BS 9 from the western basin.

Range (cm)	C <sub>org</sub> (%)	CaCO <sub>3</sub> (%)	Al (%)	Fe (%)	Cu (ppm)	Mn (ppm)	Cr (ppm)	Sr (ppm)	Ba (ppm)	Zn (ppm)	V (ppm)	Ni (ppm)	Sc (ppm)	Co (ppm)	Mo (ppm)	As (ppm)	Sb (ppm)	Pb (ppm)
0-1	2.22	45	1.95	1.36	86	328	32	1541	1249	104	54	4.5	5	2	9	23	23	23
1-2	2.92	24	1.94	1.74	93	369	62	907	1012	110	70	4.2	6	2	8	21	21	21
2-3	-	29	1.99	2.27	98	440	84	859	859	114	73	4.1	8	2	24	20	20	20
3-4	1.55	32	1.54	2.09	70	421	70	1084	713	88	64	4.4	7	2	9	22	22	22
4-5	1.02	35	1.25	1.92	61	389	63	1119	421	70	63	4.0	8	2	22	20	20	20
5-6	0.93	35	1.41	2.15	65	429	80	1110	452	67	67	4.3	9	2	4	22	22	22
6-7	2.42	34	1.32	2.34	63	462	86	1107	363	67	76	4.2	8	2	25	21	21	21
7-8	2.59	33	1.31	2.34	64	457	88	1060	376	66	80	4.1	10	2	27	21	22	21
8-9	2.74	29	1.42	2.58	71	486	95	921	435	71	91	4.0	10	2	32	20	20	20
9-10	3.76	23	1.63	2.68	80	491	98	753	436	76	102	4.1	12	2	39	20	20	20
10-11	2.51	32	1.27	2.16	61	444	77	1282	337	63	88	4.2	11	2	29	21	21	21
11-12	2.11	39	1.41	2.20	63	444	78	1251	332	61	85	4.5	9	2	29	22	22	22
12-13	2.34	35	1.34	2.43	68	471	93	1165	429	64	89	3.9	10	2	36	20	20	20
13-14	3.66	31	1.89	2.58	78	493	97	1058	468	70	100	4.9	12	2	36	24	24	24
14-15	1.06	30	1.46	2.39	74	466	86	990	594	67	96	3.9	10	2	41	20	20	20
15-17	3.18	36	1.29	2.27	65	464	87	1166	491	61	91	3.9	10	2	36	20	20	20
17-19	3.66	48	1.28	1.87	59	428	67	1548	457	54	74	4.3	9	2	28	22	22	22
19-21	2.42	51	1.03	1.61	52	386	58	1644	342	46	62	3.9	8	2	24	20	20	20
21-23	3.77	34	1.38	2.24	69	454	77	1083	524	65	97	3.9	12	2	40	20	20	20
23-25	2.29	33	1.26	2.39	63	456	89	1058	560	65	93	4.0	10	2	40	20	20	20
25-27	2.41	38	1.27	2.33	64	478	94	1233	524	66	88	3.9	10	2	36	19	20	20
27-30	3.27	34	1.46	4.01	72	471	169	179	1023	90	121	60	18	20	70	20	20	20
30-35	3.76	43	1.00	1.90	49	411	73	1206	511	63	69	4	8	2	29	20	20	20
35-40	4.64	41	1.52	3.73	76	424	154	188	1362	166	120	58	18	20	88	20	20	20
40-45	2.13	41	1.34	3.89	67	365	167	177	1151	169	127	56	18	2	69	20	20	20
45-50	4.66	25	1.59	2.93	73	442	116	789	767	95	110	4	13	2	31	22	22	22

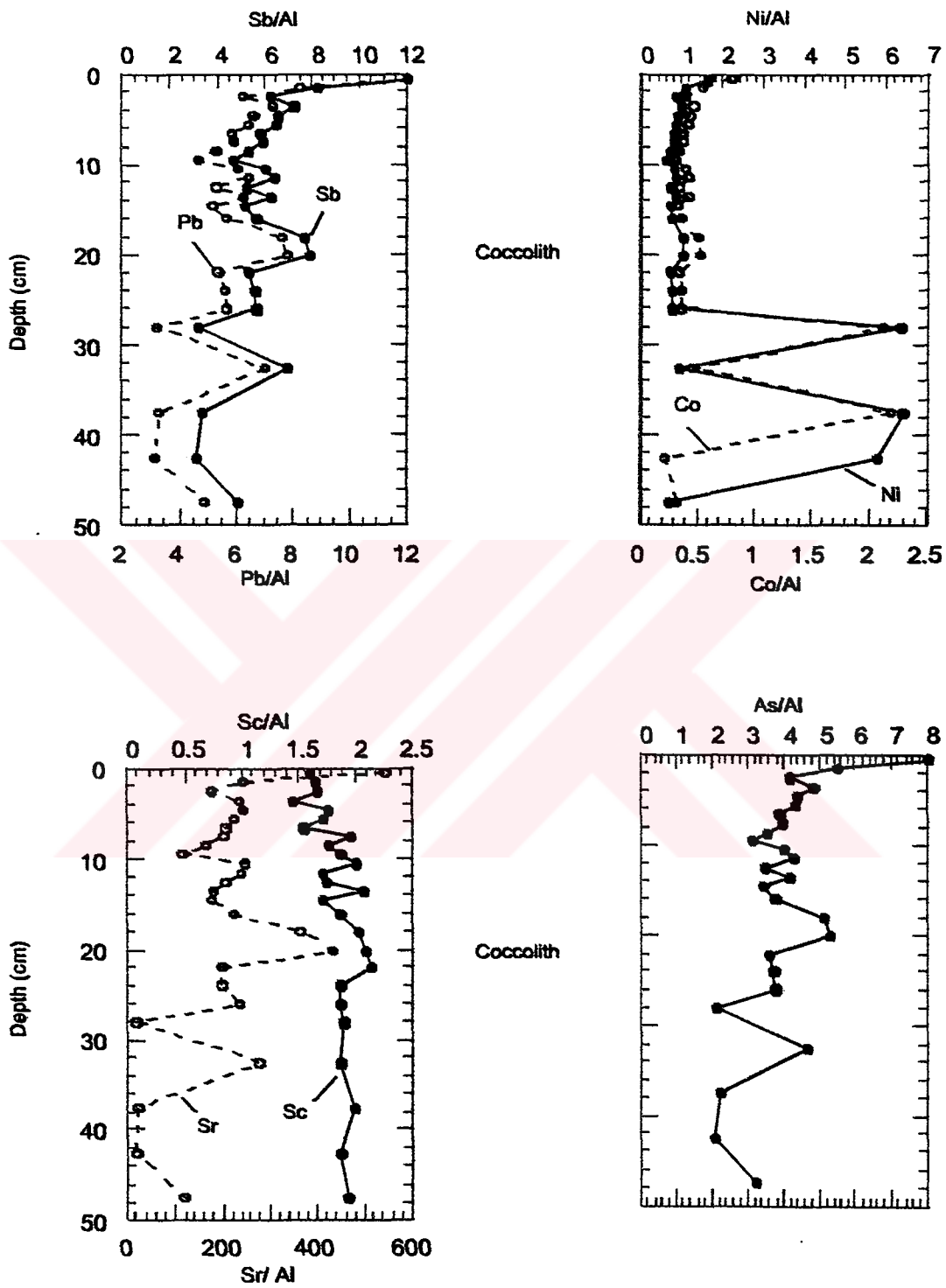


Fig 3.7. Concentration /depth profiles of Sb, Pb, Co, Ni, Sc, Sr, and As in Core BS 9  
 All metal data are as weight ratios to Al ( $\times 10^{-4}$ ).



### 3.3.2.2. Core BS 15

Aluminium normalized values of Mn and Fe demonstrate broadly similar profiles to each other and average  $89 \times 10^{-4}$  and 0.6 in the sapropel unit, respectively (Fig 3.8, Table 3.1, Table 3.2). Mn/Al show significant enrichment between 10-11 cm depth and gradual depletion in the sapropel unit. There is no Mn/Al peak just above the sapropel unit. The gradual increase of Fe/Al occur between 27.5-32.5 cm depth, followed by a gradual decrease to the base of the core. Fe/Al and Mn/Al shows a depletion in the sapropel unit relative to coccolith unit.

Aluminium normalized Pb, Cu and Zn average  $6 \times 10^{-4}$ ,  $21 \times 10^{-4}$  and  $17 \times 10^{-4}$  sapropel unit, respectively (Table 3.1). The values sharply increase in the top 2 cm, followed by a uniform profile along the rest of the core (Fig 3.8, Fig 3.9, Table 3.3). However, Cu/Al shows a slightly depletion in the sapropel compared to the coccolith unit. There is a small Pb/Al peak at 11 cm core depth in the coccolith unit (Fig 3.9).

As/Al and Sb/Al profiles are similar (Fig 3.9). They show a depletion in the sapropel unit and slight increase at top 4 cm of the core (Fig 3.9, Table 3.3). The profiles form a peak at 11 cm depth.

Aluminium normalized Sr profiles is similar to those of As and Sb, except for a more pronounced depletion in the sapropel unit (Fig 3.9).

Ba/Al and Mo/Al averages  $328 \times 10^{-4}$  and  $13 \times 10^{-4}$  in the sapropel unit. Ba/Al values show very sharp increase from 4 cm depth to the top of the core. The Ba /Al values increase gradually with depth from 4 cm depth (Fig 3.8, Table 3.1, Table 3.3). Ba and Mo are more enriched in the sapropel unit than in the coccolith unit.

Ni/Al range between  $13-20 \times 10^{-4}$  and Co/Al range between  $0.3-9 \times 10^{-4}$  in the sapropel unit (Table 3.1). Ni/Al and Co/Al gradually increase in the sapropel unit, forming peaks at depths of 17 cm and 27.5 cm in the coccolith unit (Fig 3.9). Unlike from Pb/Al, As/Al, Zn/Al, Cu/Al and Ba/Al, these elements show no enrichment at top 4 cm of the core.

Sc/Al average  $2 \times 10^{-4}$  in the sapropel unit. Sc/Al exhibit a depletion in the sapropel unit compared to the coccolith unit.

Table 3.6. Chemical composition of sediments in Core BS 15 from the western basin.

Range (cm)	C <sub>org</sub> (%)	CaCO <sub>3</sub> (%)	Al (%)	Fe (%)	Cu (ppm)	Mn (ppm)	Cr (ppm)	Sr (ppm)	Ba (ppm)	Zn (ppm)	V (ppm)	Ni (ppm)	Sc (ppm)	Co (ppm)	Mo (ppm)	As (ppm)	Sb (ppm)	Pb (ppm)
0-1	3.51	62.75	3.02	1.91	101	435	62	1159	1815	183	70	6	6	2	8	20	30	274
1-2	4.05	58.41	3.11	1.79	58	425	58	1430	514	109	57	6	6	2	7	19	28	28
2-3	3.93	57.32	3.69	2.12	65	484	71	1279	397	91	71	6	8	2	8	20	30	30
3-4	3.51	65.98	3.80	2.26	73	512	75	1270	397	85	77	6	8	2	8	20	30	30
4-5	4.15	62.16	3.01	1.78	67	440	43	1587	306	67	63	6	6	2	8	20	31	31
5-6	5.58	56.43	3.24	2.06	73	489	63	1455	400	69	67	6	6	2	8	20	30	30
6-7	4.91	62.94	3.48	2.35	87	546	71	1310	565	87	81	6	8	2	8	20	30	30
7-8	3.98	72.83	3.09	2.00	72	480	60	1482	504	62	68	6	6	2	8	20	30	30
8-9	3.46	78.51	2.20	1.44	56	396	36	1875	423	56	54	6	6	2	8	20	30	30
9-10	2.94	81.32	1.97	1.11	42	346	26	2042	507	38	50	6	6	2	8	20	30	30
10-12	4.35	67.41	1.59	1.01	36	338	4	2190	285	28	46	6	4	2	8	20	30	30
12-14	4.45	65.99	2.705	1.72	61	424	51	1718	483	51	73	6	8	2	8	20	30	30
14-16	4.20	64.63	2.89	1.88	66	447	60	1698	596	54	78	6	8	2	8	20	30	30
16-18	4.05	66.37	3.07	1.96	64	465	60	1679	509	56	86	54	8	20	24	20	30	30
18-20	4.23	70.50	2.92	2.07	60	478	58	1719	486	56	69	47	7	2	27	22	33	33
20-25	4.48	69.89	2.56	1.73	60	419	32	1881	603	46	63	6	6	2	8	20	30	30
25-30	4.13	71.89	2.44	1.74	63	414	38	1834	574	44	75	65	8	24	36	20	30	30
30-35	5.61	36.13	2.89	2.05	64	433	60	1706	1016	52	76	58	8	26	32	20	30	30
35-40	7.87	37.06	6.09	3.82	117	520	128	773	2067	95	132	77	12	32	57	20	30	30
40-45	10.40	26.26	5.36	3.14	111	356	109	853	1583	79	119	80	12	32	68	20	30	30
45-50	-	-	6.41	2.76	129	354	109	525	2090	113	153	84	14	2	89	20	30	30

V/Al and Cr/Al values are higher in sapropel unit than those in coccolith unit (Fig 3.8). They average about  $24 \times 10^{-4}$  and  $20 \times 10^{-4}$  in sapropel, respectively. (Table 3.3) These elements show a slight increase in top 2 cm of the core.

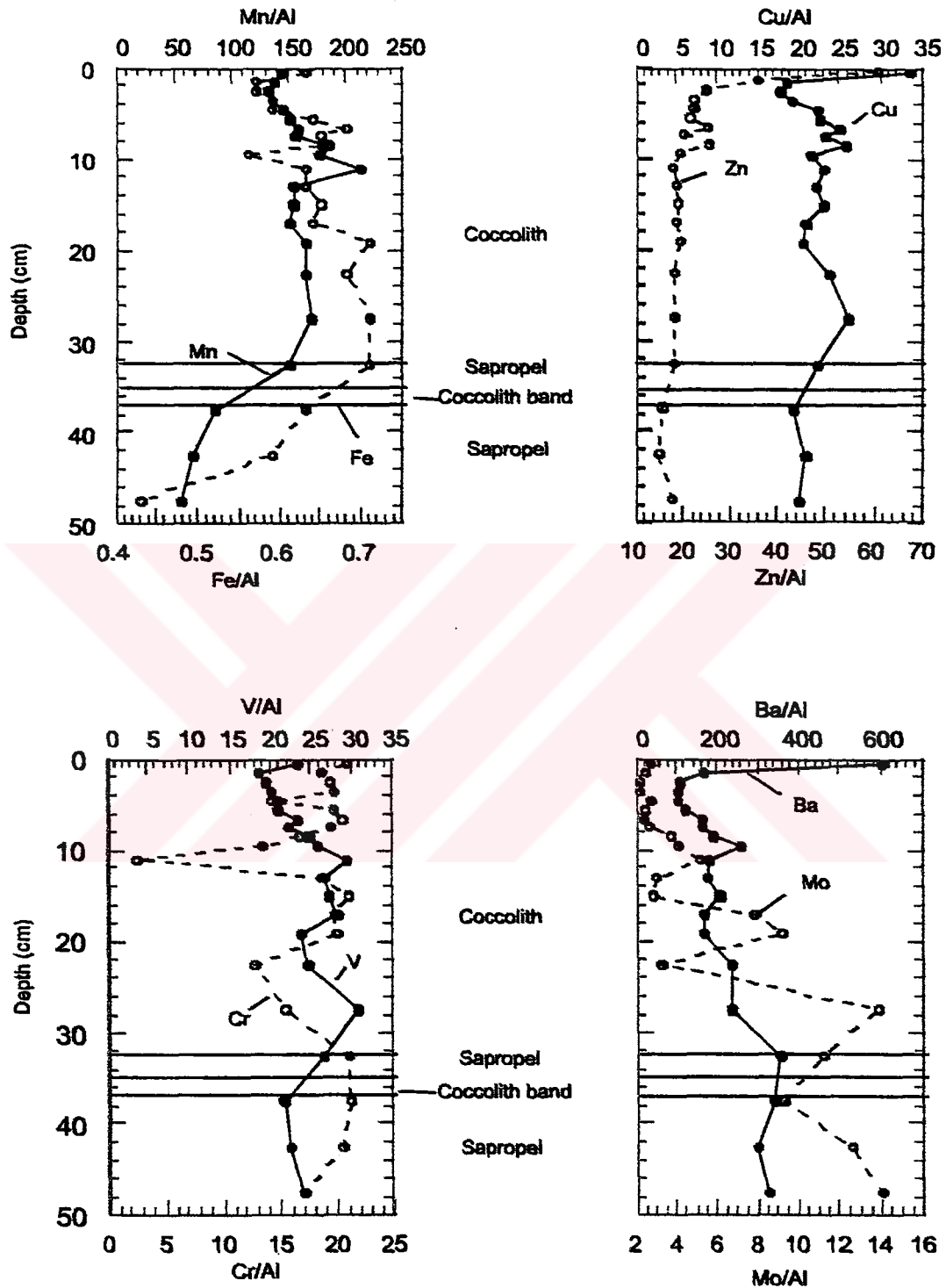


Fig 3.8. Concentration / depth profiles of Mn, Fe, Cu, Zn, V, Cr, Ba and Mo in Core BS 15. All metal data are as weight ratios to Al ( $\times 10^{-4}$ ), except for Fe ( $\times 1$ ).

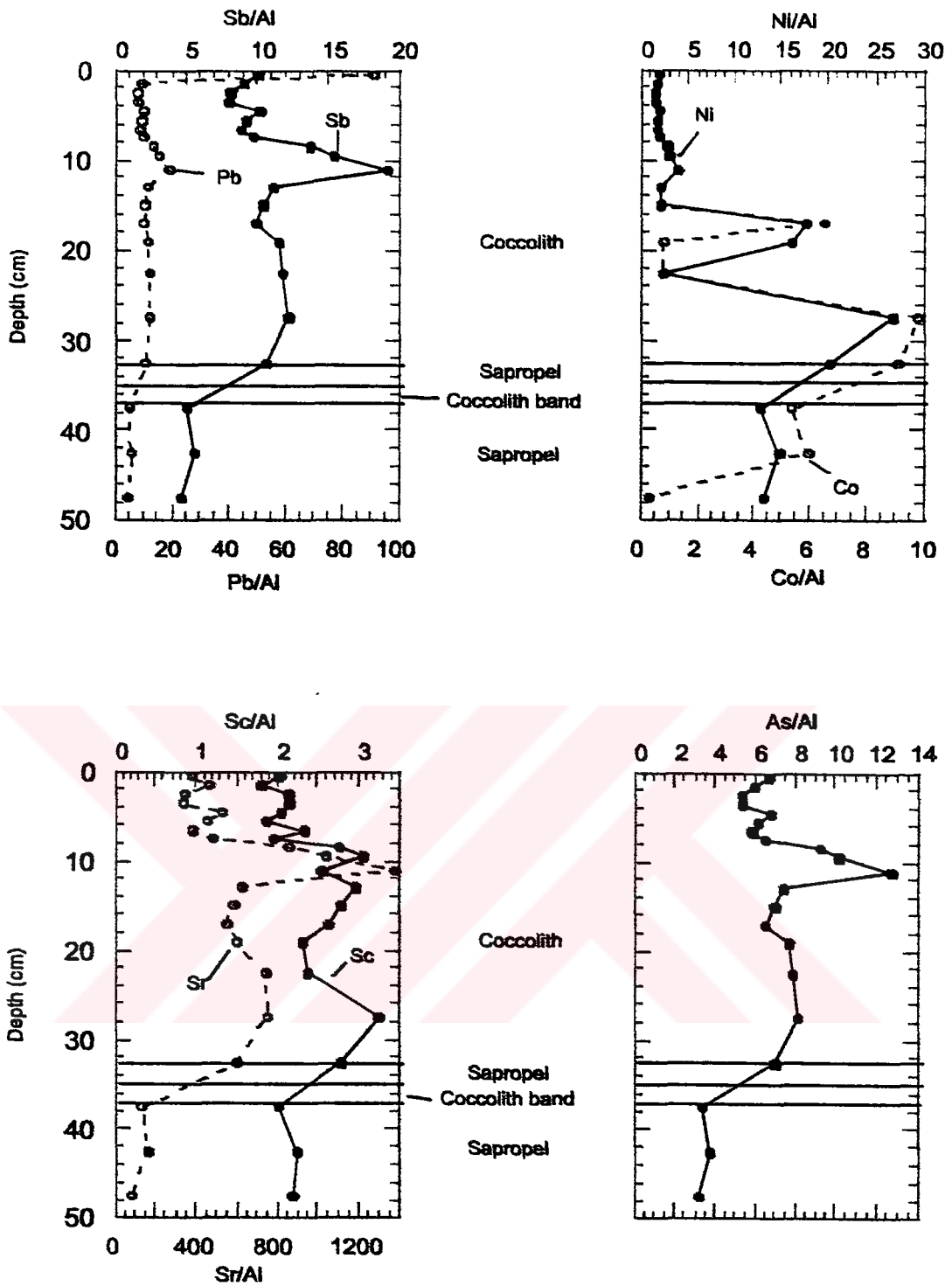


Fig 3.9. Concentration / depth profiles of Sb, Pb, Ni, Co, Sc, Sr and As in Core BS 15. All metal data are as weight ratios to Al ( $\times 10^{-4}$ ).

### 3.3.2.3. Core BS 23 (2)

Fe/Al and Mn/Al indicate elevated values in the coccolith unit relative to the sapropel unit (Fig 3.10, Table 3.3, Table 3.4, Table 3.7). Fe/Al and Mn/Al average 0.6 and  $84 \times 10^{-4}$  in sapropel unit, respectively whereas the same averages are 0.9 and  $178 \times 10^{-4}$  in the coccolith unit (Table 3.3). Compared to Fe/Al, Mn/Al show more relative depletion in the sapropel unit. Maximum values of Mn/Al and Fe/Al are observed between 10-12 cm depth interval, where there is also a total carbonate peak. The second Fe/Al peak is at 34 cm depth where Corg values are the highest in sapropel (Table 3.7).

As/Al and S/Al exhibit very similar profiles to each other and to that of Fe/Al (Fig 3.10). They average  $6 \times 10^{-4}$  and 0.6 in sapropel unit and  $9 \times 10^{-4}$  and  $0.7 \times 10^{-4}$  in the coccolith unit (Table 3.4). As and S peaks occur at the 11 cm and 33 cm depth in the coccolith unit (Table 3.7).

Cu/Al and Zn/Al profiles match in the coccolith unit, but differ in the sapropel unit (Fig 3.10). These elements sharply increase towards the core top starting at 4 cm depth (Table 3.7). Cu/Al exhibit elevated values in the latter unit, whereas Zn/Al values are uniform, being similar to those in the coccolith unit (Fig 3.10). Cu/Al has a peak at 35 cm in sapropel where there is also a Corg peak (Fig 3.5, Fig 3.10, Table 3.7). Pb/Al, Zn/Al, Cd/Al, and Sb/Al sharply increase in the top 4 cm of the core (Fig 3.10, Table 3.7). Pb/Al also show a depletion in the sapropel compared to the coccolith unit. Cd/Al profile show a slight enrichment in the sapropel unit. Sb/Al averages  $0.8 \times 10^{-4}$  in the coccolith and  $1 \times 10^{-4}$  in the sapropel unit (Table 3.4).

Ni/Al and Co/Al average  $32 \times 10^{-4}$  and  $10 \times 10^{-4}$  in the sapropel unit. They gradually increase downcore in the coccolith unit, forming a peak between 22-26 cm interval (Table 3.3, Table 3.4, Fig 3.11). Both profiles are similar to that of Fe/Al in the sapropel unit, having relatively high values in the upper part of the unit and low values near the base of the core. In contrast to Ni/Al, the average of Co/Al in the sapropel unit is lower than that in the coccolith unit.

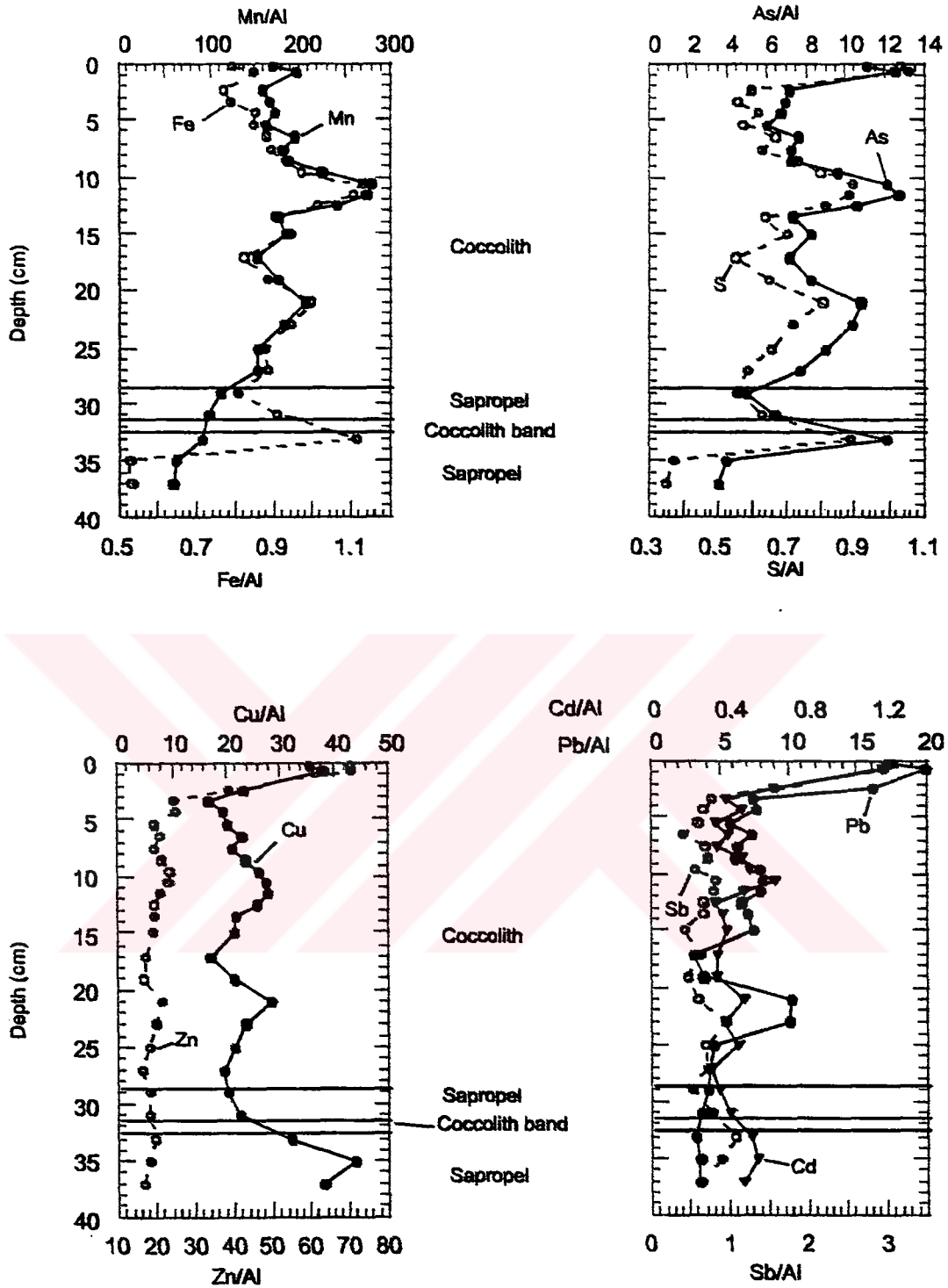


Fig 3.10. Concentration / depth profiles of Mn, Fe, As, S, Cu, Zn, Cd, Pb, and Sb in Core BS 23 (2). All metal data are as weight ratios to Al( $\times 10^{-4}$ ), except for Fe and S (x1).

Table 3.3. The range and average values of  $C_{org}$ ,  $CaCO_3$  and metals in sapropel and coccolith unit in Cores BS23 (2) & 46 from the eastern Black Sea basin.

	CORE BS23 (2)				CORE 46			
	Coccolith Unit		Sapropel Unit		Coccolith Unit		Sapropel Unit	
	Range	Average	Range	Average	Range	Average	Range	Average
Corg (%)	3.22-7.71	4.77	10.41-10.8	10.65	0.86-5.38	2.39	12.37-14.25	13.05
CaCO <sub>3</sub> (%)	3-65	38.64	5.8-24.6	15.18	3-65	38.64	5.8-24.6	15.18
Al (%)	1.2-3.7	2.4	4.6-5.7	5.1	2.4-7.2	5.4	4-7.4	5.3
Fe (%)	1.2-4.2	2.2	2.4-4.9	3.6	1.8-4.5	3.6	2.5-4.3	3.0
S (%)	1.1-3.3	1.7	1.7-3.4	2.5	1.1-1.8	1.4	1.2-2.7	2.1
Mg (%)	0.6-1.4	0.9	1.5-1.7	1.6	0.8-2.6	1.9	1.1-2	1.5
Na (%)	1.9-11.6	3.8	2.7-4.6	3.6	1.4-1.8	1.6	1.7-3.1	2.6
K (%)	0.4-1.2	0.8	1.5-1.7	1.6	0.7-1.8	1.4	1.2-2.1	1.5
P (%)	0.05-0.08	0.06	0.08-0.1	0.09	0.06-0.07	0.06	0.07-0.1	0.098
Ti (%)	0.05-0.16	0.01	0.2-0.23	0.2	0.1-0.4	0.2	0.2-0.3	0.2
Mo (ppm)	18-85	33	74-108	92	6.7-46.2	22	46-197	117
Cu (ppm)	34-119	53	15-202	155	44-66	40	46-197	154
Pb (ppm)	8-41	18	16-23	19	9-25	16	14-21	18
Zn (ppm)	26-115	55	80-103	90	36-81	66	66-108	80
Ni (ppm)	37-129	64	126-138	133	69-169	119	128-189	155
Co (ppm)	14-70	32	21-61	39	27-41	33	22-39	32
Mn (ppm)	264-544	373	284-630	431	403-834	623	255-787	405
As (ppm)	15-45	20	17-34	24	14-20	17	14-28	19
U (ppm)	3-21	15	12-18	14	2-13	7	6-16	12
Th (ppm)	2-5	4	6-7	7	4-8	7	5-7	6
Sr (ppm)	504-1474	1023	317-432	371	251-1127	476	159-546	260
Cd (ppm)	0.5-2	1	2-3	2	0.2-1	0.5	0.4-1.9	1
Sb (ppm)	1-5	2	3-4	4	1-2	1	1-4	3
V (ppm)	55-197	87	185-317	260	89-135	124	116-336	290
Ca (%)	9.9-27.8	19	5-8	6	5.79-21.3	12	2.07-11.2	4
La (ppm)	8-16	13	17-21	19	12-23	20	13-21	16
Cr (ppm)	17-51	30	62-78	70	39-167	116	62-131	77
Ba (ppm)	126-333	199	304-418	360	144-337	251	78-189	131
Zr (ppm)	14-35.4	21	47-49	48	25.5-68.5	49	31.4-48.5	39
Ce (ppm)	13-27	22	29-36	33	21-40	34	25-33	28
Y (ppm)	10-18	13	19-21	20	12.7-16.7	15	11.5-17.6	15
Nb (ppm)	1-4	2	4-5	5	2.4-7.7	6	3.5-6.2	4
Ta (ppm)	0.3-0.9	0.5	1.1-1.3	1	0.6-1.8	1	0.8-1.6	1
Sc (ppm)	3-9	5	12	12	5-16	12	9-13	11
Li (ppm)	9-28	17	35-42	39	28-49	37	28-50	37
Rb (ppm)	20-61	38	76-91	84	38-102	80	64-106	82

Table 3.4. The range and average values of Corg, CaCO<sub>3</sub> and metal/Al ratios in sapropel and coccolith unit in Cores BS23 (2) & 46 from the eastern Black Sea basin.

	CORE 46				CORE BS23 (2)			
	Coccolith Unit		Sapropel Unit		Coccolith Unit		Sapropel Unit	
	Range	Average	Range	Average	Range	Average	Range	Average
Corg (%)	0.86-5.38	2.39	12.37-14.25	13.05	3.22-7.71	4.77	10.41-10.8	10.65
CaCO <sub>3</sub> (%)	4.6-61	40.65	3.2-28	8.04	3-65	38.64	5.8-24.6	15.18
Fe /Al	0.60-0.76	0.64	0.48-0.63	0.56	0.79-1.3	0.9	0.53-1.16	0.595
S /Al	0.16-0.53	0.30	0.22-0.57	0.39	0.55-1.05	0.72	0.37-0.88	0.56
Mg /Al	0.24-0.37	0.30	0.27-0.35	0.28	0.32-0.89	0.4	0.28-0.36	0.32
Na /Al	0.21-0.64	0.40	0.3-0.67	0.53	0.76-7.14	1.79	0.5-1.0	0.75
K/Al	0.25-0.31	0.28	0.27-0.31	0.29	0.32-0.5	0.34	0.30-0.34	0.32
P /Al	0.01-0.02	0.014	0.01-0.03	0.041	0.017-0.04	0.026	0.013-0.02	0.018
Ti /Al	0.04-0.06	0.05	0.04-0.06	0.045	0.04-0.044	0.041	0.038-0.04	0.039
Mo/Al	1-26	11	14-36	24	8-22	14	13-24	19
Cu /Al	6-33	17	8-41	32	17-38	24	20-44	31
Pb/Al	2-4	3	3-4	4	3-20	8	3-4	4
Zn /Al	11-22	14	12-18.	17	16-71	25	17-19	18
Ni /Al	21-30	25	23-36	30	20-39	27	22-35	32
Co /Al	4-11	7	4-8	6	8-19	11	4-19	10
Mn /Al	76-132	102	55-131	72	151-278	178	59-110	84
As /Al	2-7	4	2-4	4	6-13	9	4-12	6
U /Al	1-5	2	1-3	2	2-13	7	2-5	3
Th /Al	1-2	2	0.9-1	1	1-2	2	1	1
Sr /Al	35-472	108	33-137	52	13-1169	463	65-81	85
Cd /Al	0.03-0.4	0.2	0.1-0.4	0.3	0.3-0.7	0.5	0.4-0.5	0.5
Sb /Al	0.1-0.5	0.3	0.4-1	0.5	0.4-3	0.8	1	1
V /Al	19-57	31	21-70	55	25-46	38	32-69	52
Ca /Al	1-4	2	0.4-3	1	4-22	9	1-2.7	2
La /Al	3-5	4	3-4	3	5-7	6	4-4.3	4
Cr /Al	14-24	17	13-24	14	13-15	14	13-14	14
Ba /Al	25-102	42	17-35	24	45-227	98	63-78	71
Zr /Al	7-11	9	7-9	8	8-11	10	8-10	9
Ce /Al	5-9	6	5-8	6	8-11	9	6-7	7
Y /Al	2-5	3	2-3	3	4-9	6	3-5	4
Nb /Al	1	1	0.7-1.11	1	1-1.4	1	0.9-1	1
Ta /Al	0.18-0.26	0.2	0.2-0.3	0.1	0.1-0.3	0.2	0.2-0.3	0.2
Sc /Al	2-2.2	2	2	2	2	2.	2-3	2
Li /Al	6-8	7	6-7.63	7	6-8	7	7-8	8
Rb /Al	13-17	18	14-17	15	15-17	16	16-17	16



Ba/Al, P/Al and Mo/Al profiles is similar to each other and to that of As, S and Fe (Fig 3.10, Fig 3.11, Table 3.3, Table 3.4). Ba/Al and P/Al show a depletion, but Mo/Al show an enrichment in the sapropel unit. Ba/Al, Mo/Al and P/Al increase in the top 1 cm depth and show peaks between 10-12 cm and 20-22cm interval (Table 3.7).

The distributions of U/Al and Th/Al are in general similar to each other along the core depth (Fig 3.11). They display lower values in the sapropel than in the coccolith units. The average of these two elements are  $3 \times 10^{-4}$  and  $1 \times 10^{-4}$  in the sapropel unit (Table 3.4). The U/Al peaks occur at 11cm depth and 22 cm depth, whereas Th/Al peaks are found at 13.5 cm and 19 cm depth in the coccolith unit (Table 3.7).

V/Al exhibits elevated values in top 1 cm of the core, and in 10-13 cm and 20-22 cm intervals in the coccolith unit (Fig 3.11, Table 3.7). This ratio display a relative enrichment in the sapropel unit, reaching the maximum at 35 cm. Cr/Al demonstrates more erratic profile with a significant enrichment in the top 4 cm and at 17 cm depths. The average of Cr/Al in sapropel is lower than that in coccolith unit.

Sr/Al averages  $463 \times 10^{-4}$  in the coccolith and  $85 \times 10^{-4}$  in the sapropel unit (Fig 3.12, Table 3.4). The Sr/Al profile show a similarity between Ca/Al and total carbonate (Fig 3.12, Table 3.7). Maximum contents of Sr/Al are observed at 11cm depth and then followed by a depletion toward the base of the core (Table 3.7). In contrast to Sr/Al, Rb/Al show an elevated value in the sapropel unit (Fig 3.12). The Rb/Al profile is in general similar to that of K/Al, but show greater increase in the sapropel unit (Fig 3.12). Rb/Al peak is at 11 cm depth in the coccolith unit (Table 3.7).

Ca/ Al average 1.8 in the sapropel unit (Table 3.4). Ca/Al show an enrichment in the coccolith unit and reaching maximum values at 11 cm depth (Fig 3.12, Table 3.7).

Mg/Al exhibits a different behaviour, showing a very strong enrichment in top 3 cm of the core, a gradual downcore decrease to the sapropel unit boundary, and then an increase in the sapropel unit near the base of the core (Fig 3.12, Table 3.4, Table 3.7) However, the average of Mg/Al in the sapropel unit is less than that in the coccolith unit (Fig 3.12).

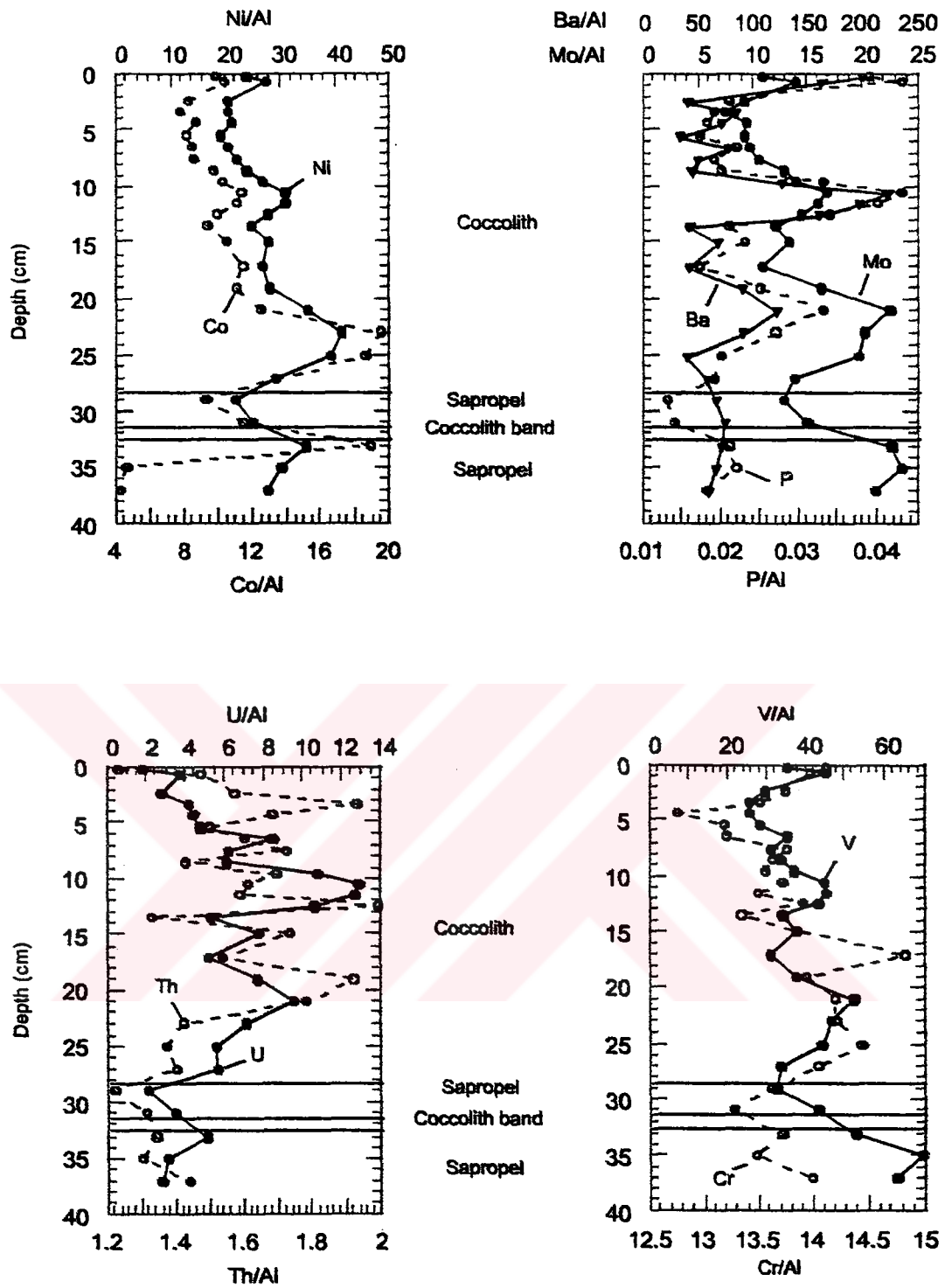


Fig 3.11. Concentration/ depth profiles of Ni, Co, Ba, Mo, P, U, Th, V, and Cr in Core BS 23 (2). All metal data are as weight ratios to Al ( $\times 10^{-4}$ ), except for P ( $\times 1$ ).

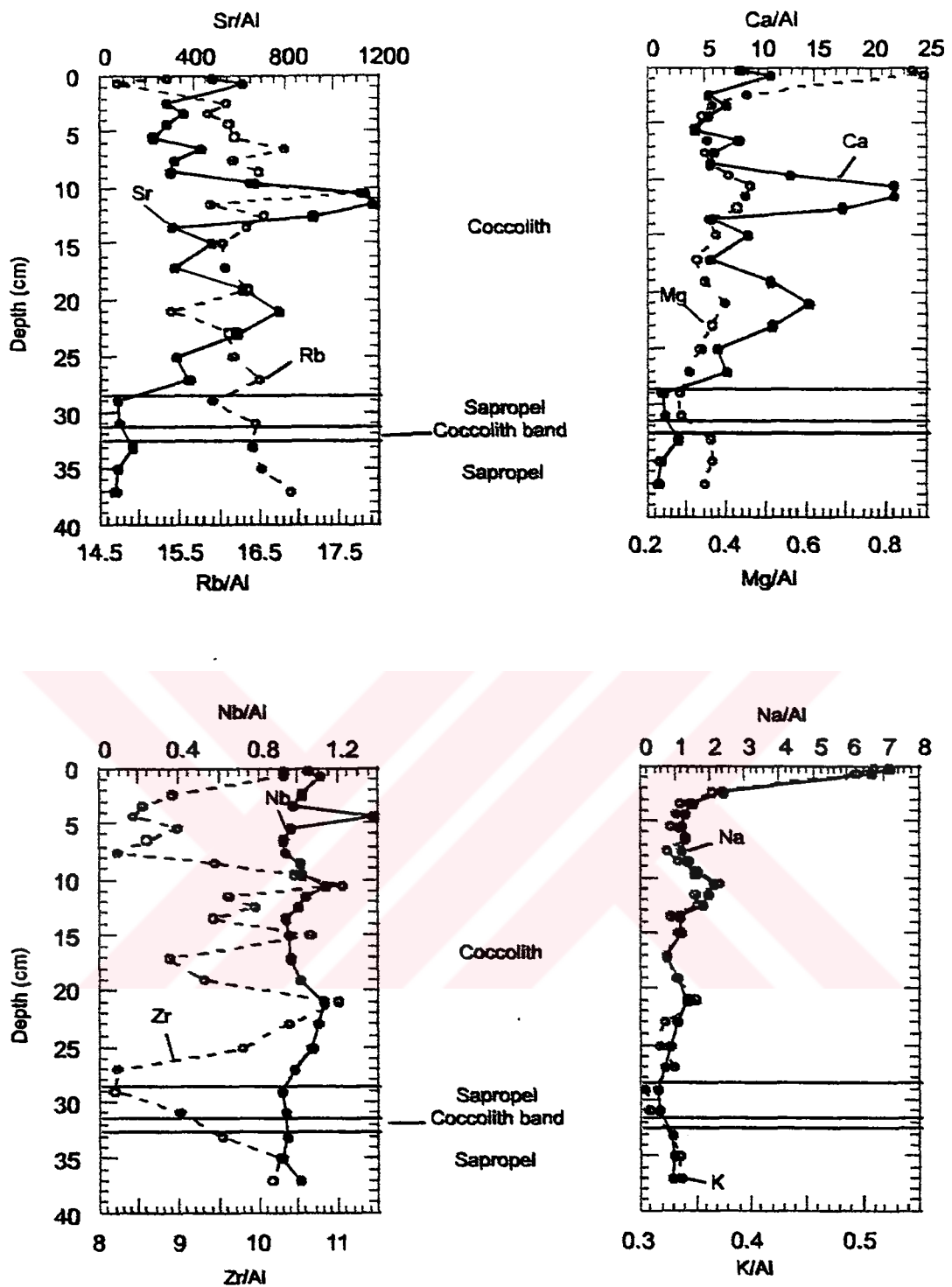


Fig 3.12. Concentration / depth profiles of Sr, Rb, Ca, Mg, Nb, Zr, Na and K in Core BS 23 (2). All metal data are as weight ratios to Al ( $\times 10^{-4}$ ), except for Ca, Mg, Na and K ( $\times 1$ ).

Table 3.7. Chemical composition of sediments in Core BS 23 (2) from the eastern basin.

Depth cm	CaCO <sub>3</sub> %	Fe %	S %	Mg %	Al %	Na %	K %	P %	Ti %	Mo ppm	Cu ppm	Pb ppm	Zn ppm	Ni ppm	Co ppm	Mn ppm	As ppm	U ppm	Th ppm	Sr ppm	Cd ppm	Sb ppm	V ppm	Ca %	La ppm	Cr ppm	Ba ppm	Zr ppm	Ce ppm	Y ppm	Nb ppm	Ta ppm	Sc ppm	Li ppm	Rb ppm	
0.25	3	1.3	1.68	1.41	1.63	1.63	0.83	0.06	0.07	18	58	28	115	39	16	279	18	3	2	776	2	5	57	13.5	11	23	333	17	17	11	2	0.3	3	11	25	
0.75	3.9	1.15	1.43	1.21	1.36	9.04	0.67	0.06	0.06	19	52	27	96	37	14	264	17	5	2	825	1.6	4	61	15	10	19	226	14	17	10	2	0.3	3	10	20	
2.25	3.4	33.9	1.96	1.52	1.14	2.55	6.18	0.93	0.05	0.11	23	59	41	98	52	21	405	18	7	4	727	1.6	4	76	13.9	14	35	111	23	21	12	3	0.7	6	18	41
3.25	3.84	40	2.03	1.44	0.94	2.59	3.78	0.87	0.05	0.11	20	43	19	63	53	20	432	18	11	5	941	1	2	65	18.7	16	35	224	22	26	14	3	0.6	5	17	41
4.25	3.98	31.2	2.53	1.84	1.01	2.98	3.89	0.99	0.05	0.12	28	58	23	73	63	26	514	20	13	5	851	1.4	2	76	16.3	16	38	224	25	26	14	4	0.7	6	23	48
5.5	3.58	29	2.82	1.92	1.07	3.34	3.87	1.09	0.06	0.14	31	67	19	65	64	27	544	20	16	5	768	1.1	2	94	14.4	16	44	126	30	27	14	3	0.8	7	23	54
6.5	4.1	40.1	2.2	1.67	0.87	2.5	3.21	0.83	0.05	0.1	24	57	18	52	51	21	484	19	21	4	1056	1	1	87	20.2	15	33	206	22	23	15	2	0.6	5	16	42
7.5	4.66	35.3	2.6	1.83	0.99	2.91	4.00	0.94	0.06	0.11	31	61	18	56	65	25	524	21	18	5	929	1	2	90	17.4	16	40	155	24	25	18	3	0.6	6	23	47
8.5	3.74	39.6	2.6	2.04	0.99	2.79	3.70	0.93	0.06	0.11	36	66	17	59	67	27	524	20	17	4	843	1.3	2	93	15.5	14	38	130	26	23	13	3	0.7	6	20	46
9.5	3.44	47.8	1.72	1.41	0.72	1.77	2.75	0.62	0.06	0.07	25	46	14	41	47	18	398	17	19	3	1178	0.9	1	65	22.9	10	24	231	19	16	11	2	0.3	4	12	29
10.5	3.22	65	1.4	1.11	0.57	1.24	2.63	0.46	0.05	0.05	21	34	10	28	38	14	345	15	16	2	1411	0.8	1	55	27.6	8	17	281	13.7	14	11	1	0.3	3	10	22
11.5	3.66	52.8	1.39	1.11	0.56	1.26	2.48	0.44	0.05	0.05	20	35	10	26	39	14	344	16	16	2	1474	0.6	1	57	27.8	9	17	252	12	13	11	1	0.3	3	9	20
12.5	4.88	54.7	1.53	1.22	0.64	1.51	2.74	0.53	0.05	0.06	22	39	10	29	42	15	364	16	16	3	1375	0.5	1	65	26.2	11	21	247	15	17	14	2	0.3	4	12	25
13.5	4.68	35.7	2.7	1.92	1.05	3	3.35	0.98	0.06	0.12	37	65	21	58	74	28	527	22	16	4	920	1.1	2	102	17.1	16	40	137	28	25	15	3	0.8	6	21	49
15	4.40	41	2.17	1.61	0.86	2.31	2.76	0.77	0.05	0.09	31	50	17	44	64	24	427	19	18	4	1097	0.9	1	86	20.8	13	32	162	24	21	14	2	0.6	5	15	37
17	4.10	37.7	2.66	1.78	1.04	3.24	2.46	1.05	0.06	0.14	35	55	10	55	86	37	494	23	17	5	1021	1.1	2	101	18.2	16	48	149	29	26	15	3	0.8	7	20	52
19	3.99	49	1.84	1.35	0.71	2.08	2.25	0.69	0.05	0.08	34	45	8	34	58	23	369	17	16	4	1257	0.7	1	78	23.1	12	29	195	19	19	12	2	0.5	5	15	34
21	4.6	53.7	1.68	1.36	0.67	1.69	2.28	0.59	0.06	0.07	38	48	17	36	59	21	346	18	16	3	1295	0.8	1	88	24.8	11	24	212	19	18	13	2	0.3	4	12	26
23	5.08	45.2	1.99	1.51	0.76	2.11	2.30	0.68	0.06	0.08	43	50	21	42	87	41	387	22	15	3	1235	0.8	2	98	23.6	13	30	199	22	22	14	2	0.5	5	15	34
25	4.44	34.4	2.54	1.9	0.96	2.91	2.42	0.92	0.06	0.12	57	63	13	52	114	54	439	16	16	4	940	1.3	2	129	18	15	42	130	28	25	14	3	0.7	7	23	47
27	7.71	40.3	2.52	1.66	0.87	2.85	1.91	0.94	0.05	0.11	39	55	12	45	83	38	432	12	16	4	1074	0.9	2	96	20.5	15	40	173	23	25	15	3	0.6	6	21	47
29	8.14	13.9	4.61	3.19	1.6	5.73	2.67	1.74	0.08	0.23	74	115	23	103	126	53	630	18	12	7	414	2	3	185	7.72	21	78	400	47	36	19	5	1.3	12	42	91
31	10.7	18.9	4.86	3.36	1.52	5.35	2.69	1.64	0.08	0.21	80	120	20	95	133	61	523	14	18	7	432	2.2	4	231	8.09	20	71	418	48	35	21	5	1.2	12	40	88
33	11.8	24.6	4.15	3.3	1.33	3.72	3.41	1.22	0.08	0.16	85	119	12	72	129	70	345	45	19	5	504	1.9	4	197	9.92	16	51	280	35	27	18	4	0.9	9	28	61
35	12.2	5.8	2.42	1.69	1.65	4.6	4.56	1.54	0.1	0.18	108	202	16	83	138	21	284	18	14	6	321	2.5	4	317	5.01	17	62	321	47	29	21	4	1.1	12	35	76
37	10.4	6.7	2.57	1.69	1.65	4.86	4.38	1.64	0.09	0.2	103	184	17	80	135	21	287	17	13	7	317	2.3	3	305	4.65	18	68	304	49	32	20	5	1.3	12	38	82

Nb/Al has a relatively uniform profile with an elevated value at 4cm depth in the coccolith unit (Table 3.7, Fig 3.12). The average of Nb/Al is lesser in the sapropel unit than in the coccolith unit.

The average of Zr/Al in the sapropel unit is lesser than in the coccolith unit (Fig 3.12, Table 3.7). It exhibits variable values with a significant enrichment in the top 3 cm and at 10 cm depth in the coccolith unit.

Na/Al and K/Al show a similar profile along the core. Elevated K/Al and Na/Al values are found in the top of the core, which increase steeply from 4cm depth to the core top, followed by a gradual decrease to the base of the core (Fig 3.12, Table 3.4, Table 3.7). There is therefore depletion of these elements in the sapropel unit. Na/Al and K/Al display a small peak at 10 cm core depth (Table 3.7).

Ce/Al show a relatively uniform values along the core, but the average of Ce/Al in the sapropel is smaller than that in the coccolith unit (Fig 3.13). Ta/Al show a more erratic profile in coccolith and has gradual increase with in the sapropel unit (Fig 3.13).

Li has a uniform profile through the core showing the similar behaviours of Al and Ti (Table 3.7). The average of Li/ Al in the coccolith unit is slightly higher than that in the sapropel unit. Unlike Li/Al profile, Ti/Al display more erratic profile along the core.

La/Al and Y/Al profiles exhibit similar downcore distribution pattern which show a general decrease to the base of the core (Fig 3.13). Maximum contents of these elements are observed between 10-13 cm and at 21 cm depth in the coccolith unit. (Table 3.7). The values show a gradual decrease in the sapropel unit

Sc/Al has uniform profile, with a small peak between 10-13 cm depth in the coccolith unit (Fig 3.13, Table 3.7). However, the average of Sc in the coccolith unit is smaller than that in sapropel unit.

Mg/Ca, Cd/Ca, and Sr/Ca profiles show an increase in the sapropel unit compared to the coccolith unit (Fig 3.14). All three profiles show relatively uniform values from the core top to the sapropel unit boundary, followed by elevated values in the sapropel unit.

U/Th exhibit a different behaviour, showing a relative increase between 10-13 cm depth in the coccolith unit and a decrease in the sapropel unit (Fig 3.14, Table 3.7).

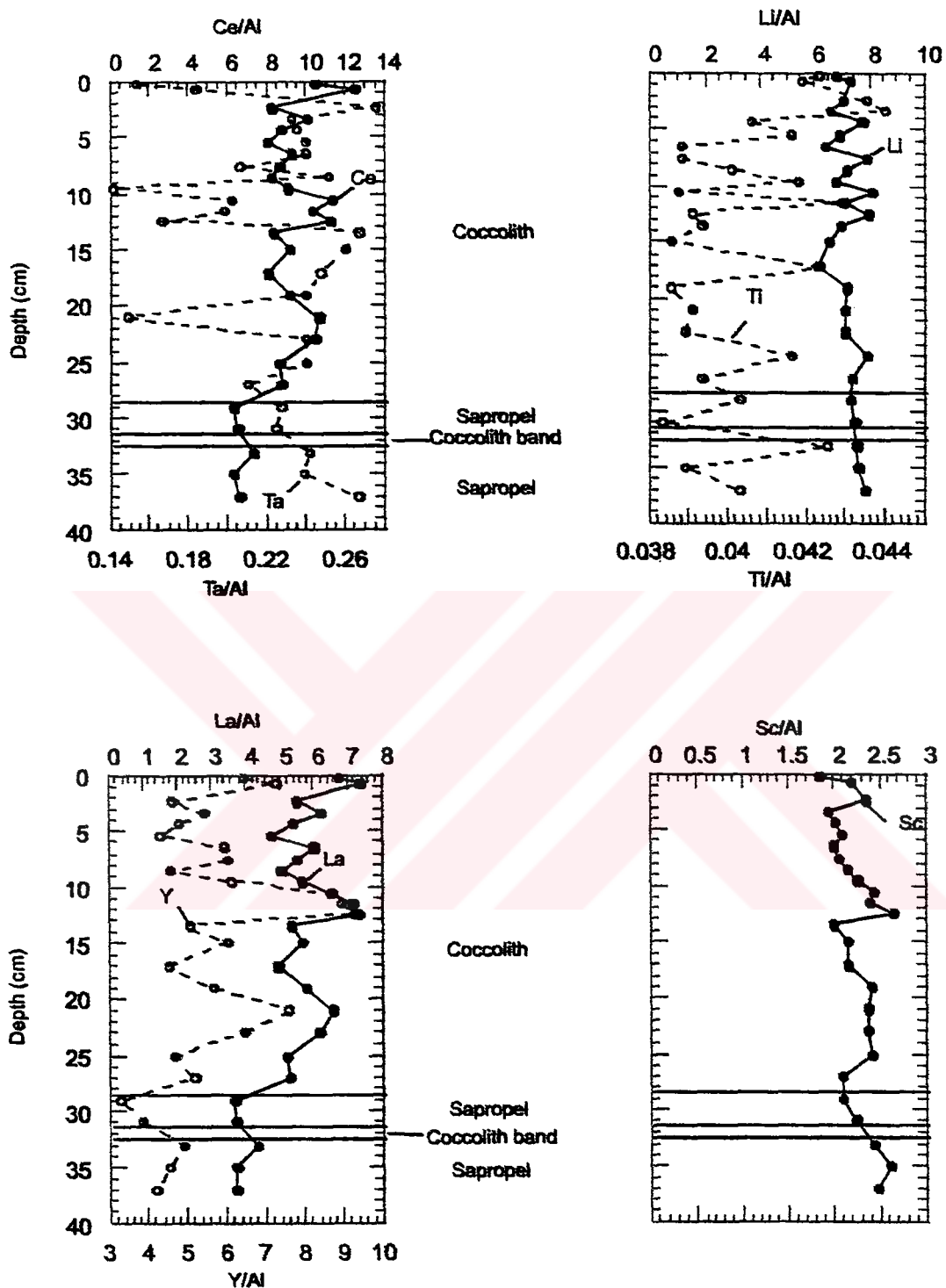


Fig 3.13. Concentration / depth profiles of Ce, Ta, Li, Ti, La, Y and Sc in Core BS 23 (2). All metal data are as weight ratios to Al ( $\times 10^{-4}$ ), except for Ti ( $\times 1$ ).

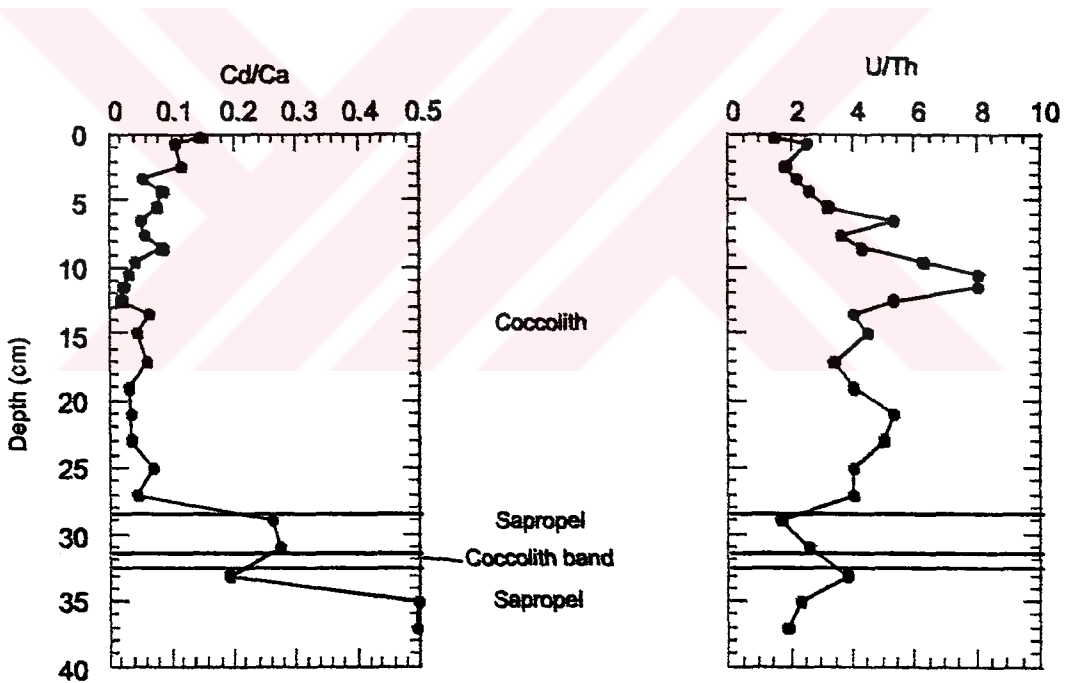
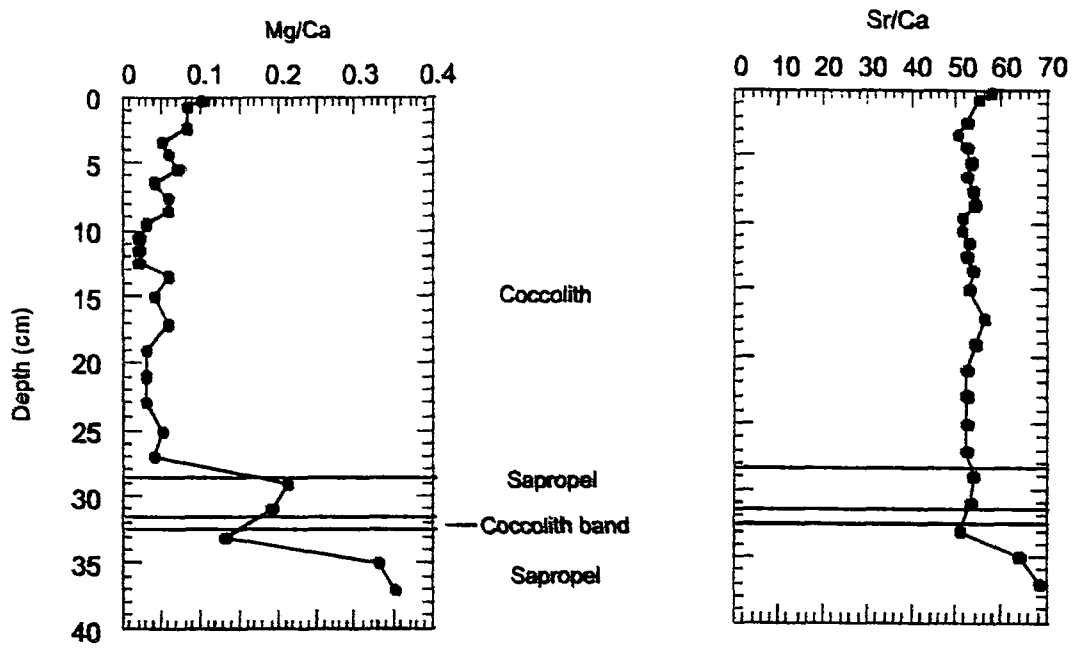


Fig 3.14. Concentration / depth profiles of Mg/Ca, Sr/ Ca, Cd/Ca and U/Th in Core BS 23 (2).

#### 3.3.2.4. Core 46

Mn/Al and Fe/Al exhibit similar downcore distribution patterns from the core top to core base (Fig 3.15). Both Mn/Al and Fe/Al show a strong depletion in the sapropel unit relative to the coccolith unit. Maximum contents of these elements are observed at 37 cm, 95 cm, 123 cm depth in the coccolith unit (Table 3.3, Table 3.4). There is no Mn/Al peak observed just above the sapropel unit (Fig 3.15, Table 3.8).

As/Al and S/Al show similar profiles with significant enrichment at 20 cm, 37 cm, and 43 cm depth in the coccolith unit followed by a relative enrichment in the sapropel unit (Fig 3.15, Table 3.8).

Aluminium normalized Cu and Zn values have similar profiles along the core depth (Fig 3.15). Cu/Al display a depletion in the coccolith unit, followed by a strong enrichment in the sapropel unit, reaching a peak at 49.5 cm depth and a maximum content in the sapropel unit near the base of the core (Table 3.8). Zn/Al show a decrease in the coccolith unit and then followed by enrichment in the sapropel unit, reaching the maximum values at 106.5 cm depth. The average Cu/Al and Zn/Al in the sapropel are higher than in the coccolith unit. There are no steep peaks in the coccolith unit at core top because of low sampling resolution in this case.

Pb/Al shows a relatively uniform values along the core, whereas Cd/Al exhibits a depletion in the coccolith unit and the enrichments between 46-95 cm depth and 107 cm in the sapropel unit (Fig 3.15, Table 3.8). Sb/Al is similar to Cd/Al in the coccolith unit. It shows a gradual increase in the sapropel unit, with a maximum value at 92 cm depth (Table 3.8).

Ni/Al and Co/Al show somewhat contrasting trends along the core (Fig 3.16). Ni/Al exhibits depletion in the coccolith unit and enrichment in the sapropel unit, Co/Al show a more erratic profile in the coccolith unit and relatively low values in the sapropel unit (Table 3.8).

Ba, Mo and P range 78-189 ppm, 46-197 ppm, 0.07-0.12 % in the sapropel unit, respectively (Table 3.3). Ba/Al average  $42 \times 10^{-4}$  in the coccolith unit (Table 3.4). Maximum content of Ba is observed at 37 cm depth in coccolith unit, followed by a gradual decrease in the sapropel unit (Table 3.8).



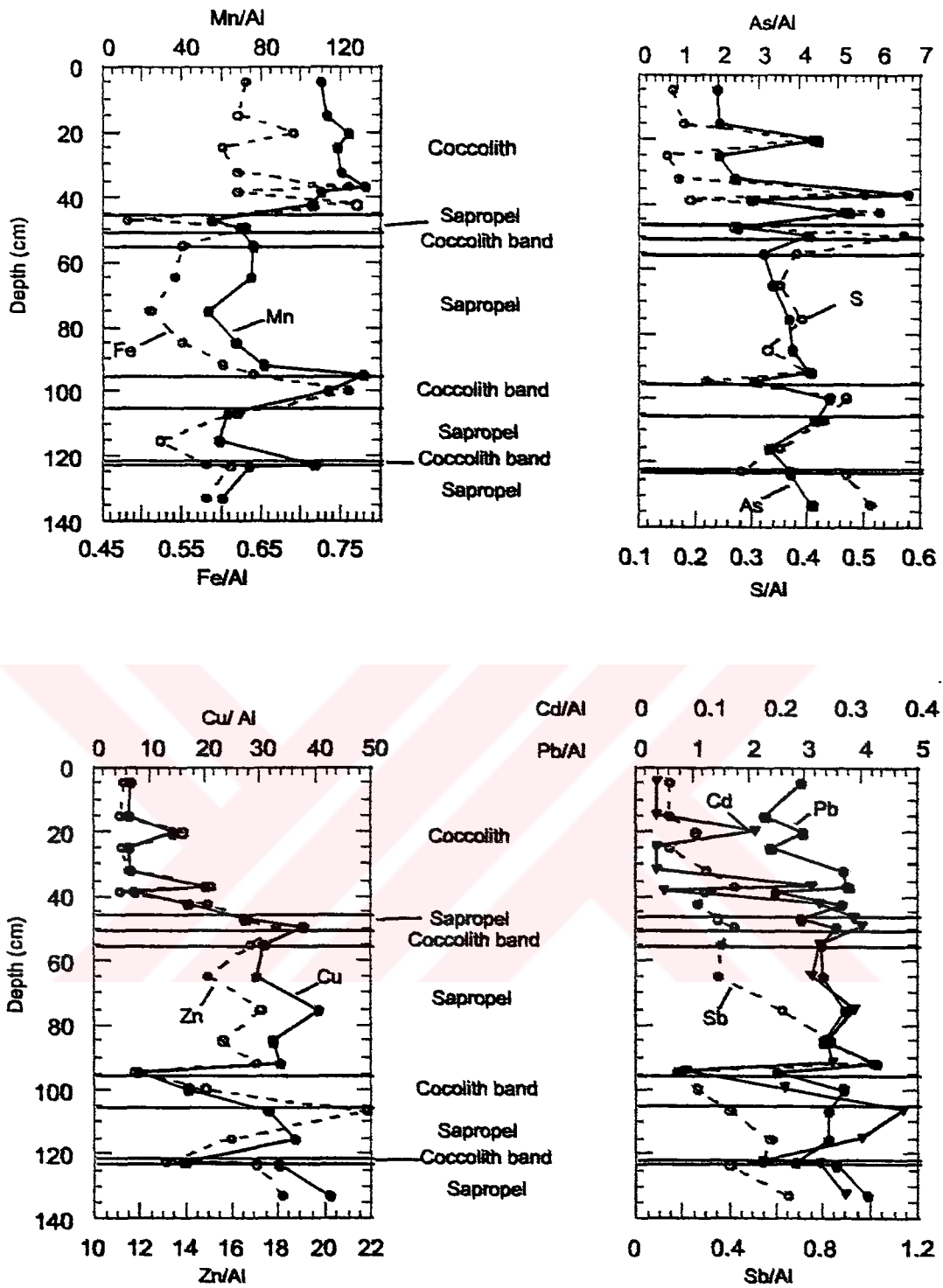


Fig 3.15. Concentration / depth profiles of Mn, Fe, As, S, Cu, Zn, Cd, Pb and Sb in Core 46. All metal data are as weight ratios to Al ( $\times 10^{-4}$ ), except for Fe and S ( $\times 1$ ).

Table.3.8. Chemical composition of sediments in Core 46 from the eastern basin.

Depth cm	Coag %	CaCO <sub>3</sub> %	Fe %	S %	Mg %	Al %	Na %	K %	P %	Ti %	Mo ppm	Cu ppm	Pb ppm	Zn ppm	Ni ppm	Co ppm	Mn ppm	As ppm	U ppm	Th ppm	Sr ppm	Cd ppm	Sb ppm	V ppm	Ca %	La ppm	Cr ppm	Ba ppm	Zr ppm	Ce ppm	Y ppm	Nb ppm	Ta ppm	Sc ppm	Li ppm	Rb ppm
5	0,86	13,6	4,48	1,14	2,57	7,16	1,65	1,82	0,08	0,39	7	49	21	81	163	37	783	14	2	8	251	0,2	1	135	6	23	166	260	69	38	16	7,7	2	16	49	101
15	0,86	15,4	4,33	1,28	2,55	6,95	1,57	1,79	0,06	0,41	8	44	16	77	162	30	779	14	2	8	278	0,2	1	129	6	22	167	282	59	37	16	7,6	2	15	44	94
20	3,15	-	2,78	1,65	1,11	4,04	1,45	1,18	0,06	0,16	22	57	12	56	88	35	502	18	11	5	826	0,7	1	117	16	17	82	180	38	30	14	4	1	8	29	67
25	0,87	15,8	4,25	1,08	2,54	7,08	1,54	1,83	0,06	0,38	9	45	17	78	161	28	834	14	2	8	300	0,2	1	133	7	22	167	286	65	39	16	8	2	15	47	102
32,5	0,87	15,8	4,21	1,16	2,53	6,76	1,54	1,81	0,06	0,39	13	45	25	78	162	29	810	16	3	8	327	0,2	2	135	8	23	164	337	61	38	15	8	2	14	44	80
36,5	3,57	61,4	1,81	1,2	0,8	2,39	1,53	0,69	0,07	0,1	30	48	9	36	69	27	315	16	12	4	1127	0,6	1	89	21	12	39	244	28	21	13	3	0,5	5	17	38
38,5	1,18	20,3	4,29	1,32	2,43	6,91	1,42	1,79	0,06	0,37	20	52	17	77	169	32	757	19	3	8	386	0,3	2	131	7,8	23	163	286	59	40	17	8	2	15	46	101
42,5	1,18	41,4	2,84	2,02	1,08	3,83	1,68	1,13	0,07	0,16	46	66	14	67	91	41	403	20	15	5	739	1	1	123	16	17	56	214	33	31	15	4	1	8	28	65
47	12,37	11,6	2,78	1,58	1,55	5,77	2,49	1,69	0,08	0,22	83	159	17	96	128	22	315	14	15	6	275	1,8	2	270	5	16	75	189	49	33	18	5	1	13	44	98
49,5	12,37	5,8	3,00	2,69	1,39	4,76	2,87	1,38	0,1	0,18	150	180	17	85	155	39	328	20	14	5	187	2	2	329	3	13	64	131	39	25	14	4	1	11	34	77
55	12,37	-	2,99	2,06	1,5	5,47	2,83	1,53	0,12	0,2	136	169	18	92	163	34	414	17	16	5	228	1	2	301	3,5	16	75	149	38,8	27	17	4,3	1	12	39	83
65	12,37	4,8	3,08	2,02	1,52	5,7	2,33	1,57	0,11	0,2	126	169	19	85	155	33	428	19	15	6	211	1	2	317	3	17	74	111	38	30	16	4	1	12	40	86
75	12,37	3,1	2,45	1,89	1,43	4,82	2,85	1,41	0,11	0,18	152	195	18	83	166	28	255	16	10	5	159	2	3	323	2	14	89	126	31	23	12	4	1	11	35	72
85	12,37	5,8	3,30	1,97	1,63	6,02	2,84	1,7	0,11	0,22	131	194	20	94	189	33	405	23	12	6	202	2	5	338	3	16	85	110	40	29	16	4	1	13	42	92
92	12,37	-	2,39	1,58	1,14	3,98	2,47	1,16	0,08	0,15	109	134	17	88	142	30	325	17	13	5	544	1	4	238	10	14	59	140	34	25	13	3	1	9	28	64
94,5	5,38	28,1	3,67	1,22	1,86	5,61	1,67	1,49	0,07	0,31	17	46	14	66	134	28	734	16	6	7	546	0,4	1	116	11	21	131	158	46	36	15	6	2	12	32	77
100	5,38	43,2	2,89	1,76	1,1	3,78	1,75	1,11	0,07	0,16	42	65	14	56	90	36	428	18	13	5	789	1	1	120	16	18	57	144	32	31	15	4	1	8	28	65
109,5	5,38	-	3,06	2,13	1,41	4,97	2,46	1,52	0,09	0,18	102	157	17	108	136	39	312	22	15	6	283	2	2	282	5	17	71	142	41	31	17	4,2	1	11	37	85
115	14,25	4,8	2,75	1,82	1,44	5,27	2,83	1,54	0,1	0,19	129	182	18	84	162	28	308	17	11	5	185	2	3	321	3	15	74	107	35	28	15	3,7	1	11	39	85
122,5	14,25	7,8	4,27	2,04	1,8	7,41	2,21	2,08	0,07	0,28	86	120	21	97	156	31	787	28	11	7	213	1	4	308	4	20	97	183	46	35	16	5	1	15	50	108
123	14,25	4,6	3,06	2,35	1,37	5,04	2,76	1,45	0,11	0,18	129	167	18	86	144	34	373	19	11	5	175	1	2	303	3	14	83	83	33	25	14	4	1	11	34	76
133	14,25	3,6	2,68	2,34	1,33	4,63	3,09	1,37	0,12	0,16	167	197	19	84	162	38	278	20	12	5	173	1	3	324	2	13	82	78	33	23	13	4	1	11	32	70

Mo/Al and P/Al profiles are similar, showing an increase in the upper part of the sapropel unit with maximum contents in the sapropel unit near the base of the core (Fig 3.16). In addition, Elevated P/Al values are found at 37cm depth (Fig 3.16, Table 3.8).

U/Al and Th/Al display different behaviour to each other along the core (Fig 3.16). The elevated U/Al value occur in the sapropel unit in contrast to Th/Al. U/Al exhibits an erratic profile in the coccolith unit, with a maximum value at 37 cm depth, followed by a gradual decrease in the sapropel unit. The average of U/Al in the sapropel unit is higher than that in the coccolith unit. Th/Al shows a significant enrichment at 37 cm depth and a gradual decrease towards the sapropel unit (Fig 3.16, Table 3.8).

V and Cr show a contrasting trends along the core (Fig 3.16). Low values of V/Al are observed in the coccolith unit relative to the sapropel unit. The V/Al increase between 50 and 95 cm depth in the sapropel unit, with the maximum content occurring at the base of the core in sapropel unit (Table 3.8). On the other hand, Cr/Al exhibit a more erratic profile in coccolith unit, followed by a decrease in the sapropel unit (Fig 3.16).

The highest values of Sr/Al is found in coccolith unit, with a maximum content at 37cm depth (Fig 3.17, Table 3.8). The values show a sharp decrease between 46-95 cm depth in the sapropel unit (Fig 3.17). Rb/Al shows more fluctuated values along the core and decrease gradually toward the sapropel unit (Fig 3.17). Sr/Al and Rb/Al values in the sapropel unit are lower than those in the coccolith unit. Sr and Rb in sapropel average  $52 \times 10^{-4}$  and  $15 \times 10^{-4}$  (Fig 3.17, Table 3.4). They show similar profile along the core. Their concentrations decrease in the sapropel unit compare to the coccolith unit.

Ca/Al display a similar profile to that of Sr/Al. It also has a significant enrichment at 37cm depth in the coccolith unit, followed by a gradual depletion in the sapropel unit (Fig 3.17, Table 3.8). The Mg/Al profile is in general different from those of Ca/Al and Sr/Al (Fig 3.17). The fluctuating values of Mg/Al is observed in the coccolith unit, with maximum contents at 15 cm and between 32.5-37 cm depth, and with a gradual depletion in sapropel unit (Table 3.8).

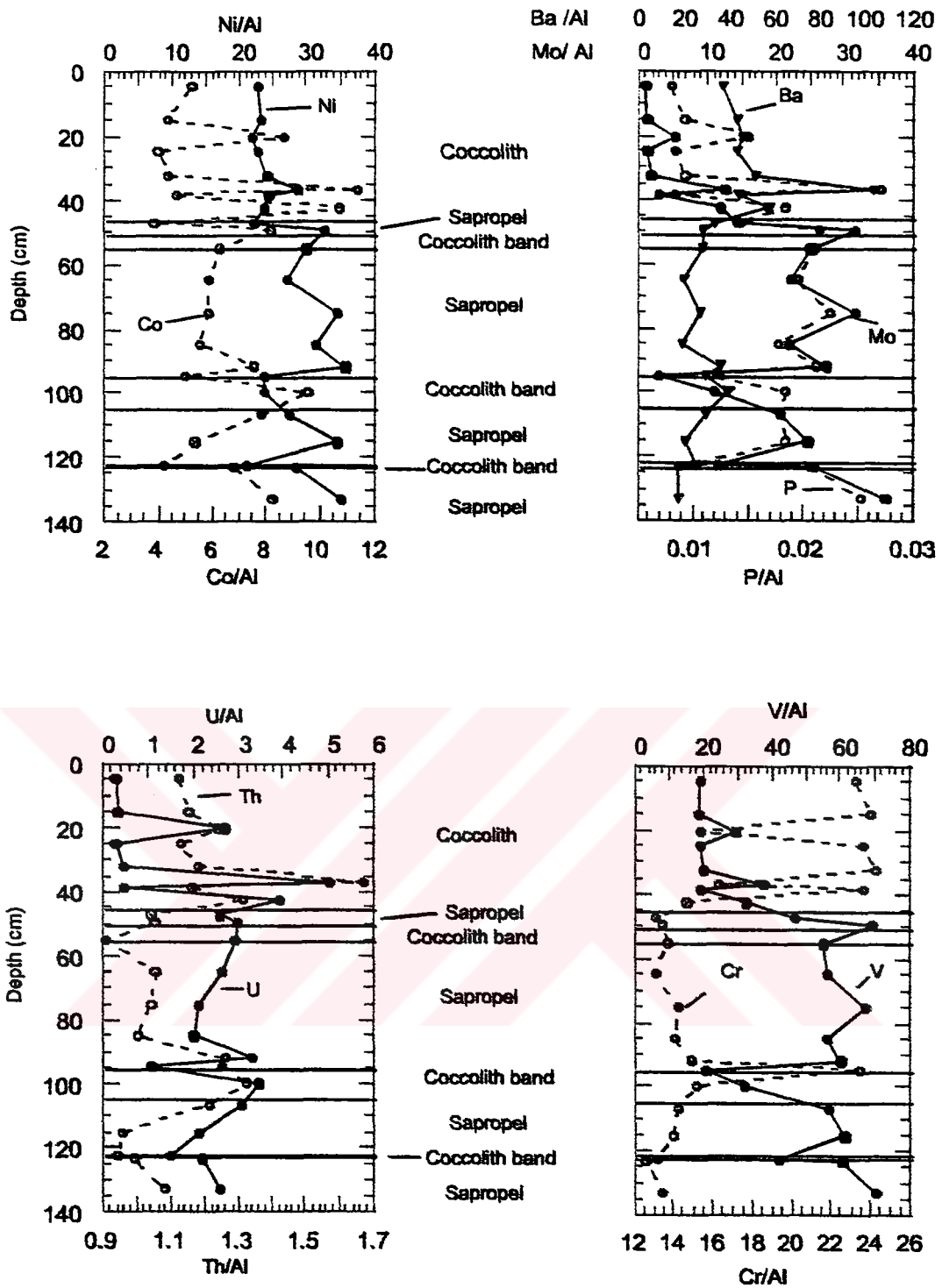


Fig 3.16. Concentration / depth profiles of Ni, Co, Ba, Mo, P, U, Th, V and Cr in Core 46. All metal data are as weight ratios to Al ( $\times 10^{-4}$ ).

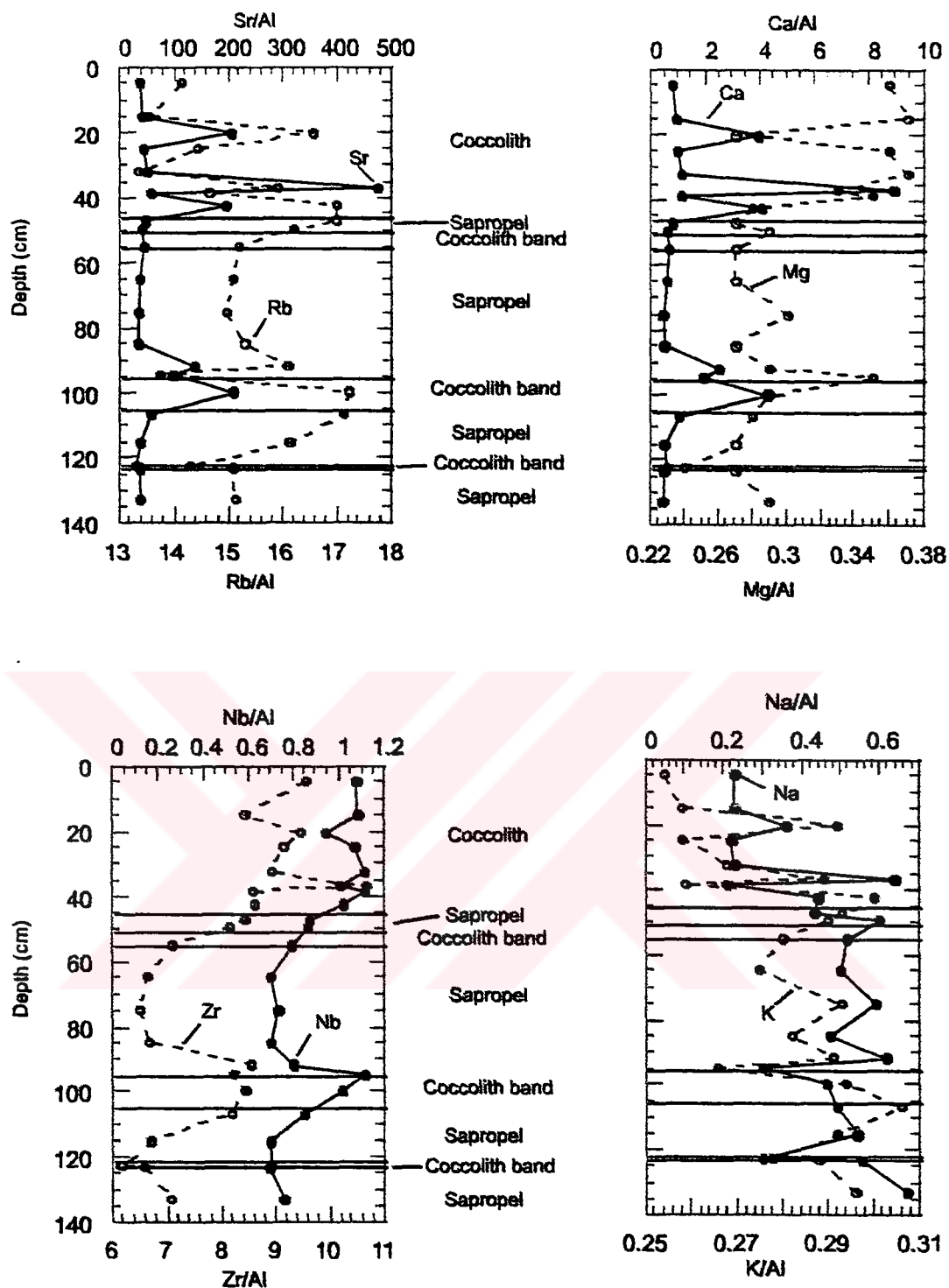


Fig 3.17. Concentration / depth profiles of Sr, Rb, Ca, Mg, Nb, Zr, Na and K in Core 46. All metal data are as weight ratios to Al ( $\times 10^{-4}$ ), except for Ca, Mg, Na and K ( $\times 1$ )

The profiles of Nb/Al and Zr/Al are in general similar to each other, and exhibit a depletion in the sapropel unit compared to the coccolith unit (Fig 3.17).

Na/Al and K/Al display more erratic profile along the core (Fig 3.17). The elevated Na/Al and K/Al values are found at 37 cm depth in the coccolith unit (Table 3.8). The average of Na/Al and K/Al in the coccolith unit is lower than in the sapropel unit.

Ce/Al and Ta/Al show a variable values in the coccolith unit, and a gradual decrease in the sapropel unit. Maximum content of Ce/Al is found at 37 cm depth and that of Ta/Al is found between 32.5-37 cm depth in the coccolith unit (Fig 3.18, Table 3.8). These elements exhibit higher values in the coccolith unit relative to those in the sapropel unit.

Li/Al and Ti/Al exhibit different profiles along the core (Fig 3.18). Li/Al profiles gives uniform values along the core. The average values of Li/Al in the sapropel and coccolith units are  $7 \times 10^{-4}$  (Table 3.4). Ti/Al profile show variable values in the coccolith unit and uniformly low values in the sapropel unit, except for a peak at a depth of 90 cm (Fig 3.18, Table 3.8).

La/Al and Y/Al profiles are similar to each other (Fig 3.18). They have a higher values at core top, and maximum values at 37 cm depth in the coccolith unit (Table 3.8). They exhibit a gradual decrease in the sapropel unit compared to the coccolith unit (Fig 3.18). Sc/Al show a very uniform profile along the core (Fig 3.18).

The elevated values of Mg/Ca, Sr/Ca, Cd/Ca and U/Th are observed in the sapropel unit (Fig 3.19). The highest Cd/Ca and Mg/Ca are found at 75 cm depth (Table 3.8). The elevated values of Sr/Ca are observed at the base of the core. U/Th has a highest value at 37 cm depth (Table 3.8).

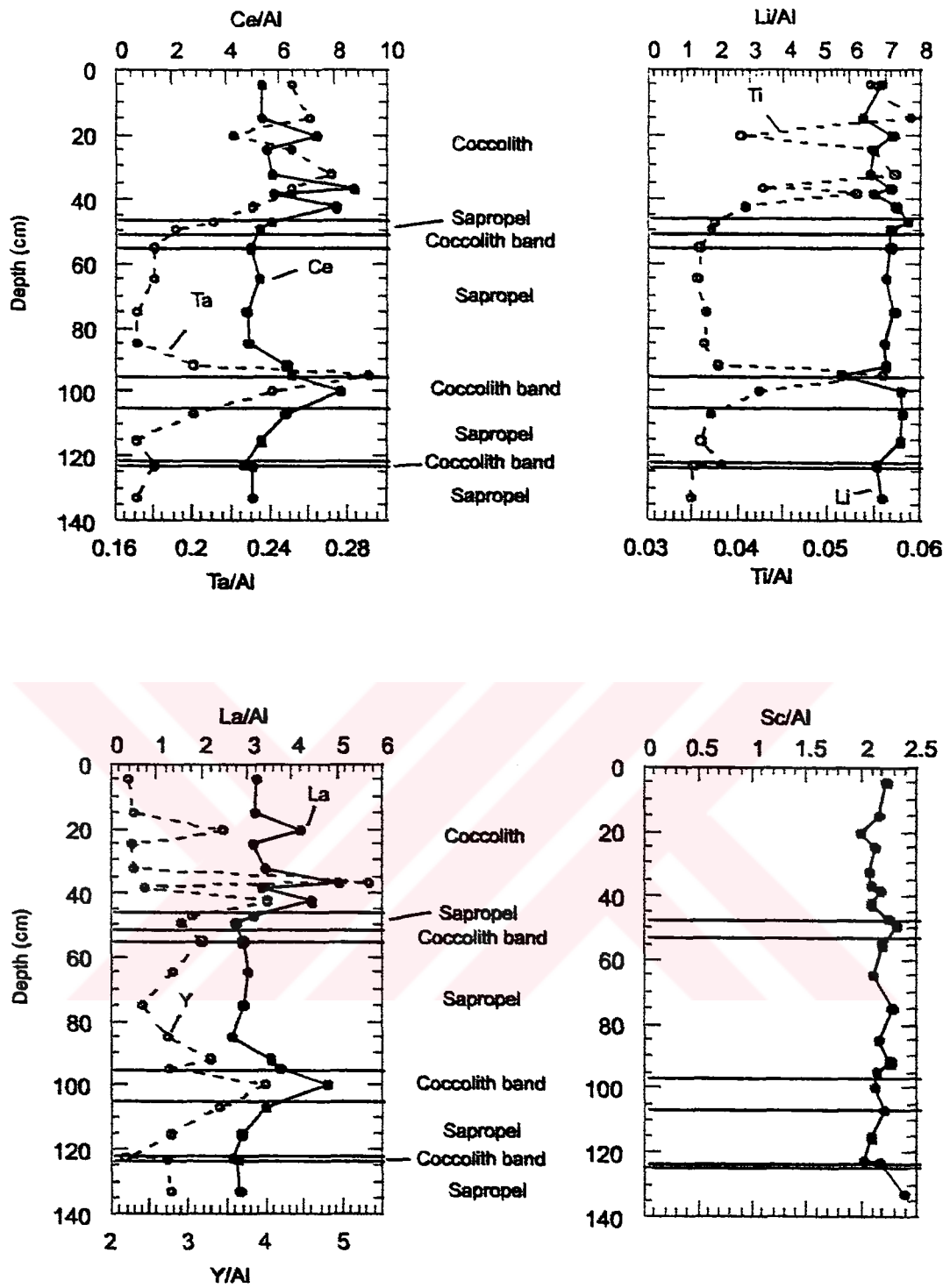


Fig 3.18. Concentration / depth profiles of the Ce, Ta, Li, Ti, La, Y and Sc in Core 46. All metal data are as weight ratios to Al ( $\times 10^{-4}$ ), except for Ti ( $\times 1$ ).

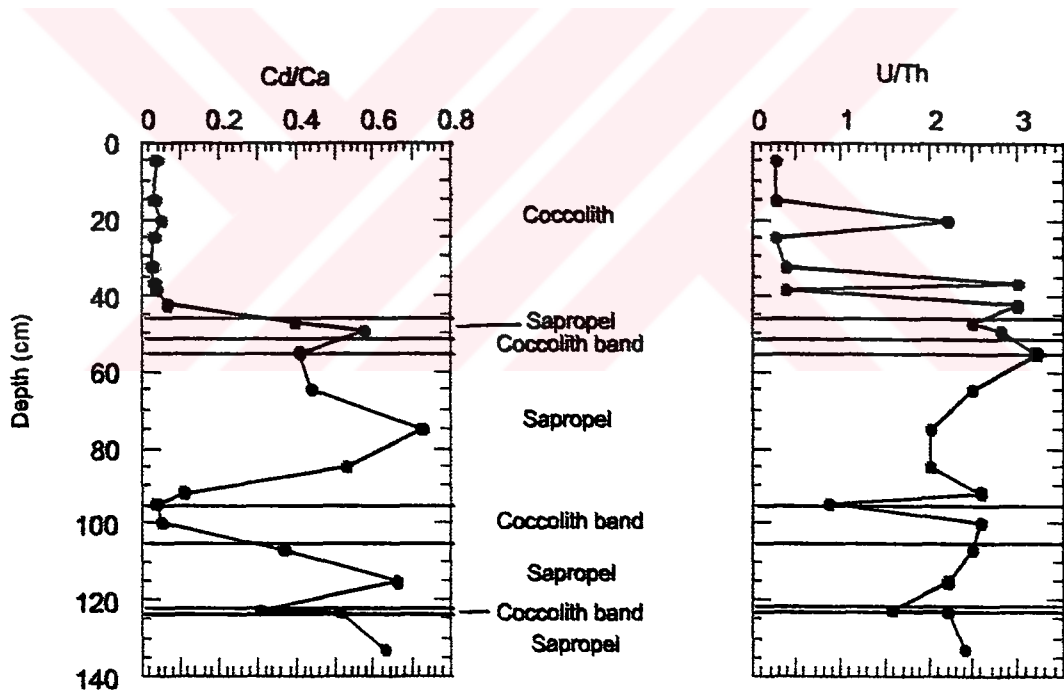
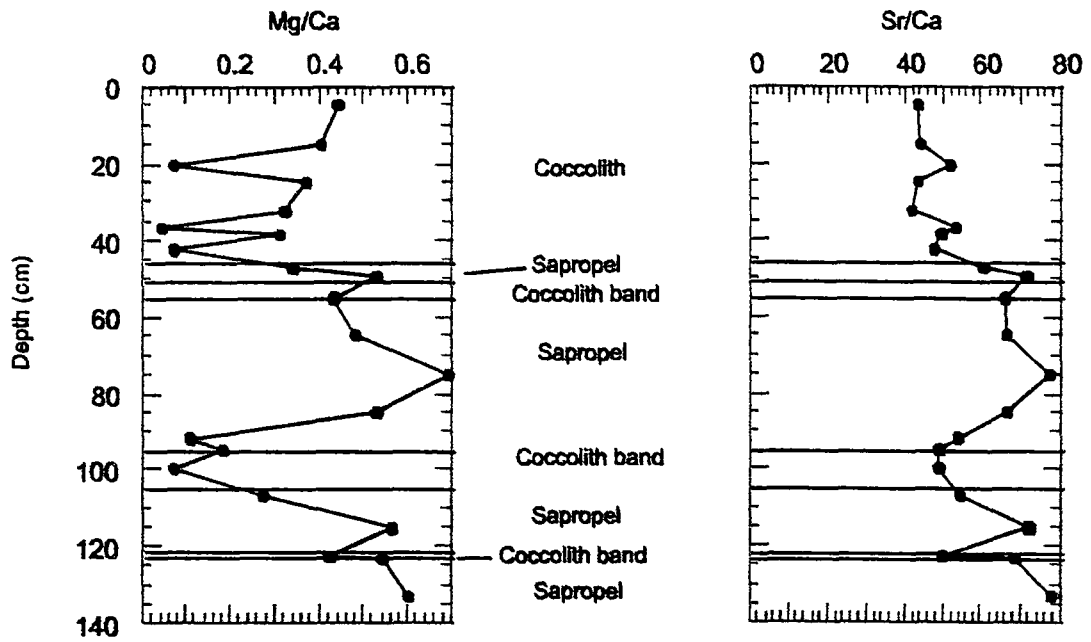


Fig 3.19. Concentration / depth profiles of Mg /Ca, Sr/Ca, Cd/Ca and U/Th in Core 46.



## 4. DISCUSSIONS AND CONCLUSIONS

### 4.1. Discussions

#### 4.1.1. Detrital Input

The main components of the Black Sea sediments in the studied cores are the biogenic carbonate and detrital mineral matter. The former component is the most abundant in the coccolith unit, in which total carbonate contents reach maximum values because of high concentrations of calcite coccoliths of *Emiliana huxleyi* forming white laminae in this unit.

Core BS 9 includes only the coccolith unit. Cores BS 15 and BS 23 (2) have the coccolith and the upper part of the sapropel units. Core 46 contains both coccolith unit and a thick underlying sapropel unit. The *Emiliana huxleyi* coccoliths form < 1 mm thick laminae in the basinal and lower slope sediments. These laminae are the product of annual summer plankton blooms when the light intensity and temperature are optimal for a maximum growth (Degens *et al.*, 1970).

The total carbonate, Ca/Al, and Sr/Al profiles are very similar to each other in Cores BS 15, BS 23 (2) and 46 (Fig 3.5, Fig 3.12, Fig 3.17). In these cores carbonate, Ca/Al and Sr/Al profiles show a decrease in the sapropel unit compared to the overlying coccolith unit. Carbonate, Ca/Al and Sr/Al values are higher in the western Black Sea basin than in the eastern Black Sea basin. This indicates greater biogenic carbonate flux and relatively low detrital input in the former basin compared to the latter basin. The elevated values in Sr/Al profile are observed in the coccolith unit relative to that in the sapropel unit in Core BS15, BS23 (2) and 46.

The high values of Sr/Al are especially observed in the coccolith unit in Core BS 15 in the western basin. Sr/Al shows enrichment in both the sapropel and coccolith units to a higher degree in the western basin than in the eastern basin. Sr/Al in the sapropel unit from the western basin is three times higher than that in the eastern basin. High Sr/Al values in the western basin are due to high biogenic carbonate content in general, and to the greater contribution of aragonitic shells to the total carbonate content in this basin in particular. The ease of the substitution of Sr in aragonite structure is well known (e.g., Krauskopf, 1979). Strontium can replace Ca in other mineral lattices such as calcite and plagioclase feldspar. Ca and Sr relationship in the Black Sea sediments is supported by a strong correlation coefficient between these two metals in both the coccolith and sapropel units in all cores (Table 3.10, Table 3.12).

In addition to *E. huxleyi*, coccolithophore species *Braarudosphaera bigelowi* and *Scyphosphaera sp.* are observed in general at all levels along the Core BS 23(2). However, *B. bigelowi* is found mainly in the lower part of the coccolith unit and in the sapropel unit. This coccolith species were not observed in high surface salinities such as Red Sea (salinity:37-41 ‰). The greatest amount of this species is found in coastal waters of low salinity, such as Gulf of Maine (salinity:31.8-32.7‰), (Grand and Braarud,1935) and Gulf of Panama (salinity:26.8-32.5‰) (Smayada,1966). The widespread occurrence of *B. bigelowi* in the Black Sea clearly indicates the ability of this species to thrive in unusually low salinities (Bukry,1974). The Black Sea sediments in Core BS 23 (2) also contain diatoms and pollens. The diatoms in this core are *Coscinodiscus marginatus*, *Thalassiosira sp.*, *Thalassiosira oestrupi(?)* and *Roperia sp.* *Coscinodiscus marginatus* is characteristic of brackish-marine water environments (Maynard,1974).

Pollens found in different levels of the Black Sea sediments belong to tree populations such as coniferae (e.g. pinus,Alnus, Quercus) and to step vegetation (e.g. chenopodiacea). Traverse (1974) suggests that the higher spore and pollen in sediments is the result of reduced sedimentation rates, which has predominantly resulted from the rise of water level in the Black sea and of the base levels of stream in the drainage area during the deposition of the sapropel and coccolith units.

Another important component of the Black Sea sediments is the detrital mineral and organic matter which have been transported to the basin via the rivers.

Table 3. 9. Correlation coefficients of elements for the coccolith unit in Cores BS 23 (2) & 46 from the eastern basin (n=30)

	Coorg %	Fe %	S %	Mg %	Al %	Na %	K %	P %	Ti %	Mo ppm	Cu ppm	Pb ppm	Zn ppm	Ni ppm	Co ppm	Mn ppm	As ppm	U ppm	Th ppm	Sr ppm	Cd ppm	Sb ppm	V ppm	Ca %	La ppm	Cr ppm	Ba ppm	Zr ppm	Ce ppm	Y ppm	Nb ppm	Ta ppm	Sc ppm	Li ppm	Rb ppm				
Coorg	1																																						
Fe	-0.68	1																																					
S	0.37	-0.08	1																																				
Mg	-0.76	0.87	-0.32	1																																			
Al	-0.76	0.98	-0.22	0.94	1																																		
Na	0.26	-0.49	0.23	-0.13	-0.42	1																																	
K	-0.73	0.97	-0.13	0.95	0.99	-0.30	1																																
P	-0.44	0.34	0.17	0.40	0.37	0.03	0.40	1																															
Ti	-0.78	0.95	-0.33	0.96	0.99	-0.39	0.97	0.36	1																														
Mo	0.36	-0.33	0.66	-0.61	-0.46	-0.12	-0.45	0.05	-0.53	1																													
Cu	0.16	0.13	0.90	-0.04	0.03	0.25	0.13	0.37	-0.08	0.32	1																												
Pb	-0.11	0.05	0.12	0.29	0.10	0.61	0.20	0.12	0.12	-0.25	0.32	1																											
Zn	-0.37	0.35	0.12	0.63	0.43	0.60	0.55	0.35	0.44	-0.43	0.36	0.78	1																										
Ni	-0.67	0.94	-0.24	0.88	0.96	-0.50	0.93	0.39	0.95	-0.29	-0.01	0.01	0.32	1																									
Co	-0.09	0.53	0.38	0.25	0.44	-0.46	0.44	0.36	0.36	0.50	0.46	-0.16	0.01	0.59	1																								
Mn	-0.67	0.96	-0.18	0.87	0.95	-0.45	0.94	0.20	0.94	-0.46	0.02	0.10	0.35	0.89	0.35	1																							
As	0.56	-0.14	0.80	-0.39	-0.28	0.05	-0.22	-0.01	-0.37	0.84	0.68	-0.01	-0.10	-0.15	0.57	-0.23	1																						
U	0.64	-0.53	0.45	-0.85	-0.67	-0.20	-0.70	-0.37	-0.72	0.68	0.17	-0.47	-0.76	-0.62	-0.02	-0.53	0.11	1																					
Th	-0.70	0.97	-0.16	0.87	0.97	-0.48	0.95	0.27	0.95	-0.41	0.05	0.07	0.37	0.90	0.43	0.94	-0.22	-0.57	1																				
Sr	0.71	-0.85	0.03	-0.93	-0.89	0.01	-0.94	-0.48	-0.88	0.47	-0.26	-0.44	-0.77	-0.80	-0.34	-0.82	0.22	0.79	-0.85	1																			
Cd	0.51	-0.60	0.65	-0.49	-0.62	0.80	-0.50	-0.03	-0.65	0.40	0.56	0.45	0.33	-0.65	-0.16	-0.62	0.11	0.24	-0.62	0.25	1																		
Sb	0.22	-0.25	0.28	0.06	-0.19	0.87	-0.06	0.11	-0.18	-0.02	0.37	0.74	0.73	-0.22	-0.15	-0.24	0.34	-0.36	-0.25	-0.19	0.74	1																	
V	-0.56	0.90	0.05	0.71	0.86	-0.55	0.84	0.50	0.81	0.00	0.28	-0.04	0.22	0.92	0.77	0.79	0.10	-0.39	0.83	-0.72	-0.53	-0.28	1																
Ca	0.67	-0.83	-0.01	-0.92	-0.86	-0.05	-0.92	-0.47	-0.85	0.46	-0.31	-0.46	-0.80	-0.77	-0.32	-0.79	0.18	0.79	-0.82	0.99	0.19	-0.25	-0.69	1															
La	-0.64	0.97	-0.03	0.87	0.96	-0.39	0.97	0.33	0.93	-0.33	0.19	0.17	0.46	0.91	0.52	0.93	-0.08	-0.58	0.97	-0.88	-0.51	-0.13	0.87	-0.86	1														
Cr	-0.78	0.94	-0.38	0.96	0.98	-0.39	0.96	0.35	1.00	-0.55	-0.12	0.10	0.42	0.95	0.34	0.93	-0.39	-0.73	0.93	-0.86	-0.68	-0.19	0.80	-0.83	0.91	1													
Ba	-0.52	0.23	-0.69	0.33	0.37	0.02	0.34	0.24	0.46	-0.67	-0.62	0.03	0.22	0.35	-0.29	0.28	-0.68	-0.62	0.27	-0.30	-0.44	-0.05	0.07	-0.26	0.22	0.50	1												
Zr	-0.77	0.97	-0.26	0.94	0.99	-0.43	0.97	0.39	0.98	-0.46	0.00	0.09	0.41	0.96	0.45	0.94	-0.11	-0.68	0.95	-0.88	-0.64	-0.21	0.87	-0.85	0.98	0.38	1												
Ce	-0.67	0.97	-0.05	0.87	0.97	-0.43	0.97	0.39	0.93	-0.31	0.18	0.11	0.43	0.92	0.55	0.91	-0.10	-0.59	0.97	-0.88	-0.33	-0.16	0.89	-0.85	0.99	0.91	0.25	0.95	1										
Y	-0.29	0.78	0.17	0.52	0.69	-0.52	0.68	0.16	0.63	-0.03	0.26	-0.08	0.07	0.66	0.52	0.73	0.18	-0.11	0.77	-0.52	-0.49	-0.33	0.72	-0.50	0.81	0.61	-0.03	0.65	0.78	1									
Nb	-0.77	0.97	-0.26	0.94	0.99	-0.40	0.98	0.36	0.99	-0.47	-0.01	0.13	0.44	0.95	0.42	0.94	-0.30	-0.70	0.96	-0.89	-0.61	-0.18	0.83	-0.86	0.94	0.98	0.42	0.98	0.95	0.66	1								
Ta	-0.76	0.98	-0.22	0.93	0.99	-0.43	0.98	0.36	0.98	-0.44	0.03	0.13	0.43	0.95	0.44	0.95	-0.26	-0.66	0.97	-0.89	-0.61	-0.19	0.86	-0.86	0.96	0.97	0.33	0.99	0.96	0.68	0.98	1							
Sc	-0.76	0.97	-0.26	0.93	0.99	-0.44	0.97	0.34	0.99	-0.44	-0.01	0.09	0.40	0.97	0.45	0.94	-0.28	-0.67	0.96	-0.87	-0.63	-0.21	0.86	-0.84	0.94	0.98	0.36	0.99	0.95	0.68	0.99	1							
Li	-0.74	0.98	-0.19	0.92	0.99	-0.43	0.98	0.37	0.98	-0.41	0.07	0.09	0.42	0.95	0.48	0.94	-0.24	-0.65	0.96	-0.89	-0.61	-0.20	0.88	-0.86	0.96	0.97	0.34	0.99	0.97	0.71	0.99	0.98	0.99	1					
Rb	-0.73	0.98	-0.14	0.90	0.99	-0.45	0.98	0.38	0.96	-0.39	0.10	0.07	0.41	0.94	0.50	0.94	-0.21	-0.62	0.97	-0.88	-0.60	-0.22	0.88	-0.85	0.97	0.95	0.30	0.98	0.98	0.73	0.98	0.98	0.98	0.99	1				

Table 3.10. Correlation coefficients of elements for the sapropel unit in Cores BS 23 (2) & 46 from the eastern Black Sea basin. (n=18)

	Co	Fe	S	Mg	Al	Na	K	P	Ti	Mo	Cu	Pb	Zn	Ni	Co	Mn	As	U	Th	Sr	Cd	Sb	V	Ca	La	Cr	Ba	Zr	Ce	Y	Nb	Ta	Sc	Li	Rb			
Co	1																																					
Co	1																																					
Fe	-0.18	1																																				
S	0.09	0.70	1																																			
Mg	-0.07	0.33	0.20	1																																		
Al	0.20	0.40	-0.08	0.74	1																																	
Na	0.38	-0.28	0.11	0.07	-0.24	1																																
K	0.20	0.42	0.03	0.76	0.93	0.06	1																															
P	0.59	-0.31	-0.04	-0.18	-0.01	0.38	-0.06	1																														
Ti	-0.24	0.47	-0.21	0.88	0.78	0.38	0.68	-0.42	1																													
Mo	0.71	-0.45	0.11	-0.30	-0.05	0.42	-0.04	0.92	-0.53	1																												
Cu	0.66	-0.52	-0.04	-0.09	0.01	0.66	0.14	0.84	-0.45	0.89	1																											
Pb	0.32	0.32	0.26	0.25	0.66	-0.04	0.68	0.27	0.25	0.33	0.30	1																										
Zn	0.18	0.32	0.34	0.33	0.62	0.10	0.72	0.25	0.21	0.30	0.40	0.71	1																									
Ni	0.65	-0.19	-0.09	0.22	0.40	0.17	0.31	0.69	0.06	0.72	0.67	0.67	0.42	0.35	1																							
Co	-0.14	0.75	0.09	-0.25	-0.22	-0.10	-0.17	-0.25	-0.16	-0.15	-0.33	0.00	0.10	-0.24	1																							
Mn	-0.29	0.72	0.09	0.59	0.64	-0.54	0.51	-0.36	0.84	-0.62	-0.70	0.29	0.09	-0.16	0.19	1																						
As	0.01	0.77	0.81	-0.03	-0.05	0.08	0.06	-0.33	-0.03	-0.18	-0.23	-0.01	0.14	-0.14	0.89	0.25	1																					
U	0.11	0.22	0.56	-0.38	-0.29	0.33	-0.13	0.06	-0.50	0.12	0.14	-0.12	0.21	-0.21	0.55	-0.33	0.12	1																				
Th	-0.34	0.55	0.03	0.77	0.60	0.01	0.72	-0.51	0.75	-0.54	-0.33	0.37	0.36	-0.19	0.00	0.65	0.6	-0.14	1																			
Sr	-0.67	0.21	-0.02	-0.24	-0.47	-0.33	-0.48	-0.75	-0.01	-0.79	-0.81	-0.50	-0.63	-0.79	0.29	0.26	0.20	0.08	0.10	1																		
Cd	0.21	0.11	0.41	0.08	-0.03	0.77	0.32	0.13	-0.28	0.25	0.53	0.24	0.52	0.40	0.18	-0.38	0.1	0.56	0.24	-0.29	1																	
Sb	0.48	0.23	0.29	0.08	0.11	0.45	0.27	0.07	-0.11	0.27	0.35	0.33	0.24	0.40	0.22	-0.06	0.49	0.24	0.14	-0.18	0.51	1																
V	0.74	-0.40	-0.06	0.04	0.27	0.51	0.34	0.79	-0.25	0.87	0.93	0.42	0.49	0.76	-0.36	-0.47	-0.83	0.09	-0.22	-0.91	0.40	0.36	1															
Ca	-0.69	0.27	-0.01	-0.22	-0.41	-0.40	-0.45	-0.78	0.05	-0.82	-0.86	-0.49	-0.60	-0.79	0.31	0.33	0.23	0.05	0.12	0.99	-0.34	-0.20	-0.93	1														
La	-0.55	0.64	0.04	0.62	0.47	-0.24	0.53	-0.72	0.73	-0.82	-0.65	0.15	0.16	-0.47	0.14	0.76	0.23	-0.07	0.86	0.43	0.06	-0.07	-0.57	0.46	1													
Cr	-0.28	0.30	-0.36	0.82	0.68	-0.45	0.52	-0.31	0.95	-0.45	-0.41	0.15	0.10	0.17	-0.26	0.74	-0.18	-0.63	0.60	-0.02	-0.44	-0.20	-0.24	0.04	0.58	1												
Ba	-0.23	0.58	0.50	0.27	0.01	0.37	0.28	-0.49	0.14	-0.42	-0.23	0.14	0.20	-0.44	0.44	0.25	0.31	0.39	0.61	0.33	0.64	0.34	-0.32	0.30	0.62	-0.06	1											
Zr	-0.22	0.39	0.00	0.74	0.51	0.22	0.69	-0.43	0.61	-0.45	-0.15	0.23	0.41	-0.20	-0.09	0.41	0.07	0.07	0.87	0.03	0.46	0.13	-0.09	0.02	0.74	0.45	0.68	1										
Ce	-0.52	0.62	0.02	0.62	0.53	-0.27	0.59	-0.72	0.74	-0.79	-0.60	0.19	0.24	-0.42	0.09	0.73	0.17	-0.06	0.88	0.36	0.08	-0.09	-0.49	0.40	0.97	0.59	0.57	0.79	1									
Y	-0.22	0.40	0.25	0.41	0.14	0.48	0.41	-0.34	0.19	-0.39	-0.08	0.03	0.29	-0.34	0.21	0.16	0.35	0.50	0.62	0.19	0.69	0.26	-0.13	0.16	0.63	0.00	0.82	0.79	0.62	1								
Nb	-0.42	0.50	-0.09	0.83	0.62	-0.21	0.64	-0.55	0.88	-0.64	-0.48	0.18	0.25	-0.22	-0.07	0.72	0.00	-0.26	0.87	0.15	-0.02	-0.18	-0.36	0.18	0.85	0.79	0.45	0.84	0.87	0.50	1							
Ta	-0.41	0.47	-0.13	0.85	0.56	-0.11	0.61	-0.59	0.87	-0.69	-0.49	0.11	0.16	-0.27	-0.10	0.71	0.02	-0.28	0.90	0.20	0.03	-0.13	-0.39	0.22	0.87	0.76	0.50	0.85	0.88	0.55	0.97	1						
Sc	0.28	0.28	-0.10	0.82	0.93	0.08	0.95	0.09	0.71	0.05	0.21	0.60	0.66	0.42	-0.30	0.46	-0.07	-0.19	0.65	-0.57	0.22	0.23	0.42	-0.54	0.42	0.59	0.14	0.66	0.46	0.31	0.63	0.51	0.90	1				
Li	0.26	0.35	0.03	0.60	0.91	-0.02	0.96	0.03	0.56	0.05	0.21	0.72	0.76	0.35	-0.18	0.40	0.00	-0.02	0.58	-0.52	0.31	0.23	0.40	-0.49	0.44	0.40	0.18	0.58	0.51	0.33	0.51	0.45	0.90	1				
Rb	0.14	0.37	-0.02	0.63	0.92	-0.13	0.94	-0.07	0.63	-0.06	0.10	0.67	0.75	0.27	-0.19	0.46	-0.04	-0.06	0.63	-0.44	0.24	0.14	0.31	-0.40	0.51	0.49	0.16	0.64	0.60	0.34	0.60	0.33	0.89	0.98	1			

The mineralogical composition and grain size of detrital input in sediments in Cores BS 23 (2) and BS 15 were investigated. This is also shown by enrichment in the coccolith unit of lithophile elements, such as K, Na, Mg, Rb, Cr, Ti and Zr. Enrichment of these metals, together with sharp increases in heavy metals of anthropogenic origin (Cu, Zn, Pb, Sb and As), in the top few cm of the cores are due to anthropogenic effects, such as industrial and agricultural activities in the last few hundred years. The differences in the depth of the onset of the enrichment in different cores are because of different sedimentation rates at different core sites.

The depth of the onset of metal enrichment increases in the order: Core BS 23(2), Core BS 15 and Core BS 9. Core 46 from the eastern basin was not sampled at sufficiently high resolution to determine the corresponding metal enrichment depth near the core top. The sequence of this depth distribution indicates that the sedimentation rate is in the order: Core BS 9 > Core BS 15 > Core BS 23(2). This conclusion is supported by  $^{210}\text{Pb}$  mass accumulation rate (MAR) data of Çağatay *et al.* (2001) at sites Cores BS 9 and BS 15. These authors determined the sedimentation rates of  $72\text{ cm kyr}^{-1}$  (MAR:  $171.5\text{ gm}^{-2}\text{y}^{-1}$ ) and  $24\text{ cm kyr}^{-1}$  (MAR:  $71.25\text{ gm}^{-2}\text{y}^{-1}$ ) in Core BS 9 and BS 15, respectively. The sedimentation rate at the site of Core BS 9 is therefore about 3 times higher than at the site of Core BS 15. It is also concluded that the average MAR for the last 125 yr are considerably higher than those for the last 2000 years, computed from published  $^{14}\text{C}$  ages (Arthur and Dean, 1999) suggesting that the sedimentation rate has considerably increased in recent times probably over the last few hundred years. The high sedimentation rate at the former site is in line with the fact that its location is closer to the sediment source than the site of BS15 on the Danube submarine fan.

The 2000 yr old coccolith/sapropel boundary occurs at 32.5 cm and 28.5 cm in Cores BS 15 and BS 23(2), respectively. This suggests that the that sedimentation rates for the last about 2000 yrs are also higher at the site of Core BS15 than those at the site of Core BS 23(2). This conclusion is in agreement with the grain size data and lithophile element distributions discussed above.

Some lithophile elements, such as Cr, Mg, K, Rb, La, Ce, Th and Ta, provide useful information on the composition of the detrital fraction.

The elevated Cr values are observed in the sapropel unit in Core BS15 whereas in Core BS 23 (2) and 46 there is depletion of Cr and Mg in the sapropel unit (Fig 3.9, Fig 3.11, Fig 3.16).

Cr substitute readily for Mg minerals such as chlorite (Petruk 1964; Muller and Stoffers, 1974). This suggests higher input of chlorite to the western basin compared to the eastern basin during the sapropel deposition. Cr is higher in the coccolith unit than in the sapropel unit suggesting higher chlorite enrichment in the coccolith unit compared to the sapropel unit. Mg/Al values in the eastern basin cores decrease in the sapropel unit relative to the coccolith unit. Mg/Al enrichment in the coccolith unit relative to the sapropel unit is controlled by the amount of chlorite. Rb/Al decrease in sapropel unit at Core BS 23 (2), BS15 and Core 46 (Fig 3.12, Fig 3.17).

Mg/Ca ratio is higher in the sapropel unit than in the coccolith unit. This is mainly due to the high carbonate, and therefore high Ca contents and/or high chlorite contents in the latter unit. Mg/Ca ratio in biogenic carbonate is considered to be a measure of water temperature (Fischer and Wefer, 1999; Watanabe *et al.*, 2001). However, in the Black Sea cores because the total sediment Mg/Ca ratio is determined, it can not used to deduce the relative changes in the water temperature.

Rb, Zr and Nb are present entirely in aluminosilicate fraction, but they may not show the same distribution in the various components of this fraction. Rubidium is always camouflaged in K-bearing minerals and its abundance will therefore be largely controlled by the distribution of K-feldspar and micas. Zirconium occurs in sediments almost entirely in zircon, which because of its density, is transported with the coarse silt and the fine sand fractions; hence, the concentration of Zr should vary with the quartz content. Both Zr and Nb occur in higher concentration in felsic rocks (Francois, 1988). Zr/Al values increase in Core BS 23 and in the upper 40 cm of Core 46 (Fig 12, Fig 3.17). The rest of the Core 46 shows in general a depletion of Zr/Al. Nb values decrease in sapropel unit in Core 46 and shows uniform values in Core BS 23 (2) (Fig 3.12, Fig 3.17).

Na/Al and K/Al increase in the sapropel unit in Core 46. These metals show profiles with uniform values in this unit at Core BS 23 (2). Ce/Al, La/Al and Y /Al values show a depletion in the sapropel unit in the eastern basin and Li/Al and Sc/Al display profile with uniform values along the eastern basin cores.

Table 3.11. Correlation coefficients of elements for the coccolith unit in Cores BS 9, BS 15, BS 23(2) and 46. (n=70)

	Corg	Al	Fe	Cu	Mn	Cr	Sr	Ba	Zn	V	Ni	Sc	Co	Mo	As	Sb	Pb
	%	%	%	ppm	ppm	ppm	ppm	ppm	ppm	ppm	ppm	ppm	ppm	ppm	ppm	ppm	ppm
Corg	1																
Al	0,05	1															
Fe	-0,04	0,80	1														
Cu	0,02	0,31	0,07	1													
Mn	-0,04	0,51	0,81	-0,03	1												
Cr	0,00	0,95	0,88	0,20	0,68	1											
Sr	0,05	-0,67	-0,82	-0,11	-0,50	-0,68	1										
Ba	-0,05	0,39	0,06	0,65	-0,16	0,33	-0,07	1									
Zn	-0,04	0,50	0,34	0,62	0,08	0,48	-0,50	0,73	1								
V	-0,01	0,69	0,90	0,05	0,66	0,73	-0,77	-0,04	0,20	1							
Ni	-0,11	0,18	0,67	-0,42	0,63	0,36	-0,59	-0,34	-0,05	0,70	1						
Sc	0,00	0,96	0,84	0,21	0,59	0,95	-0,63	0,33	0,42	0,75	0,30	1					
Co	-0,10	-0,09	0,42	-0,37	0,33	0,01	-0,45	-0,45	-0,19	0,58	0,87	0,01	1				
Mo	0,03	0,42	0,32	0,10	-0,16	0,24	-0,43	0,14	0,15	0,50	0,13	0,40	0,28	1			
As	0,16	0,05	-0,18	0,54	-0,27	-0,13	0,26	0,23	0,09	-0,09	-0,45	-0,02	-0,24	0,27	1		
Sb	0,12	0,31	-0,21	0,57	-0,21	0,19	0,38	0,60	0,29	-0,31	-0,75	0,25	-0,84	-0,06	0,52	1	
Pb	0,02	0,02	-0,09	0,47	-0,05	0,04	0,06	0,63	0,54	-0,14	-0,24	0,00	-0,28	-0,15	0,14	0,31	1

Table 3.12. Correlation coefficients of elements for the sapropel unit in Core BS 15, BS 23(2) and 46. (n=22)

	Corg	Al	Fe	Cu	Mn	Cr	Sr	Ba	Zn	V	Ni	Sc	Co	Mo	As	Sb	Pb
	%	%	%	ppm	ppm	ppm	ppm	ppm	ppm	ppm	ppm	ppm	ppm	ppm	ppm	ppm	ppm
Corg	1																
Al	0,24	1															
Fe	-0,32	0,42	1														
Cu	0,70	0,15	-0,37	1													
Mn	-0,34	0,50	0,71	-0,62	1												
Cr	-0,22	0,66	0,28	-0,36	0,55	1											
Sr	-0,58	-0,49	-0,05	-0,73	0,15	0,12	1										
Ba	-0,32	0,15	0,06	-0,33	0,06	0,60	0,54	1									
Zn	0,19	0,73	0,31	0,41	0,05	0,30	-0,54	0,21	1								
V	0,71	0,25	-0,20	0,90	-0,35	-0,41	-0,85	-0,63	0,36	1							
Ni	0,62	0,27	-0,03	0,70	-0,12	-0,28	-0,84	-0,76	0,23	0,88	1						
Sc	0,30	0,94	0,29	0,28	0,34	0,59	-0,49	0,19	0,76	0,32	0,25	1					
Co	-0,24	-0,20	0,69	-0,14	0,19	-0,33	-0,06	-0,32	-0,07	0,88	0,15	-0,32	1				
Mo	0,73	0,08	-0,33	0,91	-0,56	-0,43	-0,73	-0,41	0,33	0,88	0,74	0,14	-0,01	1			
As	-0,13	-0,04	0,74	-0,19	0,25	-0,18	0,03	0,00	0,11	-0,11	-0,02	-0,07	0,79	-0,12	1		
Sb	-0,27	-0,01	-0,06	-0,36	0,02	0,49	0,70	0,94	0,02	-0,64	-0,77	0,04	-0,34	-0,41	-0,04	1	
Pb	-0,19	0,22	0,06	-0,24	0,15	0,50	0,55	0,86	0,23	-0,47	-0,61	0,24	-0,32	-0,27	-0,08	0,91	1



Ta/Al decrease in sapropel unit at Core 46 and these metals show a profile with fluctuating values in core BS 23 (2). Scandium is expected to be captured by ferromagnesian minerals. The high degree of correlation coefficients between Al, K, Sc, Rb, Li between Core 46 and BS 23(2) in the sapropel unit is probably accounted for by the presence of potassium feldspar, mica, and mafic minerals. The presence of detrital silicates in the sapropel unit is shown by strong positive correlation between Mg, Al, Ti, Nb, Ta, Th and Cr (Table 3.10 and 3.12).

#### 4.1.2. Organic Productivity

Barium is an important proxy for organic productivity in marine sediments (Brumsack, 1986; Calvert, 1990; Bishop, 1988; Dymond, 1985; Schmitz, 1987; Thomson *et al.*, 1995). Calvert and Fontugne (1987), Revelle *et al.* (1955), Goldberg (1958), Goldberg and Arrhenius (1958); and Gurvich *et al.* (1978) showed that the Ba contents of pelagic sediments are highest in areas of high productivity, and especially so in siliceous sediments. Therefore, Barium is used as a proxy for paleoproductivity, with high Ba contents being often found in organic rich sediments, including sapropel (Brumsack, 1986; Calvert, 1990; Bishop, 1988; Dymond, 1985; Schmitz, 1987; Thomson *et al.*, 1995).

In such sediments, Ba occurs as biologically secreted 1-3  $\mu\text{m}$  barite crystals (Brumsack, 1986; Calvert, 1990; Dymond *et al.*, 1992; Chow and Goldberg, 1960; Goldberg, 1958). Although no barite crystals have yet been reported from the Black Sea sapropel, it is reasonable to assume that Ba occurs as micro barite crystals in the organic rich water (Calvert, 1990; Hirst, 1974).

The trends of Ba/Al profiles are generally conformable with those of Corg profiles in the studied cores, indicating the proxy character of this ratio for organic productivity in the Black Sea sediments (Fig 3.5., Fig 3.8). High Ba, Mo, P, Ni and V show strong correlation between each other in organic-rich sediments. Ba/Al and Mo/Al values increase at Core BS 15, BS 23 (2), and between 27.5-38.5 cm of Core 46 (Fig 3.8, Fig 3.11, Fig 3.16). The highest Ba values are found in the western basin. Its concentration in the sapropel unit is 5 and 13 times that in the coccolith unit in Cores BS 23 and 46, respectively (Table 3.3, Table 3.4). Ba shows a general depletion in the sapropel unit in Core 46.

Ba/Al ratio is the highest in the sapropel unit in Core BS 15, followed by Core BS 23(2) and Core 46. These trends suggest that the organic productivity was higher in the western basin than in the eastern basin during the sapropel deposition. In the coccolith unit, Ba/Al ratio increases in the order: Core 46 < BS 23(2) < BS 9 < BS15, again suggesting higher organic productivity in the western Black Sea basin compared to the eastern Black Sea basin during the last 3000 years.

The enrichment of Ba in the organic rich horizons of coccolith and sapropel units and in the top 2-4 cm of the cores can be interpreted as a reflection of increased fertility of Black Sea during the deposition of these layers. The sharp enrichment of Ba in the few cm-thick core tops is an important indicator of the recent eutrophication of the Black Sea.

Higher Ba contents and lower detrital input in the upper part of the sapropel unit in Core BS 15, BS 23 (2) and in the upper part of the Core 46 show that the organic carbon is composed mainly of marine origin. This result is supported by elemental C/N analysis of sapropel in Core 46 in the eastern Black Sea by Çağatay (1999). The elemental data suggest that the organic carbon is probably mainly of marine origin, with a significant contributions of terrestrial material. Detailed C/N analysis, Rock Eval Pyrolysis and C isotope analysis by Tolun *et al.*(1999) in the same core show that the organic matter in the lower part of the sapropel starts with predominantly terrestrial organic matter input, followed by a marine contribution towards the upper part of the coccolith unit.

The elevated values of Mo, Ni and V are observed in the sapropel unit in Core BS 15, BS 23 (2) and 46 (Fig 3.8, Fig 3.9, Fig 3.11, Fig.3.16). In this unit Cu, Ni, Mo and V values show a strong correlation with C<sub>org</sub> values suggesting a genetic relationship between these metals and organic matter (Table 3.10, Table 3.12). The highest enrichment of these elements in the sapropel unit is found in the western Black Sea basin, where the detrital input is less than that in the eastern Black Sea basin. Volkov and Fomina (1974) and Philipchuk and Volkov (1974) suggest that Mo, Ni and V are mostly concentrated in both the organic and sulphide fractions, with V being present mainly in the organic and Mo and Ni mainly coprecipitated with iron sulphides as their sulphide phases. In the anoxic basin sulphide precipitation start in the anoxic water layer (Brewer and Spencer, 1974; Jacos *et al.*, 1985; Landing and Lewis, 1991; Spencer *et al.*, 1972).

V enrichment probably occurs by surface surface adsorption of vanadyl ions ( $\text{VO}_2^+$ ) on organic matter or precipitation of  $\text{V}_2\text{O}_3$  or  $\text{V}(\text{OH})_3$  (Calvert and Pedersen, 1993), although V (and Ni) could also be present as metal porphyrins (Mason, 1982). P/Al distribution is similar to that of Mo in the sapropel unit in the eastern basin cores supporting the association of P and Mo with the organic matter.

#### 4.1.3. Redox Conditions During the Sapropel Deposition

Metal contents of marine sediments, in particular those of redox sensitive elements such as Mn and Fe, provide significant information for discussion of the depositional conditions of the sapropel unit. Mn/Al in the sapropel unit averages  $89 \times 10^{-4}$ ,  $84 \times 10^{-4}$  and  $72 \times 10^{-4}$  in Core BS 15, BS 23 and 46, respectively. The same ratio in the coccolith unit in the same cores averages  $154 \times 10^{-4}$ ,  $178 \times 10^{-4}$  and  $101 \times 10^{-4}$ , respectively. The values in the sapropel unit are therefore lower than those in the coccolith unit. Fe shows a similar behaviour to Mn in the sapropel unit; Fe values decrease in the sapropel unit compared to the coccolith unit in Core BS 15, BS 23 (2) and 46. There is no enrichment just above the sapropel unit in any of these cores. Çağatay (1999) found that there is no significant difference between Mn contents of the sapropel and coccolith units.

Manganese and Fe exist as Mn (IV) oxyhydroxide and Fe(III) colloids in the oxic, and as a dissolved Mn (II) and Fe (II) in the anoxic water layers of the Black Sea Basin (Spencer et al., 1971). In the anoxic sediment column, it precipitates as Mn (II) carbonate, provided sufficient alkalinity is reached (Calvert, 1990). In most surface oxic sediments of deep basins and shelves, Mn is highly enriched as Mn-oxyhydroxide crust and nodules (Cronan, 1980; Shaw *et al.*, 1990).

This enrichment occurs by the upward diffusion of dissolved Mn (II) from the sulfate reduction zone and its precipitation as oxyhydroxides in the surface oxic layer (Froelich *et al.*, 1979). The recycling of Mn between oxic and anoxic zones of a sediment column and its enrichment in the oxic layer can obviously occur under oxic water column conditions (Calvert, 1990). Using this criteria, Calvert (1990), Pedersen and Calvert (1990) and Calvert and Pedersen (1993) interpreted the relatively high levels of Mn in sapropel in the core from the central Black Sea to infer that the basin waters were oxygenated during the formation of the sapropel unit.

These types of enrichments of Mn, Fe and other redox sensitive elements above S-1 sapropel in the Mediterranean are well documented (Pruysers *et al.*, 1993; Higgs *et al.*, 1994; Thomson *et al.*, 1995). These enrichments are attributed to diagenetic deposition of Fe and Mn-oxyhydroxides above the sapropel under oxic bottom water conditions. Because of well known sorptive and coprecipitation capacities of hydroxides, many elements show similar profiles that of Fe and Mn above the S-1 sapropel. However, such an enrichment above the Black Sea sapropel is not observed both eastern and western part of the Black Sea basin. These data are consistent with earlier studies by Çağatay (1999). The absence of such clear enrichments of redox sensitive elements, such as Mn and Fe, above the Black Sea sapropel suggest that oxic bottom water conditions never prevailed during or after the deposition of sapropel unit. Although it can be argued that later anoxic conditions might have eliminated such oxyhydroxide-enriched profiles, depletion of Mn within the Black Sea sapropel in cores BS15, BS23(2) and 46 strongly testifies against oxic bottom water conditions during the sapropel deposition (Calvert and Pedersen, 1993; Pruyers *et al.*, 1993; Higgs *et al.*, 1994; Thomson *et al.*, 1995).

In anoxic basins, the dissolved concentrations of chalcophile elements, such as Cd, Cu and Zn, decrease from the upper oxic water mass into underlying anoxic waters (Jacobs and Emerson, 1982; Jacobs *et al.*, 1985; Landing and Lewis, 1991; Haraldsson and Westerlund, 1988, 1991). This decrease is most likely due to the precipitation of the respective solid sulphides in the presence of dissolved sulphide ions in the anoxic waters. Pb, Cu, Zn, Cd, Ni and Zn are chalcophile elements and occur in sulphide phases and are concentrated in the sediments of the anoxic basins (Calvert and Pedersen, 1993). The enrichment of these elements in the Black Sea sapropel also strongly suggests that this layer was deposited under anoxic bottom water conditions. Cu/Al, Pb/Al and Zn/Al show uniform profile in the sapropel unit in Core BS15. Sb/Al shows a relative depletion in sapropel unit in Core BS 15. The western basin cores (Core BS 9 and BS 15) display general enrichment of Cu/Al in the sapropel unit.

As/Al and S/Al values in Core BS 23 (2) and Core 46 increase in the sapropel unit relative to the coccolith unit. These enrichments are consistent with elevated Fe and Co values in the sapropel unit in these cores.

In addition, the higher correlation coefficient between Co, As and S supports the close association of these metals in sulphide phases in the sapropel unit. However, As/Al show a relative depletion in this unit in Core BS 15. S and As exhibit similar behaviour in the Black Sea cores. Co/Al values increase in Core BS 15, in Core BS 23(2) and in the top 40 cm of Core 46 (Fig 3.9, Fig 3.11, and Fig 3.16). There is a strong correlation coefficient between Co and As and S in the sapropel unit (Table 3.12). The distribution of Co/Al is somewhat similar to that of Cu/Al, Mo/Al and V/Al (Fig 3.9, Fig 3.11, Fig3.16). Co/Al is high at the Corg peak in the sapropel in Core BS 23 (Fig 3.5, Fig3.11).

The elevated values of Mo, Ni and V are observed in sapropel unit in Core BS 15, BS 23 (2) and 46 (Fig 3.8, Fig 3.9, Fig 3.11, Fig3.16). Mo, Ni and V are mostly concentrated in both the organic and sulphide fractions, Mo are coprecipitated with iron sulphides in their sulphide phases. In the anoxic basin sulphide precipitation start in the anoxic water layer (Brewer and Spencer, 1974; Spencer and Brewer, 1971; Jacos *et al.*, 1985; Landing and Lewis, 1991; Spencer *et al.*, 1972). The Mo/Al maximum concentration occurs at the Corg peak and whereas S and As reach maximum values at a depth of 33 cm in Core BS 23(2) and at the base of the Core 46 (Fig 3.5, Fig 3.11, Fig 3.16, Table 3.7, Table 3.8). Korolev (1958) and Bertine (1972) have shown experimentally that Mo is removed very effectively by its coprecipitation with FeS from thio-molybdate solutions and from anoxic sea water, respectively. Hence Mo may be present to a greater extent in sulphide fraction compared with Cu and V in the sapropel.

## 4.2. Conclusions

As a result of the studies carried out during this thesis, the following conclusions are reached:

1. Carbonate, Ca/Al and Sr/Al values are higher in the western Black Sea basin than in the eastern Black Sea basin. This indicates greater biogenic carbonate flux and relatively low detrital input in the former basin compared to the latter basin. Significantly high Sr/Al values in both the sapropel and coccolith units in the western basin may be due to greater total biogenic carbonate input and/or to greater contribution of aragonitic shells to the total carbonate content in this basin.

2. The presence of *B. bigelowi* in the sapropel unit (and in the lower part of the coccolith unit) clearly indicates unusually low salinities (Bukry, 1974) during the deposition of the sapropel unit
3. Smear slide studies in Cores BS 23 (2) and BS 15 demonstrate that the amount and the size of the quartz, detrital calcite, opaque mineral, chlorite and biotite show an increase in the coccolith unit compared to the sapropel unit. This is also shown by enrichment in the coccolith unit of lithophile elements such as K, Na, Mg, Rb, Cr, Ti and Zr, all indicating that detrital mineral input during the deposition of the sapropel unit was lower than that during the deposition of the coccolith unit.
4. Enrichment of the lithophile elements, together with sharp increases in heavy metals of anthropogenic origin (Cu, Zn, Pb, Sb and As) in the top few cm of the cores, are due to anthropogenic activity in the last few hundred years. The differences in the depth of the onset of the enrichment of metals in different cores indicate that the sedimentation rate decreases in the order: Core BS 9 > Core BS 15 > Core BS 23(2). This conclusion is supported by <sup>210</sup>Pb mass accumulation rate (MAR) data of Çağatay et al. (2001) at sites Cores BS9 and BS15. Core 46 from the eastern basin was not sampled at sufficiently high resolution to determine the corresponding metal enrichment depth near the core top
5. The 2000 yr old coccolith/sapropel boundary occurs at 32.5 cm and 28.5 cm in Cores BS 15 and BS 23(2), respectively. This suggests that the that sedimentation rates for the last about 2000 yrs are also higher at the site of Core BS15 than those at the site of Core BS 23(2). This conclusion is in agreement with the grain size data and lithophile element distributions discussed above.
6. The elevated Cr values are observed in the sapropel unit in Core BS15, whereas in Core BS 23 (2) and 46 there is depletion of Cr and Mg in the sapropel unit (Fig 3.9, Fig 3.11, Fig 3.16). Cr and Mg occur in mafic minerals such as chlorite (Petruk 1964; Muller and Stoffers, 1974). This suggests that there was a higher input of chlorite to the western basin compared to the eastern basin during the sapropel deposition. Cr is generally higher in the coccolith unit than in the sapropel unit.

7. The high degree of correlation coefficients between Al, K, Sc, Rb, and Li in the sapropel unit in Cores 46 and BS 23(2) is probably accounted for by the presence of potassium feldspar, mica, and mafic minerals. The presence of detrital silicates in the sapropel unit is shown by close degree of correlation between Mg, Al, Ti, Nb, Ta, Th and Cr.
8. The trends of Ba/Al profiles are generally conformable with those of Corg profiles in the studied cores, indicating the proxy character of this ratio for organic productivity in the Black Sea sediments. The highest Ba values are found in the western basin. Its concentration in the sapropel unit is 5 and 13 times that in the coccolith unit in Cores BS 23 and 46, respectively (Table 3.3, Table 3.4). Ba shows a general depletion in the sapropel unit in Core 46. Ba/Al ratio is the highest in the sapropel unit in Core BS 15, followed by Core BS 23(2) and Core 46. These trends suggest that the organic productivity was higher in the western basin than in the eastern basin during the sapropel deposition. In the coccolith unit, Ba/Al ratio increases in the order: Core 46 < BS 23(2) < BS 9 < BS15, again suggesting higher organic productivity in the western Black Sea basin compared to the eastern Black Sea basin during the last 3000 years.
9. The enrichment of Ba in the organic rich horizons of coccolith and sapropel units and in the top 2-4 cm of the cores can be interpreted as a reflection of the recent eutrophication of the Black Sea.
10. Higher Ba contents and lower detrital input in the upper part of the sapropel unit in Core BS 15, BS 23 (2) and in the upper part of the Core 46 show that the organic carbon is composed mainly marine origin. This result is supported by the earlier organic geochemical analysis by Tolun et al. (1999) and Tolun (2001), which indicate that in the Black Sea sapropel the marine component of organic carbon increases towards the top of the unit.
11. High Mo, P, Ni, V and Ba concentrations show strong correlation between each other in sapropel unit. The highest enrichment of these element in this unit is found the western part of the basin compared to the eastern basin. Mo, Ni and V are mostly concentrated in both the organic and sulphide fractions. P/Al distribution is similar to that of Mo in the sapropel unit in the eastern basin cores showing the association of P and Mo with the organic matter.

13. The contents of Mn as a redox-sensitive element in the sapropel unit are lower than those of the coccolith unit. Fe shows a similar behaviour to Mn in the sapropel unit. There is no enrichment of Mn and Fe just above the sapropel unit in any of these cores in the eastern and western Black Sea basins. The absence of such clear enrichments of redox sensitive elements, such as Mn and Fe, above and within the Black Sea sapropel strongly suggest that oxic bottom water conditions never prevailed during or after the deposition of sapropel unit.
14. Enrichment of chalcophile elements such as Zn, Cu, Ni, As, and S in the sapropel unit also strongly suggests that this layer was deposited under anoxic bottom water conditions.





## REFERENCES

- Arkangel'skii, A.D. and Strakhov, N.M.**, 1938. Geologic structure and history of the development of the Black Sea, *Moscow and Leningrad, Izdatel'stvo Akademii Navk SSSR* (in Russian), 200p.
- Arthur, M.A. and Dean, W.E.**, 1998. Organic matter production and preservation and evolution of anoxia in the Holocene Black Sea, *Paleoceanography*, 13, 395-411.
- Bertine, K.K.**, 1972. The deposition of molybdenum in anoxic waters, *Mar. Chem.*, 1, 43-53.
- Bishop, J.K.B.**, 1988. The barite opal-organic carbon association in oceanic particulate matter, *Nature*, 332, 341-343.
- Braarud, T.**, 1963. Reproduction in the Marine coccolithophorid coccoliths *huxleyi* in culture, *Napoli Zool. Sta. Pub.*, 23, 110-116.
- Brewer P.G. and Spencer, D.W.**, 1974. Distribution of some trace elements in Black Sea and their flux between dissolved and particulate phases, in: E.T. Degens and D.A. Ross (Eds), *The Black Sea-Geology, Chemistry and Biology*, *Am. Assoc. Pet. Geol. Bull.*, 20, 137-144.
- Brown, S.D., Chiavari, G., Ediger, V., Fabbri, D., Gaines, A.F., Galletti, G., Karayığit, A.L., Love, G.D., Snape, C.E., Sirkecioğlu, O., Toprak, S.**, 2000. Black Sea sapropels: relationship to kerogen and fossil fuel precursors, *Fuel* 79, 1725-1742.
- Brumsack, H.J.**, 1986. The inorganic geochemistry of Cretaceous black shales (DSDP Leg 41) in comparison to modern upwelling sediment from the Gulf of California. In: C.P. Summerhayes and N.J. Shackleton (Editors). *North Atlantic Paleoceanography*, *Geol. Soc.*, pp. 137-151.
- Bukry, D.A.**, 1974. Coccolith as paleosalinity indicators-evidence from the Black Sea, In: Degens E.T. and Ross D.A. (Eds), *The Black Sea-Geology, Chemistry and Biology*, *Am. Assoc. Pet. Geol. Bull.*, 20, 353-363.

- Calvert, S.E.**, 1990. Geochemistry and origin of the Holocene Sapropel in the Black Sea. In: V. Ittekkot, S. Kempe, W. Michaelis and A. Spitay (Eds) Springer, Berlin, *Facets of modern biogeochemistry*, pp. 326-32.
- Calvert, S.E., and Fontugne, M.R.**, 1987. Stable carbon isotopic evidence for the marine origin of the organic matter in the Holocene Black Sea Sapropel, *Chemical Geology*, 66, 315-322.
- Calvert, S.E., and Pedersen, T.F.**, 1993. Geochemistry of recent oxic and anoxic marine sediments: Implications for the geological record, *Marine Geology*, 113, 67-88.
- Calvert, S.E. and Pedersen, T.F.**, 1992. Organic carbon accumulation and preservation in marine sediments: How important is anoxia? In: J.K. Whelan and J.W. Farrington (Editors), *Productivity Accumulation and preservation of Organic matter in Recent and Ancient Sediments*, Columbia Univ. Press, New York, pp. 231-263.
- Calvert, S.E., Vogel, J.S. and Southon, J.R.**, 1987. Carbon accumulation rates and the origin of the Holocene sapropel in the Black Sea, *Geology*, 15, 918-921.
- Calvert, S.E., Price, N.B.**, 1983. Geochemistry of Namibian Shelf sediments. In: Thiede J. And Suess E (Editors), *Coastal upwelling: its sediment record*, vol 1, Plenum, New York, pp. 337-375.
- Chow, T.J. and Goldberg E.D.**, 1960. On the marine geochemistry of barium, *Geochim. Cosmochim. Acta*, 20, 192-198.
- Cronan, D.S.**, 1980. *Underwater minerals*, Academic press, London, 362 pp.
- Çağatay, M.N., Saltoğlu, T., Gedik, A.**, 1987. Geochemistry of recent Black Sea sediments, *Geological Engineering*, 30, 47- 64.
- Çağatay, M.N., Saltoğlu, T. and Gedik, A.**, 1990. Geochemistry of uranium in the late Pleistocene sediments from the southern part of the Black Sea basin, *Chemical Geology*, 82, 129-144.
- Çağatay, M.N., Güngör, E., Güngör, N., Yılmaz, Y.Z., Sarı, E.**, 2001. Sediment organic carbon and carbonate mass accumulation rates on the western continental margin of the Black Sea. 36. CIESM Congress Proceedings, Volume 36, p.114.
- Degens, E.T. and Ross, D.A.**, 1972. Chronology of Black Sea over the last 25.000 years, *Chem. Geol.*, 10, 1-16.
- Degens, E.T., Watson, S.W. and Remsen, C.C.**, 1970. Fossil membranes and cell wall fragments from a 7.000-year old Black Sea sediment, *Science*, 168, 1207-1208.

- Degens, E.T., Michealis, W., Garassi, C., Mopper, K., Kempe, S. and Ittekkot, V.A., 1980.** Warvenchronologie und frühdiagenetische Umsetzungen organischer Substanzen Holozäner Sedimente des Schwarzen Meeres, *Neues Jahrb. Geol. Paleontol. Monatsch.*, 2, 65-86.
- Demaison, G.J. and Moore, J.T., 1980.** Anoxic environments and oil source bed genesis, *Organic Geochemistry*, 2, 9-31.
- Demaison, G.J., 1991.** Anoxia vs. productivity: what controls the formation of organic-carbon-rich sediments and sedimentary rocks?, *Am. Assoc. Petrol. Geol. Bull.*, 64, 1179-1203.
- Didyk, B.M., Simoneit, B.R.T., Brassel, S.C., and Eglinton, G., 1978.** Organic geochemical indicators of paleoenvironmental conditions sedimentation, *Nature*, 272, 216-222.
- Dymond, J., Suess, E. and Lyle, M., 1992.** Barium in deep sea sediment: A geochemical proxy for paleoproductivity, *Paleoceanography*, 7, 163-181.
- Dymond, J., 1985.** Particulate barium fluxes in the oceans: An indicator of new productivity. *Trans. Am. Geophys. Union*, 66, 1275.
- Emeis, K.C, Zhan, R., 1996.** Sapropels, Mediterranean climate and oceanography since the Miocene, *ODP legs 160 and 161 shipboard scientific party*, ODP First Euro Colloquium, Oldenburg, p 2.
- Emerson, S. and Hedges, J.L., 1988.** Processes controlling the organic carbon content of open ocean sediments, *Paleoceanography*, 3, 139-162.
- Ergin, M., Gaines, A., Galetti, G.C., Chiavari, G., Fabbri, D., Yücesoy-Eryılmaz, F., 1996.** Early diagenesis of organic matter in recent Black Sea sediments: characterization and source assessment, *Applied Geochemistry*, 11, 711-720.
- Espitalié, J., Laporte, J.L., Madec, M., Marquis, F., Leplat, P. And Paulet, J., 1977.** Methode rapide de caractérisation des roches mères, de leur potential pétrolier et de leur degré évolution, *Revue dél Inst. Frencais du Pétr.*, 32, 23 43.
- Fischer, G. and Wefer, G., 1999.** *Use of Proxies in Paleoceanography*, Berlin: Springer, 735 p.
- Francois, R., 1988.** A study on the regulation of the concentrations of some trace metals (Rb, Sr, Zn, Pb, Cu, V, Cr, Ni, Mn and Mo) in Saanich Inlet sediments, British Colombia, Canada, *Marine Geol.*, 83, 285-308.

- Froelich, P.N., Klinkhammer, G.P., Bender, M.L., Luedtke, N.A., Heath, G.R., Cullen, D., Dauphin, P., Hammond, D., Hartman, B. and Maynard, V.,** 1979. Early oxidation of organic matter in pelagic sediments of the eastern equatorial Atlantic: suboxic diagenesis, *Geochim. Cosmochim. Acta*, 43, 1075-1090.
- Gaudette, H., Flight, W., Tones, L., and Folger, D.,** 1974. An expensive titration method for the determination of organic carbon in recent sediments, *Journal Sedimentary Petrology*, 44, 249-253.
- Goldberg, E.D.,** 1958. Determination of opal in marine sediments, *J. Mar. Res.*, 17, 178-182.
- Goldberg, E.D. and Arrhenius, G.O.S.,** 1958. Chemistry of Pacific pelagic sediments, *Geochim. Cosmochim. Acta*, 13, 153-212.
- Grand, H.H., and Braarud, T.,** 1935. A quantitative study of the phytoplankton in the Bay of Fundy and the Gulf of Maine (including observation on hydrography, chemistry and turbidity), *Biol. Board Canada Jour.*, 1, n:5, 280-467.
- Gunnerson, C.G. and Özturgut, E.,** 1974. The Bosphorus, In: Degens E.T. and Ross D.A. (Eds), *The Black Sea-Geology, Chemistry and Biology*, *Am. Assoc. Pet. Geol. Bull.*, 20, 99-114.
- Gurvich, Y.G., Bogdanov, Y.A., Lisitsyn, A.P.,** 1978. Behaviour of barium in recent sedimentation in the Pacific, *Geokhim.*, 3, 359-374 (in Russian).
- Haraldsson, C. and Westerlund, S.,** 1988. Trace metals in the water columns of the Black Sea and Framwären Fjord, *Marine Chemistry*, 23, 417-424.
- Haraldsson, C. and Westerlund, S.,** 1991. Total and suspended cadmium, cobalt, copper, iron, lead, manganese, nickel and zinc in the water column of the Black Sea, In: J.W. Murray and E. Izdar (eds.), *Black Sea Oceanography*, Kluwer, Dordrecht, pp. 161-172.
- Higgs, N.C., Thomson, J., Wilson, T.R.S. and Croudace, I.W.,** 1994. Modification and complete removal of eastern Mediterranean sapropels by postdepositional oxidation, *Geology*, 22, 423-426.
- Hirst, D.M.,** 1974. Geochemistry of sediments from eleven Black Sea cores. In: Degens E.T. and Ross D.A. (Eds), *The Black Sea-Geology, Chemistry and Biology*, *Am. Assoc. Pet. Geol. Bull.*, 20, 430-455.
- Huc, A.Y., Durand, B., and Monin, J.C.,** 1978. Humic compounds and kerogens in cores from Black Sea sediments, *Deep Sea Drilling Project*, 42 (Eds. D.A. Ross and Y.P. Neprochnov et al.), US. Gov., Printing office, Washington, D.C., pp. 737-748.

- Hunt, J.M.**, 1974. Hydrocarbon geochemistry of Black Sea. In: Degens E. T. and Ross D. A. (Eds), *The Black Sea-Geology, Chemistry and Biology*, *Am. Assoc. Pet. Geol. Bull.*, 20, 499-504.
- Jacobs, L., and Emerson, S.**, 1982. Trace metal solubility in Vancouver Island, British Columbia, *J. Fish. Res. Board. Can.*, 19, 1-37.
- Jacobs, L., Emerson, S. and Skei, J.**, 1985. Partitioning and transport of metals across the O<sub>2</sub>/H<sub>2</sub>S interface in a permanently anoxic basin: Framvaren fjord, Norway, *Geochim. Cosmochim. Acta*, 49, 1433-1444.
- Jones, G.A and Gagnon, A.R.**, 1994. AMS radiocarbon dating of sediments in the Black Sea, *Deep Sea Research*, Part 1, 41, 531-557.
- Keil, R.G., Tsamakidis, E., Fuh, C.B., Giddings, J.C. and Hedges, J.I.**, 1994a. Mineralogical and textural controls on the organic matter composition of coastal marine sediments: hydrodynamic separation using SPLITT fractionation, *Geochim. Cosmochim. Acta*, 58, 879-893.
- Keil, R.G., Montlucon, Prahl, F.G. and Hedges, J.I.**, 1994 b. Sorptive preparation of labile organic matter in marine sediments, *Nature*, 370, 549-552.
- Korolev, D.T.**, 1958. The role of iron sulphides in the accumulation of molybdenum in sedimentary rocks of the reduced zone, *Geochemistry*, 4, 452-463.
- Koreneva, E.V.**, 1964. Spores and pollen from bottom sediments in the western part of the Pacific Ocean, *Akad. Nauk. SSSR Geol. Inst.*, v.109, 88p (in Russian).
- Krauskopf, K.B.**, 1979. *Introduction to Geochemistry*, 617 pp., Tokyo, McGraw-Hill Kogakuska.
- Landing, W.M. and Lewis, B.L.**, 1991. Thermodynamic modelling of trace metal speciation in the Black Sea, in J.W. Murray and E. Izdar (eds), *Black Sea Oceanography*, NATO Advanced Study Institute, Kluwer Acad. Publ., Dordrecht, pp. 125-160.
- Lee, C., Gasion, R.B., and Ferrington, J.W.**, 1980. Geochemistry of sterols in sediments from Black sea and southwest Africa shelf and slope, *Organic Geochemistry*, 2, 103-113.
- Loring, D.H. and Rantala, R.T.T.**, 1992. Manual for the geochemical analyses of marine sediments and suspended particulate matter, *Earth Science Reviews*, 32, 235-283.
- Mason, B. and Moore, C.B.**, 1982. *Principles of Geochemistry*, John Wiley & Sons, New York, 350 p.
- Mayer, L.M.**, 1994. Surface area control of organic carbon accumulation in continental shelf sediments, *Geochim. Cosmochim. Acta*, 58, 1271-1284.

- Maynard, N.G.**, 1974. Diatoms in Pleistocene Deep Black Sea sediments, in: E.T. Degens and D.A. Ross (Eds), *The Black Sea-Geology, Chemistry and Biology*, *Am. Assoc. Pet. Geol. Bull.*, 20, 389-396.
- Muller, G. and Stoffers, P.**, 1974. Mineralogy and petrology of Black sea basin sediments. In: Degens E.T. and Ross D.A. (Eds), *The Black Sea Geology, Chemistry and Biology*, *Am. Assoc. Pet. Geol. Bull.*, 20, 201-248.
- Murray, J.W, Top, Z. and Özsoy, E.**, 1991. Temperature and salinity distributions in the Black sea, *Deep Sea Research*, part A, 38, suppl. 2, 663-689.
- Özsoy, E. and Ünlüata, Ü.**, 1997. Oceanography of the Black Sea: a review of some recent results, *Earth Science Reviews*, 42, 231-272.
- Pedersen, T.F. and Calvert, S.E.**, 1990. Anoxia vs. productivity: What controls the formation of organic carbon-rich sediments and sedimentary rocks, *Am. Pet. Geol. Bull.*, 74, 454-466.
- Pedersen, T.F. and Calvert, S.E.**, 1991. Anoxia vs. productivity: What controls the formation of organic carbon-rich sediments and sedimentary rocks, Reply. *Am. Pet. Geol. Bull.*, 75, 500-501.
- Pelet, R. and Debyser, Y.**, 1977. Organic geochemistry of Black sea cores, *Geochim Cosmochim. Acta*, 41, 1575-1586.
- Petruk, W.**, 1964. Determination of the heavy atom content I chlorite by means of the X-ray diffractometer, *Am. Mineralogist*, 49, 61-71.
- Philipchuk, M.F. and Volkov, L.I.**, 1974. Behaviour of molybdenum in processes of sediment formation and diagenesis in the Black Sea. In: Degens E.T. and Ross D.A. (Eds), *The Black Sea-Geology, Chemistry and Biology*, *Am. Assoc. Pet. Geol. Bull.*, 20, 542-554.
- Pruysers, P.A., de Lange, G.J., Middelburg, J.J. and Hydes, D.J.**, 1993. The diagenetic formation of metal-rich layers in sapropel-containing sediments in the eastern Mediterranean, *Geochim. Cosmochim. Acta*, 57, 527-536.
- Ransom, B., Kim, D., Kastner, M. and Wainwright, S.**, 1998. Organic matter preservation on continental slopes: Importances of mineralogy and surface area, *Geochim. Cosmochim. Acta*, 62, 1329-1345.
- Revelle, R., Bramlette, M., Arrhenius, G., Goldberg, E.D.**, 1955. Pelagic sediments of the Pasific, in: Poldervaart W. (eds), *crust of the Earth Geol. Soc. Amer. Spec. Pap*, 62, 221-225.
- Roman, S.**, 1974. Palynoplanktologic Analysis of some Black Sea Cores, in: Degens E.T. and Ross D.A. (Eds), *The Black Sea-Geology, Chemistry and Biology*, *Am. Assoc. Pet. Geol. Bull.*, 20, 396-411.

- Ross, D.A and Degens, E.T.**, 1974. Recent sediments of the Black Sea. In: Degens E.T. and Ross D.A. (Eds), *The Black Sea-Geology, Chemistry and Biology*, *Am. Assoc. Pet. Geol. Bull.*, 20, 183-199.
- Ross, D.A., Degens, E.T. and MacIvaine, J.**, 1970. Black Sea: recent sedimentary history, *Science*, 170, 163-165.
- Ross, D.A., Uchpi, E., Prada, K.E. and MacIvaine, J.**, 1974. Bathimetry and microtopography of Black Sea, in: E.T. Degens and D.A. Ross (Eds), *The Black Sea-Geology, Chemistry and Biology*, *Am. Assoc. Pet. Geol. Bull.*, 20, 183-199.
- Ross, A.D., Stoffers, P. and Trimonis E.S.**, 1978. Black Sea sedimentary framework, *In: Initial Reports of the Deep Sea Drilling Project*, 42, Part 2, U.S. Gov. Print. Off., Washington, D.C., pp. 359-363.
- Ryan, W.B.F., Pitman III, W.C., Major, C.O., Shimkus, K., Moskalenko, V., Jones, J.A., Dimitrov, P., Görür, N., Sakıncı, M. and Yüce, H.**, 1997. An abrupt drowning of Black Sea shelf, *Marine Geology*, 138, 119-126.
- Rullkötter, J.**, 2000. Organic matter: The driving force for Early Diagenesis in *Marine Geochemistry*, pp.129-167, Eds. Schulz, H.D.&Zabel, M., Springer.
- Schmitz, B.**, 1987. Barium equatorial high productivity and northward wandering of Indian continent, *Paleoceanography*, 2, 63-78.
- Schrader, H. and Maderne, A.**, 1981. Sapropel formation in the eastern Mediterranean: evidence from preserved opal assemblages, *Micropaleontology*, 27, 191-203.
- Shaw, T.J., Gieskes, J.M. and Jahnke, R.A.**, 1990. Early diagenesis in differing depositional environments, *Geochim. Cosmochim. Acta*, 54, 1233-1246.
- Shimkus, K.M. and Trimonis, E.S.**, 1974, Modern sedimentation in Black Sea, In: *The Black Sea-Geology, Chemistry and Biology* (Eds. E.T. Degens and D.A. Ross), *Am. Assoc. Pet. Geol. Bull.*, 20, 249-278.
- Simoneit, B.R.**, 1974. Organic analyses of Black Sea cores. In: *The Black Sea Geology, Chemistry and Biology* (Eds. E.T. Degens and D.A. Ross), *Am. Assoc. Pet. Geol. Bull.*, 20, 477-498.
- Simoneit, B.R.**, 1978. Organic geochemistry of terrigenous muds and various shales from the Black Sea, DSDP Leg 42B, *Deep Sea Drilling Project*, (Eds: D.A. Ross and Y.P. Neprochnov et al.) US Gov., Printing Office, Washington, D.C., 749-753.
- Smayada, T.J.**, 1966. A quantitative analysis of the phytoplankton of the Gulf of Panama-III General ecological conditions, and the phytoplankton dynamics at 8° 45'N, 79° 23'N from November to May 1957, *Inter-Am. Tropical Tuna Comm. Bull.*, 11, no:5, 353-612.

- Spencer, D.W. and Brewer, P.G.**, 1971. Vertical advection diffusion and redox potential as controls on the distribution of manganese and other trace metals dissolved in waters of the Black Sea, *J. Geophys. Res.*, 76, 5877-5892.
- Spencer, D.W., Brewer, P.G. and Sachs, P.L.**, 1972. Aspects of the distribution and composition of suspended matter in the Black Sea, *Geochim. Cosmochim. Acta*, 36,71-86.
- Stein, R.**, 1986a. Surface-water paleoproductivity as inferred from sediment deposits on oxic and anoxic deep-water environments of Mesozoic Atlantic Oceans, *Mitt. Geol.-Paläont. Inst. Univ.Hamburg*, 60, 55-70.
- Stein, R.**, 1986b. Organic carbon and sedimentation rate- further evidence for anoxic deep-water conditions in the Cenomanian/Turonian Atlantic Ocean, *Marine Geology*, 72, 199-209.
- Stein, R.**, 1990. Organic carbon content / sedimentation rate relationship and its paleoenvironmental significance for marine sediments, *Geo-Marine Lett.*, 10,37-44.
- Stein, R.**, 1991. Accumulation of organic carbon in marine sediments, *Lect. Notes Earth Science*, 34, 1-217.
- Suess, E. and Thiede, J.**, 1983. *Coastal upwelling: its sedimentary record. Part A: Response of the sedimentary regime to present coastal upwelling*, Plenum Press, NY, 604 pp.
- Summerhayes, C.P., Prell, P.L. and Emeis, K.C.(eds)**, 1992. Upwelling systems: Evolution since the early Miocene, *Geol. Soc. Spec. Publ.*, 64, Blackwell, Oxford, 519 pp.
- Thiede, J. and Suess, E.**, 1983. *Coastal upwelling, its sediment record. Part B: Sedimentary records of ancient coastal upwelling*, Plenum. Press, NY, 610pp.
- Thomson, J., Higgs, N.C., Wilson, T.R.S., Croudace, I.W., de Lange, G.J. and van Santvoort, P.J.M.**, 1995. Redistribution of geochemical behaviour of redox sensitive elements around S1, the most recent eastern Mediterranean sapropel, *Geochim. Cosmochim. Acta*, 17, 3487-3501.
- Thunell, R.C. and Williams, D.F.**, 1989. Glacial-Holocene salinity changes in the Mediterranean Sea: hydrographic and depositional effects, *Nature*, 338, 493-496.
- Tolun, L., Çağatay, M.N. and Carrigan, W.J.**, 1999. Organic geochemistry and Origin of sapropelic sediments from Sea of Marmara and Black Sea. 19<sup>th</sup> International Meeting on Organic Geochemistry, 6-10 September 1999, Istanbul, Abstracts Part 1, pp.41-42.



- Tolun, L.** 2001. Marmara Denizi ve Karadeniz Holosen sapropellerinin Organik Jeokimyası. İ.Ü. Deniz Bilimleri Enstitüsü doktora tezi.
- Traverse, A.**, 1974. Palynologic investigation of two Black sea cores in: E. T. Degens and D.A. Ross (eds.), *The Black Sea-Geology, Chemistry and Biology*, *Am. Assoc. Pet. Geol. Bull.*, 20, 381-389.
- van de Meent, D., Brown, S.C., Philip, R.P. and Simoneit, B.R.T.**, 1980. Pyrolysis-high resolution gas chromatography-mass spectrometry of kerogens and kerogen precursors, *Geochim. Cosmochim. Acta*, 44, 999-1013.
- Volkov, I.I. and Fomina, L.S.**, 1974. Influence of organic material and processes of sulfide formation on distribution of some trace elements in deep water sediments of the Black Sea. In: Degens E. T and Ross D.A. (Eds) ,*The Black Sea-Geology, Chemistry and Biology*, *Am. Assoc. Pet. Geol. Bull.*, 20, 457-476.
- Watanabe, T., Winter, A., Oba, T.**, 2001. Seasonal changes in sea surface temperature and salinity during the little Ice Age in the Caribbean Sea deduced from Mg/Ca and  $^{18}\text{O}/^{16}\text{O}$  ratios in corals, *Marine Geology*, 173: 21-35.

## **CURRICULUM VITAE**

**Ümmühan Saadet SANCAR** was born on 30.12 1974 in Konya. She obtained her high school education in Yeni Levent Lisesi. After, she started graduate education at Istanbul Technical University, Mines Faculty, Geological Engineering Programme in 1993 and finished in 1998. After that, she started her studies towards M.Sc. degree at I.T.U Eurasia Institute of Earth Sciences on 1999. Later, she started to work at I.T.U., Mines Faculty General Geology department as a research assistant in 2000.

